

Aus der Abteilung für Transplantations- und Infektionsimmunologie  
der Medizinischen Fakultät  
der Universität des Saarlandes, Homburg/Saar  
Leitung: Univ.-Prof. Dr. rer. nat. Martina Sester

**Titanium dioxide nanoparticles and carbon nanotubes as potential stimulators  
of asthmatic reaction  
Studies in mouse model and cell culture**

**Dissertation**

Zur Erlangung des Grades eines Doktors  
der Naturwissenschaften  
der Medizinischen Fakultät  
der UNIVERSITÄT DES SAARLANDES  
2022

vorgelegt von  
**Shaza Abdunasser Harfoush**  
geb. am 22.06.1989 in Damaskus/Syrien

*To my first, endless, and eternal love of my life..... my country, Syria*

*To whom I owe my success & happiness, my soulmate and heartbeat .....*

*my husband, Dr. med. Al Farkash*

*To my little angels, the light of my eyes and my sunshine..... my children*

*To my idol, my role model, the person I admire..... my father,*

*Dr. dent. Abdalnasser*

*To the icon of affection, warmth, and tenderness, my beautiful Saint..... my mother*

*To the source of power, trust & support in my life, the ones I can rely on.....*

*my brothers and sisters*

*To my whole family, to which I am belonged and proud*

# Table of Content

<b>Table of Content</b> .....	<b>3</b>
<b>1. Summary</b> .....	<b>5</b>
<b>2. Zusammenfassung</b> .....	<b>7</b>
<b>3. Introduction</b> .....	<b>9</b>
3.1 Respiratory system.....	9
3.2 Allergic bronchial asthma .....	10
3.2.1 Symptoms and signs of asthma .....	11
3.2.2 Epidemiology and pathophysiology of asthma .....	11
3.2.3 Asthma and pharmacotherapy .....	12
3.3 Nanotechnology and nanoparticles .....	13
3.3.1 Titanium dioxide nanoparticles .....	15
3.3.2 Carbon nanotubes .....	16
<b>4. Aims of the studies</b> .....	<b>17</b>
<b>5. Materials and Methods</b> .....	<b>19</b>
5.1 Titanium dioxide nanoparticles and their physicochemical characteristics.....	19
5.2 Experimental design.....	20
5.3 Lung function measurements.....	22
5.4 Tissue sampling and ICP-MS measurements .....	24
5.5 Staining and histological analysis .....	24
5.6 BALF collection .....	27
5.7 ELISA assay.....	29
5.8 Investigation of NP phagocytosis.....	29
5.9 SEM and energy-dispersive X-ray spectroscopy (SEM-EDX) .....	30
5.10 Carbon nanotubes source and properties .....	31
5.11 Micrograph of carbon nanotubes .....	31
5.12 Cell culture and exposure .....	32
5.13 Measurement of interleukin 8 (IL-8) production.....	32
5.14 Cytotoxicity determination.....	33
5.15 Sample preparation and fixation for scanning electron microscopy (SEM) analysis.....	33
5.16 Statistical analysis.....	34
<b>6. Results</b> .....	<b>35</b>

6.1 Characterization of titanium dioxide nanoparticle.....	35
6.2 Inhaled exposure to titanium particles induces further airways inflammation in asthmatic mice .....	37
6.3 Titanium dioxide enhances eosinophil infiltration in the lungs of asthmatic mice .....	42
6.4 Intranasal administration of titanium dioxide nanoparticles during OVA-sensitization and challenge induces airway hyperresponsiveness .....	47
6.5 Titanium dioxide treatment shifts the respiratory immune reaction towards a Th2-mediated response .....	49
6.6 Cellular uptake of titanium dioxide nanoparticles .....	53
6.7 Titanium dioxide nanoparticles distribution in extrapulmonary organs .....	55
6.8 The isolation and identification of A549 cells under light microscope.....	61
6.9 Characterization of single, double, and multi-walled carbon nanotubes .....	64
6.10 Carbon nanotubes treatment affects IL-8 levels.....	66
6.11 Cytotoxicity induced by carbon nanotubes .....	71
6.12 Carbon nanotubes challenge and-cell interaction .....	75
<b>7. Discussion .....</b>	<b>80</b>
<b>8. Conclusion.....</b>	<b>86</b>
<b>9. References .....</b>	<b>87</b>
<b>10. Abbreviation .....</b>	<b>93</b>
<b>11. Publications .....</b>	<b>95</b>
<b>12. Aknowledgments / Danksagung .....</b>	<b>97</b>
<b>13. Lebenslauf .....</b>	<b>Error! Bookmark not defined.</b>

## 1. Summary

The rising productions of engineered nanomaterials (ENMs) increase the risk for harmful exposure in occupational environments. Titanium dioxide nanoparticles (TiO<sub>2</sub> NPs) and its derivatives are abundantly used in a number of medical and industrial applications.

Previous studies revealed that there is increasing number of individuals with respiratory disorders when such normal individuals are exposed to these particles in vocational settings. However, little is known about how these particles affect the preexisting airway diseases such as asthma.

In order to improve the understanding, we performed an ovalbumin (OVA)-induced mouse model of allergic airway inflammation. Control and asthmatic female BALB/c mice received TiO<sub>2</sub> NPs (21 nm) intranasally. Local tissue effects and lung function were measured primarily. Further, nanoparticle distribution into extrapulmonary organs was investigated by inductively coupled plasma mass spectrometry (ICP-MS), and scanning electron microscopy (SEM). Th1/Th2 cytokine levels were also measured in the lungs by ELISA.

Our findings indicate that mice receiving OVA with TiO<sub>2</sub> NPs developed an asthma-like airway reaction, and enhanced eosinophil infiltration in the lung tissues of asthmatic mice compared to controls. We also found a significant increase in Th2 cytokines including Interleukin (IL) IL-4, IL-5 and IL-13 following TiO<sub>2</sub> NP exposure. Adherent mouse alveolar macrophages were able to take up TiO<sub>2</sub> NPs at different time points. Using SEM and ICP-MS, we detected the nanoparticle in most of the organs of asthmatic and non-asthmatic treated mice.

Next, we performed *in vitro* study in order to describe the toxicity of another range of nanomaterials. Three different configurations of carbon nanotubes (CNTs) including single walled carbon nanotubes (SWCNT), double walled carbon nanotubes (DWCNT), and multi walled carbon nanotubes (MWCNT) were incubated with human pulmonary epithelial cells (A549). Supernatants

of epithelial cell cultures were collected in order to detect the release of IL-8 and lactate dehydrogenase (LDH) by pulmonary epithelial cells.

Emission scanning electron microscope (ESEM) was employed to characterize the CNTs, and to assess the modifications on the cellular surface following the exposure to the three different types of CNTs.

Our results revealed the distinct differences in the levels of inflammatory response, the cellular damage, and toxicity caused by CNTs (release of LDH). Images taken by ESEM showed nanotube agglomerates and morphological changes after cellular incubation with SWCNT, DWCNT, and MWCNTs.

Our data clarify the underlying mechanism of Titanium dioxide nanoparticles-induced aggravation of respiratory diseases and this suggests important implications for environmental and occupational health policy, as well as for workers and individuals exposed to these nanomaterials.

## 2. Zusammenfassung

Die steigende Produktion von technischen Nanomaterialien (ENMs) erhöht das Risiko einer schädlichen Exposition im beruflichen Umfeld. Titandioxid-Nanopartikel (TiO<sub>2</sub> NPs) und seine Derivate werden in zahlreichen medizinischen und industriellen Anwendungen eingesetzt.

Frühere Studien haben gezeigt, dass die Zahl der Personen mit Atemwegserkrankungen zunimmt, wenn solche Personen im beruflichen Umfeld diesen Partikeln ausgesetzt sind. Es ist jedoch wenig darüber bekannt, wie diese Partikel die bereits bestehenden Atemwegserkrankungen wie Asthma beeinflussen.

Um das Verständnis zu verbessern, führten wir ein Ovalbumin (OVA)-induziertes Mausmodell für allergische Atemwegsentzündungen durch. Kontroll- und asthmatische weibliche BALB/c Mäuse erhielten intranasal TiO<sub>2</sub> NPs (21 nm). Es wurden lokale Gewebefeffekte und die Lungenfunktion gemessen. Auch wurde die Verteilung von Nanopartikeln in extrapulmonalen Organen durch induktiv gekoppelte Plasmamassenspektrometrie (ICP-MS) und Rasterelektronenmikroskopie (SEM) untersucht. Der Th1/Th2-Zytokinspiegel wurde in den Mauslungen mittels ELISA gemessen.

Unsere Ergebnisse zeigen, dass die Mäuse, die OVA mit TiO<sub>2</sub>-NPs erhielten, eine asthmaähnliche Atemwegsreaktion entwickelten und die Infiltration mit Eosinophilen im Lungengewebe der asthmatischen Mäuse im Vergleich zu den Kontrolltieren verstärkt war. Auch gab es einen signifikanten Anstieg der Th2-Zytokine, einschließlich der Interleukine (IL) IL-4, IL-5 und IL-13 nach TiO<sub>2</sub> NP-Exposition. Alveolarmakrophagen der Mäuse konnten zu verschiedenen Zeitpunkten TiO<sub>2</sub> NPs aufnehmen. Mit Hilfe von SEM und ICP-MS konnten die Nanopartikel in den meisten Organen der asthmatischen und nicht asthmatischen Mäuse nachgewiesen werden.

Als nächstes führten wir eine *In-vitro*-Studie durch, um die Toxizität einer weiteren Reihe von Nanomaterialien zu beschreiben. Drei verschiedene Konfigurationen von Kohlenstoffnanoröhren

(CNTs), einschließlich einwandiger Kohlenstoffnanoröhren (SWCNT), doppelwandiger Kohlenstoffnanoröhren (DWCNT) und mehrwandiger Kohlenstoffnanoröhren (MWCNT) wurden mit humanen Lungenepithelzellen (A549) inkubiert.

Die Überstände von Epithelzellkulturen wurden gesammelt, um die Freisetzung von IL-8 und Lactatdehydrogenase (LDH) durch Lungenepithelzellen nachzuweisen. Das Rasterelektronenmikroskop (SEM) wurde verwendet, um die CNTs zu charakterisieren und die Veränderungen auf der Zelloberfläche nach der Exposition gegenüber den drei verschiedenen Arten von CNTs zu bewerten.

Unsere Ergebnisse zeigten deutliche Unterschiede im Grad der Entzündungsreaktion, der Zellschädigung und der durch CNTs verursachten Toxizität (Freisetzung von LDH). Die mit SEM aufgenommenen Bilder demonstrierten Nanoröhrenagglomerate und morphologische Veränderungen nach zellulärer Inkubation mit SWCNT, DWCNT und MWCNTs.

Unsere Daten verdeutlichen den zugrunde liegenden Mechanismus mit der durch Titandioxid-Nanopartikel verursachten Verschlechterung von Atemwegserkrankungen. Dies deutet auf wichtige Auswirkungen auf die Umwelt- und Arbeitsschutzpolitik bei Exposition mit Nanomaterialien.

### **3. Introduction**

#### **3.1 Respiratory system**

The respiratory system is the system which provides oxygenated blood to the whole tissues, cells and organs of the body and takes out carbon oxide (**Figure 1**). The respiratory system consists of the upper and lower airways. The upper airway consists of the pharynx and the nasal cavities. Its functions are heating, filtering, humidifying of inspired gas, a voice resonator, and conducting ambient air into the trachea [1][2]. The lower airway consists of the trachea, bronchi, bronchioles, and lungs. Through the respiratory tree branches, the inspired air is conducted in the lower airway to the alveoli [3]. Exposure to different allergens may stimulate allergic reactions in diseases such as allergic rhinitis, and allergic bronchial asthma [4].

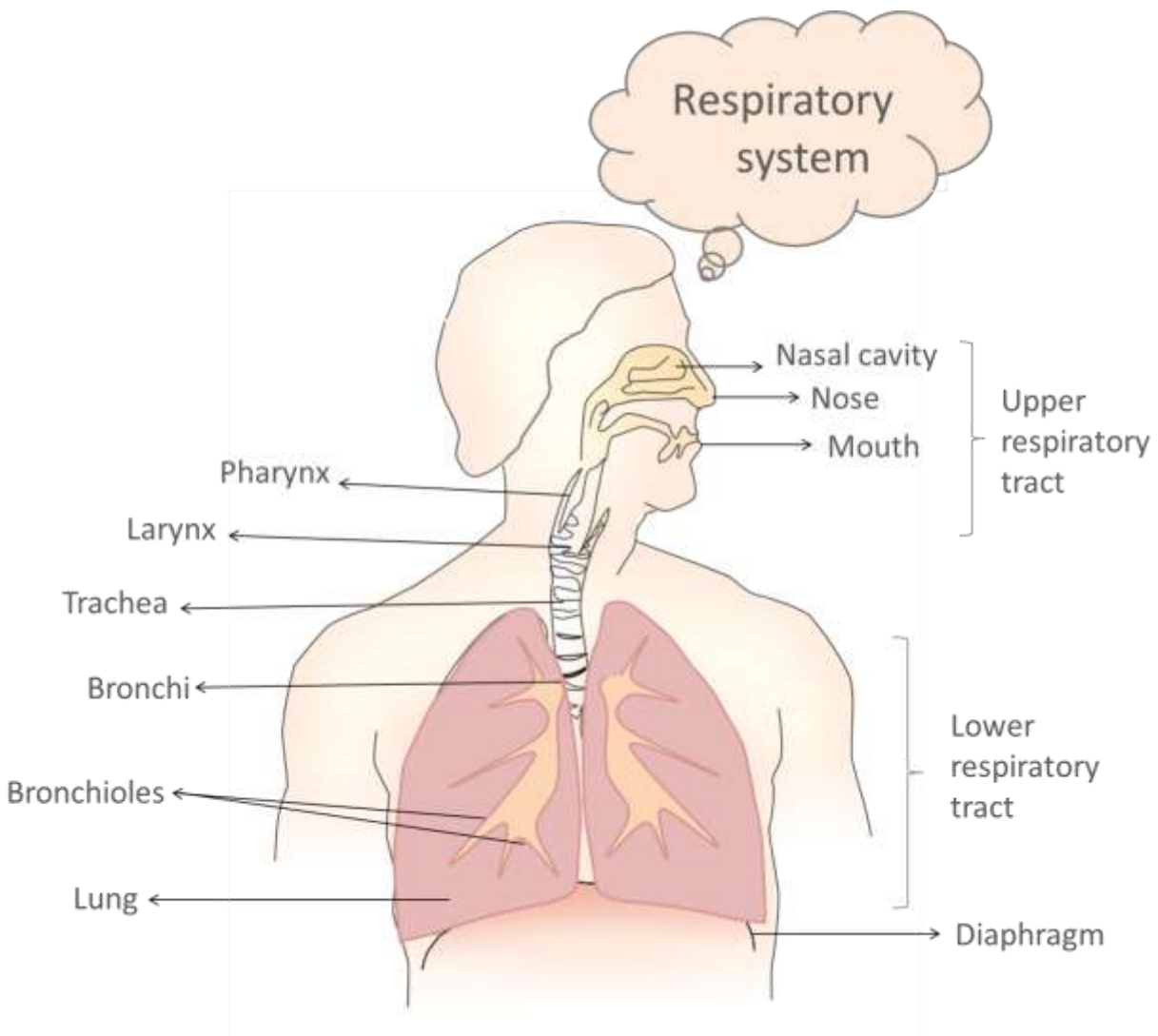


**Figure 1** The structure of human respiratory system. The respiratory system is composed of a group of blood vessels, muscles, and organs that enable us to breathe. The respiratory system organs are separated into the upper and lower respiratory tracts. The upper respiratory tract refers to the mouth, nose, nasal cavity, pharynx, and larynx. Trachea and lungs with bronchi, and bronchioles make up the lower respiratory tract.

### 3.2 Allergic bronchial asthma

Allergic bronchial asthma is a heterogeneous, complex, chronic inflammatory respiratory disease of the airways, characterized by periodic "attacks" in response to asthmatic "triggers". Asthma triggers may include:

- Infections like flu and cold
- Smoking

- Allergens such as pollen, food, and dust mites
- Air pollution and toxins
- Drugs (like NSAIDs, aspirin, and beta-blockers)
- Perfumes and fragrances
- Acid reflux

### **3.2.1 Symptoms and signs of asthma**

According to the Global Strategy for Asthma Management and Prevention GINA 2019, the symptoms and signs of asthma include:

- Shortness of breath
- Excessive coughing
- Wheezing
- Chest pain
- Tightness of chest

### **3.2.2 Epidemiology and pathophysiology of asthma**

Asthma affects around 300 million people of all the ages worldwide and this number is rising annually [5]. The asthmatic inflammatory processes start by the interplay between different cytokines produced by cells like eosinophils, basophils, dendritic cells, epithelial cells, T and B lymphocytes, mesenchymal cells, mast cells, neutrophils, lymphoid cells, and airway neurons [6]. Epithelial cells can be activated by environmental triggers which initiate the immune response by releasing different chemokines and cytokines. These substances will induce the proliferation and migration of different inflammatory cells [7][8]. Eosinophils are white blood cells associated with allergic diseases. Mast cells are the allergy-mediated cells that release chemicals such as histamine. T lymphocytes are also subgroup of white blood cells, divided in several subtypes such as T helper

1 and T helper 2 cells. T1 with the main aim for the prevention of foreign matter and infection, and T2 are participated in allergic inflammation.

These inflammatory cells are associated with the development of airway inflammation in asthma that contributes to the airflow limitation, airway hyperresponsiveness, respiratory symptoms, and chronic diseases [9].

### **3.2.3 Asthma and pharmacotherapy**

As reported by Buhl et al., the 2019 Global Initiative for Asthma (GINA) recommended the patients with asthma to take initial low-dose of inhaled corticosteroids (ICS). With moderate asthma, patients should receive increasing ICS dose with additional therapy such as the long-acting beta agonists (LABA) until they reach disease control. Long-acting muscarinic antagonists (LAMA) are a recommended additional therapy in the management of asthma. From this group has been tiotropium recently studied and approved for asthmatic patient  $\geq 6$  years and several clinical studies revealed its efficacy and safety for the treatment of uncontrolled-asthma exacerbations [76].

Moreover, biologicals and systemic steroids are potential therapies needed sometimes for patients with severe asthma. Biologicals are defined as manufactured proteins that may have therapeutic effects by inhibiting or activating different targets. Many of them are used now in clinical lung research, showing a decrease in asthma exacerbations and enhanced lung function in asthmatic patients treated with these biologicals [9,10]. The first licensed biological is the monoclonal anti-IgE antibody (omalizumab), which is approved by the US Food and Drug Administration (FDA) for patients with severe allergic asthma [9] (**Table 1**).

**Table 1** Asthma classification and pharmacotherapy: severity, symptoms, and therapy (GINA)

Severity grade	Symptoms	Pharmacotherapy
<b>1. Mild intermittent</b>	FEV <sub>1</sub> >80% < 1 daytime and 2 nighttime awakenings per week	Low dose ICS
<b>2. Mild persistent</b>	FEV <sub>1</sub> ≥80% Exacerbation of symptoms in grade 1	Low dose ICS
<b>3. Moderate persistent</b>	FEV <sub>1</sub> 60-80% > 1 nighttime awakenings	Low dose: ICS+LABA or Medium dose ICS
<b>4. Severe persistent</b>	FEV <sub>1</sub> <60% Exacerbations of symptoms at day- and nighttime Limitation of physical activities	Medium to high dose ICS+LABA
<b>5. Uncontrolled severe persistent</b>	Frequent exacerbations and stronger symptoms than in grade 4	Antibody anti-IgE (omalizumab) Anti-IL 5 (Mepolizumab) (Reslizumab) (Benzralizumab) Anti-IL-4/13 (Dupilumab)  Oral corticosteroids

ICS:inhaled corticosteroids, FEV:forced expiratory volume, LABA:long-acting betaagonists

### 3.3 Nanotechnology and nanoparticles

Nanotechnology provides promising designs for therapeutic and pharmaceutical development due to its features including biocompatibility, high biodegradability, and minimal toxicity [10-12]. It has been fundamental for medicine for many reasons including exhibiting novel approaches in treating diseases and its applications in consumer products, cosmetics, and medications like therapeutic vaccinations [13] (**Figure 2**).

Over the years many efforts are done to adopt nanotechnology for the treatment of human diseases like respiratory diseases [74].

Nanoparticles (NPs) are defined as solid particulates or particle dispersions with sizes ranging from 1 to 100 nm. NPs are recently used as efficient carriers for several pharmaceutical agents due to their unique physiochemical properties and desirable performance features [14-16]. Moreover, NPs are drug transporters because they are tiny enough to penetrate the cells, tissues, and bloodstream and remain active [17].

Conversely, definition of the side effects of NPs is also important since they may induce inflammatory reaction, tissue damage, oxidative stress, inflammasome activation, and genetic modifications [18][19]. Additionally, NPs can act as foreign particulates and might aggravate different pathologies like COPD and asthma [20] (**Figure 2**).

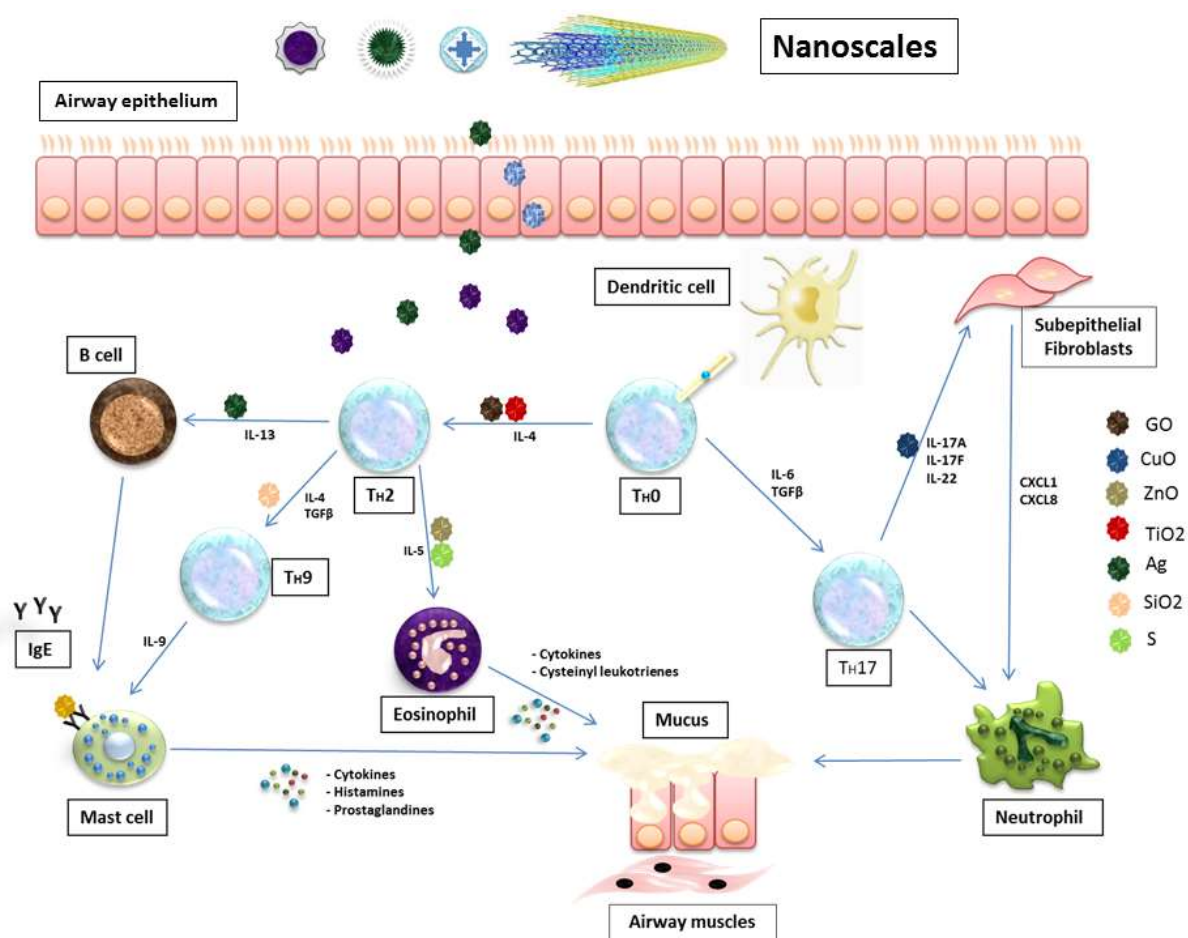


**Figure 2** Inflammatory cascade and mediators the pathogenesis of asthma. The allergic immune response starts from the respiratory epithelium where the environmental stimuli, antigens, and nanomaterials can enter and start inducing the inflammatory cells to release their mediators. These inhaled nanoscales are able to interact with the immune system and stimulate the production of chemokines, histamine, prostaglandins, and cytokines like interleukin 4 (IL-4), IL-13, IL-5 and immunoglobulin E (IgE). The released inflammatory mediators induce lung damage, bronchoconstriction, and mucus secretion (Harfoush et al., 2019).

### 3.3.1 Titanium dioxide nanoparticles

Titanium dioxide (TiO<sub>2</sub>) are widely used across a large number of applications such as solar cells, photocatalyst belts, medicine as well as in consumer products including toothpastes, deodorants, paints, food supplements, and sunscreens [21-23]. Inhalation, intratracheal instillation, and intranasal application of TiO<sub>2</sub> NPs suggest that these particles can translocate from the nasal cavity, the respiratory epithelium to localize finally in the lungs and other organs and tissues [75].

### 3.3.2 Carbon nanotubes

Among different types of nanoscales, carbon nanotubes (CNTs) are considered as one of the most attractive materials because of their distinct properties, versatile applications and chemical characteristics including their nanometer width, micrometer length, strength, as well as surface chemistry [24][25]. Such materials are currently used in biomedicine, oncology therapy, optics, computer industries, mechanical engineering, material science and electronics [26][27]. Single-walled (SWCNTs), double-walled (DWCNTs), and multi-walled (MWCNTs) are three common carbon nanotube configurations, and are composed of one or more thick graphene cylinders [28]. However, several *in vitro* studies on the effects of CNTs showed marked cytotoxicity, like cellular proliferation, the induction of oxidative stress, and apoptosis in many different cells [29-32] (Figure 3).

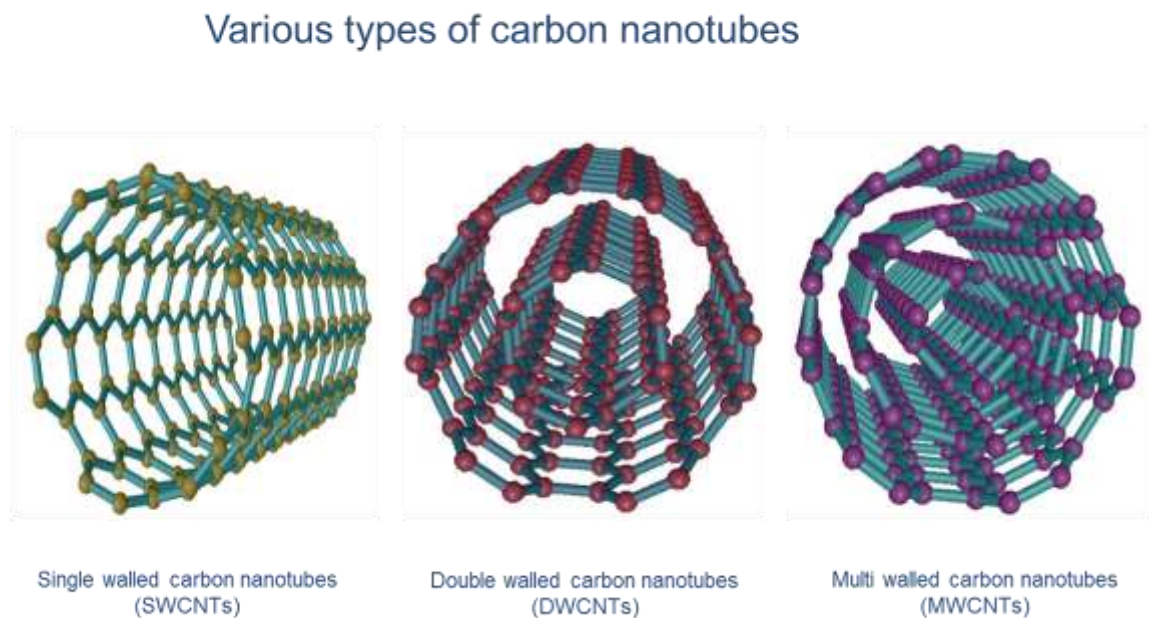


**Figure 3** Three common carbon nanotube forms: single-walled (SWCNTs), double-walled (DWCNTs), and multi-walled (MWCNTs). These structures have unique magnetic, electronic, and mechanical characteristics (Harfoush et al., 2019).

## 4. Aims of the studies

However as nanomaterials like TiO<sub>2</sub> NPs usage in consumer products, cosmetics, food supplementary, and medicine is recently increasing, it is imperative to also consider the risks induced by TiO<sub>2</sub> NPs given their harmful effects on the respiratory system and potentiality to augment allergic airway inflammation [23]. This kind of inflammation is transmitted by a complex interplay among different Th2 cytokines, like IL-4, IL-5, and IL-13. The production of cytokines is of significant importance in the pathogenesis of asthma since they further stimulate B cells and eosinophilic inflammation while inhibiting Th1 response [33][34]. The Th2-mediated allergic asthma and its crosstalk with TiO<sub>2</sub> NPs suggest the role of underlying cellular machinery in inducing allergic airway inflammation.

Some previous studies revealed that workers exposed to TiO<sub>2</sub> NPs powder by inhalation route are more susceptible to hazard risks of pulmonary diseases.

In 2017, the European Chemicals Agency (ECHA) Committee for Risk Assessment (RAC) concluded to classify TiO<sub>2</sub> as a substance suspected of causing cancer through the inhalation route. The RAC classification was made based on the hazardous characteristics of this substance. Regarding this and concerning the growing trend in the production and application of TiO<sub>2</sub> NPs, there is a rising demand for identifying the consequences of TiO<sub>2</sub> NP exposure, especially with respect to allergic and inflammatory aspects.

Therefore, the objective of our first study was to characterize TiO<sub>2</sub> NPs and investigate their effects on lung tissue morphology, non-pulmonary tissue uptake, *in vivo* modulation of allergic pulmonary inflammation, and immune response. It was hypothesized that the inhalation of TiO<sub>2</sub> NPs would have hazardous effects and might aggravate OVA-induced allergic airway inflammation.

The production of engineered CNTs has been rapidly increasing in commercial and industrial applications, including oncology therapy, biomedicine, optics, computer industries as well as in electronics. Therefore, we aimed in this *in vitro* study to assess the biological effects of industrial carbon nanotubes of different morphologies (SWCNTs, DWCNTs, and MWCNTs) on A549, a human cell cultures originating from pulmonary system. Experiments were carried out using A549 cell line since they are the most utilized cell line to study interactions of allergens with alveolar epithelium [35].

The release of the pro-inflammatory mediator IL-8 in human lung cells was investigated at different concentrations and different time points. Moreover, the cytotoxicity parameters after exposure to nanomaterials were evaluated. ESEM was employed to characterize the CNTs, to show the CNT–A549 cell interaction, and the modifications in the cellular surface after exposure to CNTs.

## 5. Materials and Methods

### 5.1 Titanium dioxide nanoparticles and their physicochemical characteristics

TiO<sub>2</sub> NPs (AEROXIDE® P25; Sigma Aldrich, Saint Louis, MO) with the primary particle size of 21 nm were used. Particles were measured by dynamic light scattering (DLS) on a Wyatt DynaPro Plate-Reader II (Wyatt Technology Europe GmbH, Dernbach, Germany) and a Malvern Zetasizer Nano-ZSP (Malvern Instruments GmbH, Herrenberg, Germany) in 96 well plates at room temperature. Samples were irradiated with a laser (semiconductor laser,  $\lambda = 830$  nm (Wyatt) or a HeNe laser,  $\lambda = 632.8$  nm (Malvern)), and the intensity fluctuations of the scattered light (detected at a backscattering angle of 156° (Wyatt) or 173° (Malvern)) were analyzed to obtain the autocorrelation function. The device software (Wyatt: DYNAMICS 7.1.9 or Malvern: Zetasizer Software 7.11) outputted the mean particle size using cumulant analysis and a size distribution using a regularization scheme by intensity or number. The mean hydrodynamic diameter is expressed as the log-normal distribution for the intensity or number density, and the dispersity  $p$  was calculated with the formula  $p = \frac{\sigma}{\mu}$ , where  $\mu$  = mean and  $\sigma$  = standard deviation.

The following assumptions were made: the suspension viscosity was assumed to be that of water, corrected for temperature, the suspension refractive index was that of water ( $n = 1.33$ ), and the calculated refractive index of the NPs was used ( $n = 2.4900$  with absorption of 0.01).

NPs were then characterized by transmission electron microscopy (TEM). TEM is a microscopy imaging technique generally uses a beam of electrons which can be transmitted over a specimen to create an image. TEM has many applications in the field of nanotechnology, cancer, semiconductor research, virology, and pollution as well as materials science.

Moreover, this assay was chosen to analyze the shape of our TiO<sub>2</sub> NPs. Nanoparticle suspensions were dried at room temperature on pioloform TEM grids and analyzed with a Tecnai 12 FEI Biotwin TEM setup (**Figure 4**).

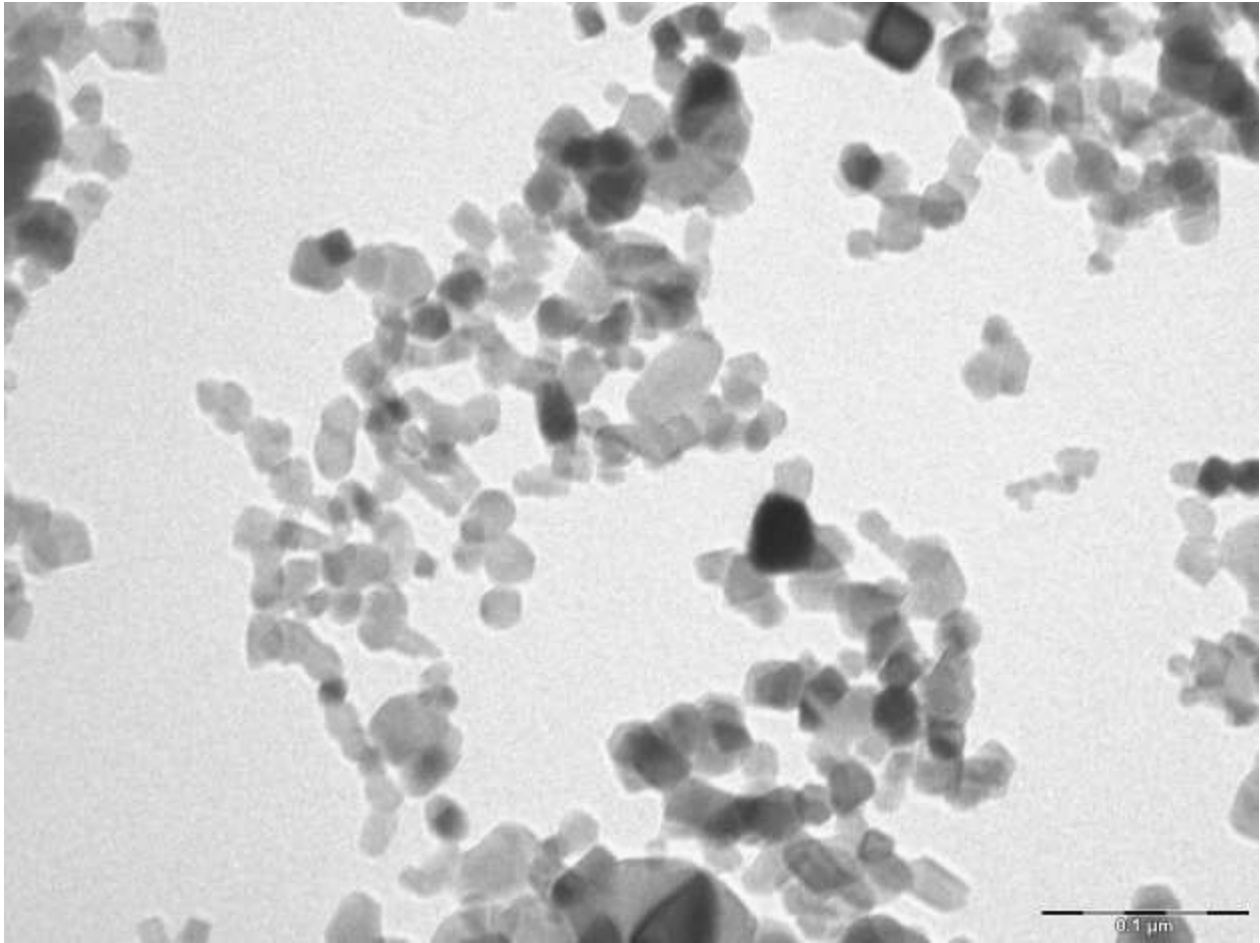


**Figure 4** TEM image of TiO<sub>2</sub> NPs. Nanoparticles had a core diameter of approximately 21 nm. TEM measurement revealed that the majority of TiO<sub>2</sub> particles were spherical and tended to associate to create relatively soft bonded agglomerates (Harfoush et al., 2020).

## 5.2 Experimental design

Nine-week-old female wild-type BALB/c-mice were obtained from Janvier Labs (Le Genest-Saint-Isle, France) and kept in a 12 h dark/light cycle at 22°C with laboratory food and tap water ad libitum. Mice were acclimatized for two weeks prior to starting the study. All animal experiments were performed in strict accordance with German animal protection laws with approval from the appropriate governmental authority (01-2014 Saarland). All experimental procedures were

approved and performed following the ethical regulations and the animal welfare protocols of state of Saarland.

In OVA mouse model, BALB/c mice were intraperitoneally sensitized to OVA (i.e., an allergen), along with aluminum hydroxide-adsorbed OVA (2 mg Al(OH)<sub>3</sub> with 20 µg OVA). On the other hand, the control animals received on days 0 and 7 only phosphate-buffered saline (PBS). Afterwards, OVA challenges were performed on days 17, 18, 19, and 20 via the intranasal route (**Figure 5**). In order to prepare the NPs, the treated TiO<sub>2</sub> NPs were dispersed in Milli-Q water, and the suspensions were ultrasonicated for 15 min to keep the maximum dispersed state. In the NPs groups, each of the BALB/c mice was treated intranasally with 25 µl TiO<sub>2</sub> NPs suspension (50 mg/mL) 1 h post-OVA-exposure on days 17 and 20 (**Figure 5**).

Day 21 was the final study endpoint. Before, sacrificing the mice, they were weighed and prepared for lung function testing. Subsequently, some organs and the bronchoalveolar lavage fluid (BALF) were isolated for the implementation of different further experiments. The three untreated groups (i.e., PBS/PBS, OVA/PBS, and OVA/OVA) consisted of 5 mice in each group (n=5). The three treated groups (i.e., PBS/TiO<sub>2</sub>/PBS, OVA/TiO<sub>2</sub>/PBS, and OVA/TiO<sub>2</sub>/OVA) had 10 mice in each group (n=10).

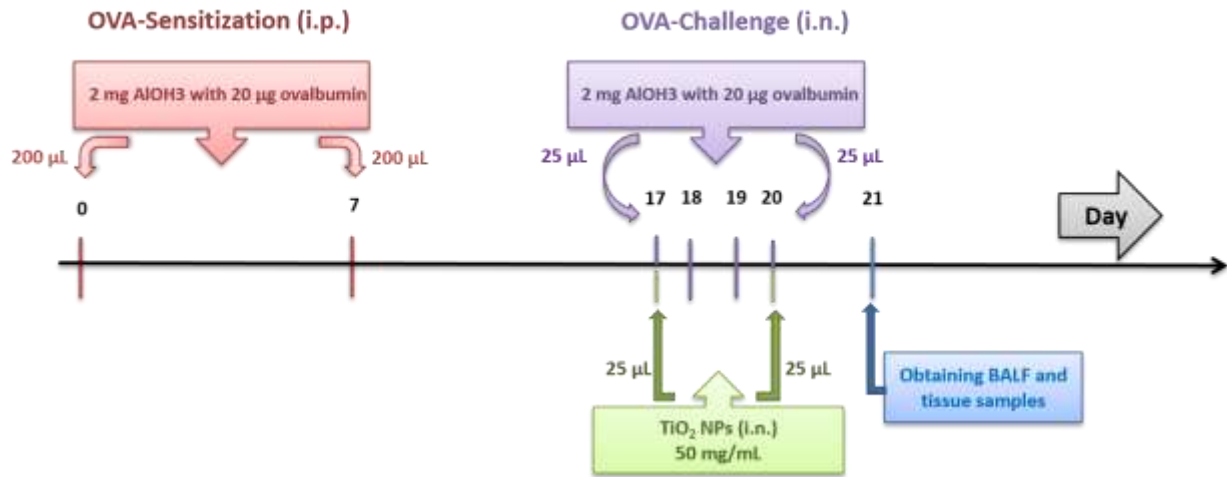


**Figure 5** OVA-sensitization and challenge in the mice. Mice in the control groups received on days 0 and 7 an intraperitoneal injection of 200 µl PBS or aluminum hydroxide-adsorbed ovalbumin (OVA; 2 mg Al(OH)<sub>3</sub> with 20 µg OVA). Moreover, the mice received intranasally 25 µl OVA for OVA challenge on days 17, 18, 19, and 20. In the nanoparticles groups, each of the BALB/c mice was exposed intranasally on days 17 and 20 to 25 µl TiO<sub>2</sub> NPs suspension (50 mg/mL) 1h post OVA exposure. Day 21 was the final study endpoint. In addition, airway resistance measurements were monitored in terms of methacholine-induced specific airway resistance. The BALF was collected for cell counting, and tissue samples were isolated for histologic analysis (Harfoush et al., 2020).

### 5.3 Lung function measurements

The lung function analysis serves to evaluate the presence and the grade of severity of bronchial hyperreactivity. It was already established and performed in our lab and represents a non-invasive measurement with conscious animals. Specific airway resistance (sRaw) was performed in a double-chamber head-out plethysmograph (DSI Buxco FinePointe NAM, MN, USA). Methacholine (MCh) was applied in increasing doses (0 mg/mL, 12.5 mg/mL, 25 mg/mL, and 50 mg/mL) via an aerosol nebulizer. After inserting the mice in the device, they were granted an acclimation period of 5 minutes to calm down. The aerosol volume was amounted to 0.02 ml and was applied in the delivery duration of 1 minute. The different concentrations of MCh were applied

within an interval of 6 minutes, including 3 minutes response time and 3 min for recovery period  
**(Figure 6).**

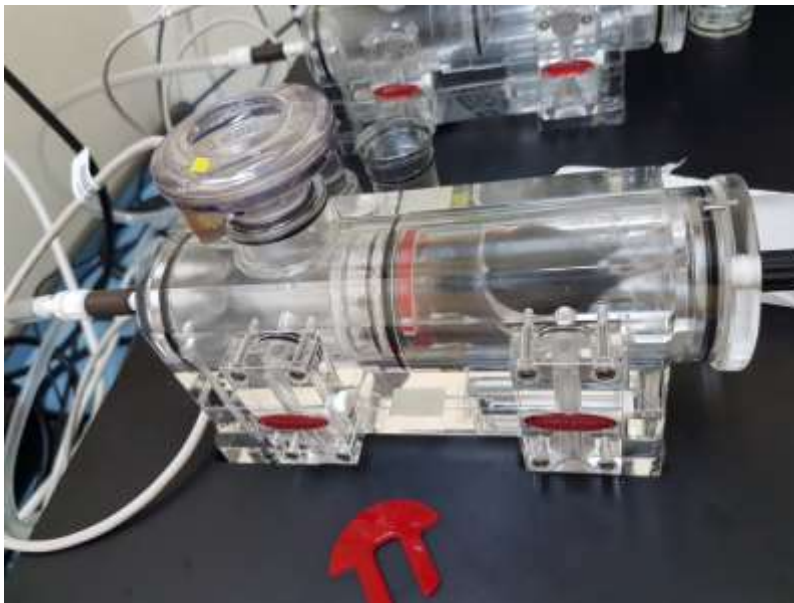


**Figure 6** In our lung function laboratory; NAM is Noninvasive Airway Mechanics also known as Double Chamber Plethysmography. This system allows the independent measurement of nasal and thoracic flows. When the mouse inhales, it draws air from the nasal chamber into the lungs. As the air moves into the lungs, the chest expands and forces the same volume of air out of the thoracic chamber. The phase difference between both flows is a measure of bronchoconstriction and called specific airway resistance (sRaw).

## **5.4 Tissue sampling and ICP-MS measurements**

BALB/c-mice were sacrificed by bleeding after the implementation of airway resistance measurements. Their organs were removed, the lungs were subjected to histological analysis, and bronchoalveolar lavage fluid (BALF) was conducted for cell counts.

Inductively coupled plasma mass spectrometry (ICP-MS) is an element analysis technique used for elemental determinations. It is widely used in the medical field, specifically, in toxicology. Relying on its unique properties, ICP-MS is a common method of testing patient's sample such as urine, blood, plasma, serum and even red blood cells.

ICP-MS was used in our project for titanium ( $^{47}\text{Ti}$ ) screening. Portions of the main organs were cut, weighed, and dissolved in 5 mL concentrated ultrapure  $\text{HNO}_3$  followed by addition of a 4% (v/v) solution of ultrapure  $\text{HCl}$  to a final volume of 10 ml. After a few days at room temperature, the samples were dissolved and analyzed using an Agilent 7500cx (Agilent Technologies, Santa Clara, CA). Scandium ( $^{45}\text{Sc}$ ) was used as an internal standard.

## **5.5 Staining and histological analysis**

It is known that most cells are transparent, therefore, stains are required to make the cells and structures more easily visible and assess lung histopathology and airway inflammation. Lung cryosections (10  $\mu\text{m}$ ) were first produced with a cryostat (CM1950, Leica, Germany). Then these sections were stained with Hematoxylin and eosin (H&E) and periodic acid Schiff (PAS).

H&E staining method is a common technique in histology. It is widely used in various medical diagnoses and for recognizing tissues by highlighting their structures. H&E stain is a combination of two dyes, hematoxylin and eosin. Eosin reacts as an acidic dye: it stains basic (or acidophilic) structures with red, pink and orange. Thus, the cytoplasm and cell walls are stained pink, by H&E

staining. Haematoxylin is a basic dye, used to stain acidic (or basophilic) structures, including the cell nucleus and organelles with purplish blue.

H&E staining protocol summary:

- Dry sections for 20 min at room temperature
- Place in Hematoxylin 3 min
- Rinse with deionized water
- Rinse hematoxylin residues with warm tap water
- Rinse again with deionized water
- Stain with eosin for 10 sec
- Dehydrate sections with:
  - 75% ethanol 1min
  - 85% ethanol 1min
  - 99% ethanol 1min
- Clear with xylene for 3 min
- Mount coverslip onto glass slides with Entellan (Merck)

Periodic acid–Schiff (PAS) is a staining method for detecting polysaccharides like glycogen, and also mucosubstances including glycolipids, glycoproteins, and mucins in different cells and tissues.

PAS staining protocol summary:

- Dry sections for 15 min at room temperature
- Dehydrate them in 1x PBS solution (pH 7,4) for 5 min
- Oxidize in 0.1% periodic acid solution for 1 min
- Rinse with warm tap water
- Rinse with deionized water
- Place in Schiff's solution (ROTH) for 20 min

- Rinse with sulfite water 3 x 2 min
- Rinse with deionized water
- Stain with Hematoxylin for 6 min
- Rinse with deionized water
- Rinse with ammonia water
- Dehydrate sections with:
  - 75% ethanol 1min
  - 85% ethanol 1min
  - 99% ethanol 1min
  - Clear with xylene for 3 min
  - Mount coverslip onto glass slides with Entellan (Merck)

Next, sections were examined with a Zeiss Axio Imager.M2 microscope (Carl Zeiss AG, Oberkochen, Germany), and the number of goblet cells in the airways was counted manually after PAS staining under the same light microscope.

Immunofluorescence staining (IF) was performed with the Shandon Sequenza system (Thermo Scientific, MA, USA). Lung sections of every mouse were dried at room temperature for 15 min. To reduce nonspecific cross reactions, sections were blocked with 5% donkey serum diluted in PBS. Afterwards, the previous sections were incubated for 1 h at room temperature with the primary antibody (diluted in 5% donkey serum). The incubation was continued overnight at 4°C. Immunolabeling was performed using primary antibodies; (i.e., antimouse F4/80 [eBioscience, San Diego, CA], antimouse Ly6G [Abcam, Cambridge, UK], antimouse Siglec-F [eBioscience, San Diego, CA], and antimouse CD3ε [Biolegend, San Diego, CA]).

On the second day, sections were rinsed twice with PBS and then incubated with secondary fluorescein-conjugated antibodies (i.e., donkey antirabbit IgG cyanine Cy3, donkey antirat IgG

Cy5, and goat anti-Armenian hamster IgG Cy3) for 2 h at room temperature. All secondary antibodies were obtained all from Jackson Immunoresearch, West Grove, PA. The cryosections were counterstained with 80  $\mu$ L 4, 6-diamidino-2-phenylindole (DAPI; 0.5  $\mu$ g mL<sup>-1</sup>, Carl Roth, Karlsruhe, Germany) for 15 min, washed several times with PBS and once with double-distilled water, and mounted with Fluoroshield<sup>TM</sup> fluorescence mounting medium (Sigma-Aldrich, St Louis, MI). Finally, fluorescence microscopy was performed by means of the Zeiss Axio Imager M2 microscope (Carl Zeiss AG) (**Table 2**).

**Table 2** Primary antibodies used in this study.

Primary antibodies	Dilution	Supplier
Rabbit antibody against mouse, F4/80	1:150	eBioscience, San Diego, CA
Rat antibody against mouse, Siglec-F	1:200	eBioscience, San Diego, CA
Rat antibody against mouse, Ly6G	1:400	Abcam, Cambridge, UK
Armenian hamster antibody against mouse, CD3 $\epsilon$	1:100	Biologend, San Diego, CA

**Table 3** Secondary antibodies used in this study.

Secondary antibodies	Dilution	Supplier
Cy3 conjugated donkey anti-rabbit IgG	1:300	Jackson Immunoresearch, West Grove, PA
Cy5 conjugated donkey anti-rat IgG	1:200	Jackson Immunoresearch, West Grove, PA
Cy3 goat anti-Armenian hamster	1:200	Jackson Immunoresearch, West Grove, PA

## 5.6 BALF collection

Bronchoalveolar lavage fluid (BALF) is a useful tool in animal laboratory in which a bronchoscope can pass deeply into the lungs to recollect the fluid for various examinations. BAL is considered as the most common method used to sample the compositions of the epithelial lining fluid and to analyze the cells as well as the protein components of the respiratory airways.

For the collection of BALF, the trachea was exposed by a midline incision in the neck, and 1 ml of ice-cold PBS (pH 7.4) containing protease inhibitors [36][37] was injected into the lungs through the trachea and withdrawn after 10 s. Afterwards, the recovered fluid was centrifuged at 1200 rpm for 10 min at 4°C, the supernatants were separated, and the cell pellets were resuspended in 0.5 mL PBS.

In the following stages, the total cell count was determined, the cells were enumerated by means of a Neubauer cell counting chamber Casy®. Next, 100µl of BAL fluid from each mouse was taken for cytospot preparation by using cytopsin (Tharmacspin).

Cytospot-slides were prepared and stained with Diff-Quick (Medion Diagnostics AG) staining solution for differential cell counts evaluation.

"Diff-Quick" is a modification of a Romanowski stain, consists of eosin dye and thiazine dyes that combined Methylene Blue and Azure A. In this study, it was used to discriminate and count immune cells like macrophages, neutrophils, eosinophils and lymphocytes in BALF.

Procedure:

- Dry sections for 15 min at room temperature
- Dip slides into Stain 1. for 45 sec
- Dip slides into Stain 2. for 45 sec
- Rinse slides in distilled water
- Mount coverslip onto glass slides with Entellan (Merck)

After the staining, cell counts were evaluated depending on their morphological characteristics using our light microscope.

## **5.7 ELISA assay**

ELISA (enzyme-linked immunosorbent assay) is a plate-based analytical assay used in both experimental and diagnostic fields and designed to detect and quantify different substances including proteins, antibodies, hormones and peptides.

At the end of the treatment, mice were sacrificed and blood samples were collected. The blood was centrifuged and obtained sera were stored at  $-80^{\circ}\text{C}$  until analysis.

Serum concentrations of total immunoglobulin (Ig)E were measured using the commercially available enzyme-linked immunosorbent assay (ELISA) kits (885046022, Invitrogen, Vienna, Austria). In order to determine the protein level in the homogenates, a Pierce BCA protein assay (23227, ThermoFisher Science, Germany) was performed on the homogenized snap-frozen lungs. After adjusting the protein level in each sample, we conducted ELISA to analyze the cytokine levels of IL-4 (DY404-05, R&D Systems Inc., USA), IL-5 (DY405-05, R&D Systems Inc., USA), IL-13 (DY413-05, R&D Systems Inc., USA), and interferon-gamma (IFN- $\gamma$ ) (DY485-05, R&D Systems Inc., USA) according to the manufacturer's protocol.

## **5.8 Investigation of NP phagocytosis**

Macrophages are cells of the innate immune system. They have a defensive function that gives them the ability to phagocytose bacteria, pathogens and other foreign agents [38].

The phagocytic ability of primary murine macrophages was analyzed *in vitro*. Alveolar macrophages were isolated from the BALF of control BALB/c mice (without OVA neither TiO<sub>2</sub> NPs). Subsequently, the samples were grown as adherent cultures in RPMI 1640 medium containing 10% FBS and 1% penicillin/streptomycin in eight-chamber culture dishes at  $37^{\circ}\text{C}$ . The macrophages were then treated with 0.0125, 0.025, and 1 mg/mL freshly prepared TiO<sub>2</sub> NP dispersions for 1, 2, 4, 8, and 24 h. Afterwards, they were fixed with ice-cold acetone and stained

with DAPI. Many images were randomly generated by using an epifluorescence microscope (Zeiss Axio Imager M2).

## **5.9 SEM and energy-dispersive X-ray spectroscopy (SEM-EDX)**

A scanning electron microscope (SEM) is a type of electron microscope that creates an image of a sample by scanning the surface with a focused beam of electrons. The electrons in the beam interact with the sample, generating different signals that can be employed to get information about the external morphology, surface composition and topography.

The sections isolated from the heart, lung, brain, stomach, kidney, spleen, and liver were scanned for TiO<sub>2</sub> NPs via SEM-EDX electron microscope (FEI/Philips XL 30 FEG ESEM; Eindhoven, NL). In addition, the macrophages in the BALF samples were first stained with Diff-Quick and then scanned for NPs by using the same previous microscope. The tissues, fixed in 2.5% glutardialdehyde and dehydrated in an ascending series of ethanol, dried in 1,1,1,3,3,3-hexamethyldisilazane (Sigma-Aldrich; Taufkirchen, Germany), and coated with carbon, were also evaluated with this setup.

## 5.10 Carbon nanotubes source and properties

Carbon nanotubes (CNTs), also called buckytube, nanoscale tubes made of carbon with diameters measured in nanometers. The unique of their nanostructure, the concomitant properties and strength of the bonds between carbon atoms endow carbon nanotubes with special natures, rendering them with unlimited nanotechnology-associated applications [42].

Carbon-based nanomaterials like graphene and carbon nanotubes, and its derivatives, fullerenes, nano-diamond, and other types of nanosized carbon materials have recently attracted a high degree of attention among the research community because of their enormous potential for a huge number of applications arising from their high thermal and electrical and conductivity, good mechanical properties, and large specific surface area [43].

In our study three different types of carbon nanotubes were used: single walled carbon nanotubes (SWCNTs,  $D \times L$ : 4-5 nm  $\times$  0.5-1.5  $\mu$ m, Sigma Aldrich, Saint Louis, MO), double walled carbon nanotubes (DWCNTs, O.D.  $\times$  I.D.  $\times$  L: 5 nm  $\times$  1.3-2.0 nm  $\times$  50  $\mu$ m Sigma Aldrich, Saint Louis, MO), and multi walled carbon nanotubes (MWCNTs,  $D \times L$ : 2.5-3 nm  $\times$  2-6  $\mu$ m Sigma Aldrich, Saint Louis, MO).

## 5.11 Micrograph of carbon nanotubes

Carbon nanotubes powder (SWCNTs, DWCNTs, and MWCNTs) were poured onto SEM sample-stubs and carbon-tabs, and then coated with coal. Microphotograph and characterization of carbon nanotube materials were performed by using scanning electron microscopy (ThermoFisher XL 30 FEG ESEM; Eindhoven).

## 5.12 Cell culture and exposure

A549 cells a human lung carcinoma epithelial cell line were employed for testing, which is a widely used and well-characterized cell cultured line (table 4). A549 cells were cultured in RPMI 1640 medium supplemented with 10% fetal calf serum and 1% penicillin/streptomycin. The culture was maintained at 37 °C in a humidified atmosphere of 5% CO<sub>2</sub>. For experimental use the cells were grown to confluence in different dishes or wells as indicated in the individual experiments. Unexposed cells were used as controls.

**Table 4** Identification of A549 cells used in our study

General Information	Characteristics
Organism	human
Tissue	lung
Cell Type	epithelial
Format	frozen
Morphology	epithelial-like
Culture Properties	adherent
Applications	This cell line is a suitable transfection host.
Storage Conditions	liquid nitrogen vapor phase
Disease	Carcinoma
Source	Prof. Dieter Gruenert Lab, Institute of human genetics, University of California, San Francisco

## 5.13 Measurement of interleukin 8 (IL-8) production

A549 cells were first seeded into 24-well cell culture plates at a density of  $5 \times 10^5$  cells/well. After seeding, the cells were treated with the three different types of CNTs (SWCNTs, DWCNTs, and

MWCNTs) at 0.3, 3, and 30  $\mu\text{g/mL}$  for 2, 4 and 6 h. The supernatants prepared were assayed for IL-8 content using a commercially available human IL-8 ELISA kit (Human IL-8/CXCL8, DuoSet ELISA DY208, R&D Systems Inc., USA), according to the manufacturer's instructions. A standard calibration curve was established for the kit, and the unit of IL-8 measurement was picograms/milliliter ( $\text{pg/mL}$ ).

#### **5.14 Cytotoxicity determination**

Cell toxicity produced by CNTs was measured by lactate dehydrogenase (LDH) assay. A549 cells were treated with different types of CNTs at (0.3, 3, 30, and 300 $\mu\text{g/mL}$ ) for 4, 6, and 24 h. LDH content was determined using a colorimetric method and assessed by a cytotoxicity assay Kit (Abcam, ab65393, Germany) according to the manufacturer's instructions. The optical density of the samples was determined using a microplate reader set to 450 nm. The activity of the released LDH was reported to that of control cells (not exposed to CNTs). A positive control consisted of the cellular LDH released after cells lysis.

#### **5.15 Sample preparation and fixation for scanning electron microscopy (SEM) analysis**

Approximately  $7 \times 10^4$  A549 cells were plated and grown on coverslips for 24 h. Then they were exposed to SWCNTs, DWCNTs, and MWCNTs at 3  $\mu\text{g/mL}$  in culture media RPMI 1640 (Gibco, Paisley, UK) for 4 h. Unexposed cells were used as negative controls. After incubation time, control and treated cells were fixed with 2 % glutaraldehyde solution (in 0.1 M cacodylate buffer, PH= 7.4 at room temperature), rinsed 4 times with cacodylate buffer for 10 min, and post-fixed in 2% osmium tetroxide (1: 1 with 0.2 M cacodylate buffer) for 1 h. Fixation was followed by five times rinsing with distilled  $\text{H}_2\text{O}$  for 10 min, the samples were then dehydrated through graded ethanol

series (10%, 20%, 30%, 40%, 50%, 60%, 70%, 80%, 90%, 100%) for 3 min each. 100% ethanol: HMDS (mixture 1:1) (1,1,1,3,3,3-hexamethyldisilazane, Sigma-Aldrich GmbH, Taufkirchen, Germany). Afterwards, samples were dried under the hood. When the drying process was completed, the test specimens Leit-Tabs (Plano GmbH, Wetzlar) were mounted on aluminum sample stubs (Specimen Stubs, Agar Scientific Ltd, Essex, England) and coated with coal vaporization (Balzers SCD 030, Lichtenstein). The subsequent investigations were performed by using scanning electron microscope (FEI / Philips XL 30 ESEM FEG, Hillsboro), magnifications up to 50,000 times and each individual characteristic areas was digital photographic captured and recorded.

### **5.16 Statistical analysis**

The data were presented as mean  $\pm$  SEM. Statistical analyses were carried out in GraphPad Prism 5.02 (GraphPad Software, Inc., La Jolla, CA). Significance was assessed by one-way ANOVA followed by Tukey's test (comparing all pairs of columns). A p-value less than 0.05 was considered statistically significant.

Asterisks indicate significance at p-values <0.05 (\*), <0.01 (\*\*), and <0.001 (\*\*\*)).

## 6. Results

### 6.1 Characterization of titanium dioxide nanoparticle

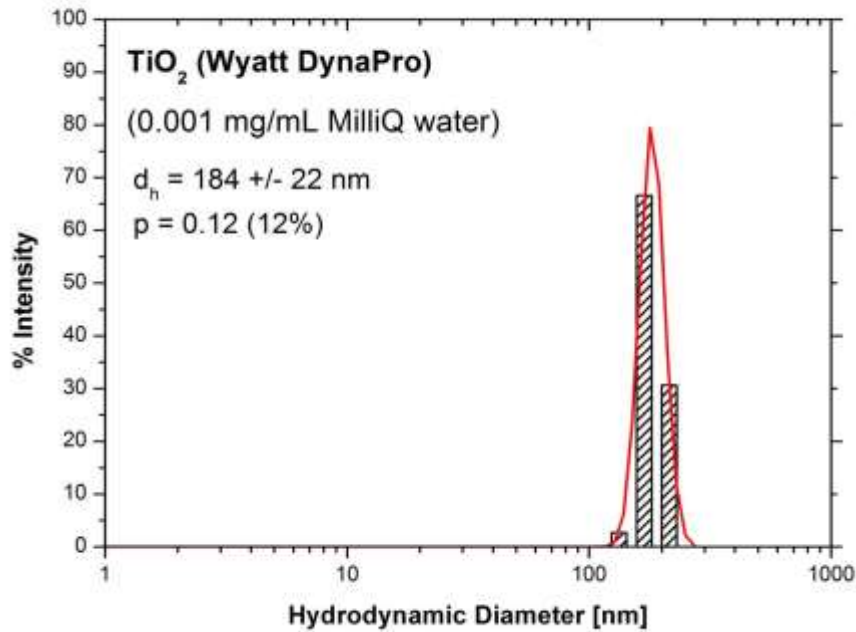
TiO<sub>2</sub> NPs used in our current study had a diameter size of 21 nm. The size and also the distribution of NPs in pure water were determined by DLS. The physicochemical characterizations of TiO<sub>2</sub> NPs are presented in (Table 5).

**Table 5** The physicochemical characterizations of titanium dioxide NPs (Harfoush et al., 2020).

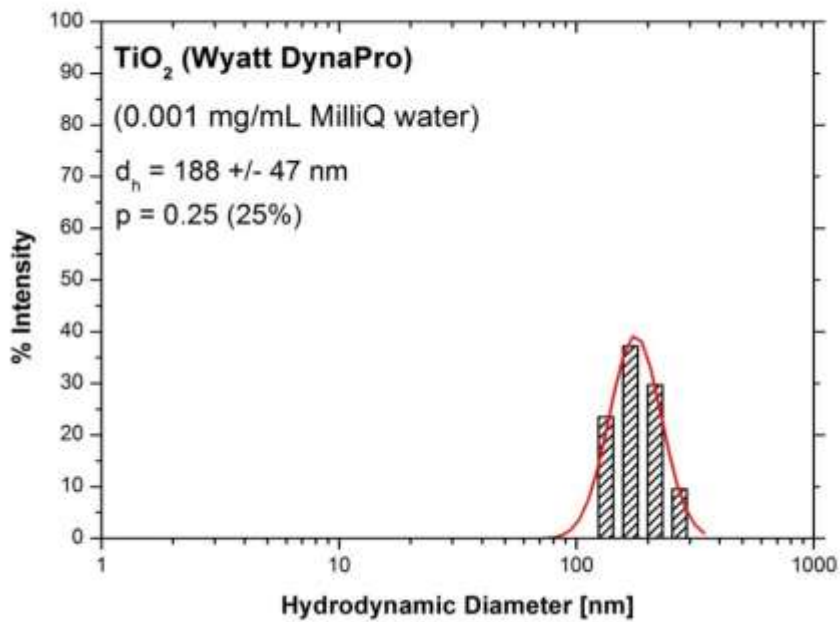
Property	TiO <sub>2</sub>
Crystalline structure	Mixture of anatase and rutile with predominantly anatase
Primary particle size	21 nm
Hydrodynamic diameter	185 ± 18 nm
Form	Nanopowder
Surface area	35-65 m <sup>2</sup> /g
Density	4.26 g/mL at 25 °C

The DLS analysis demonstrated the monomodal size distribution of both fresh and two-hour-old samples with a mean hydrodynamic diameter of around 185±18 nm. The dispersity of the freshly prepared sample (12%; **Figure 7A**) was about half of that of the two-hour-old sample (25%; **Figure 7B**), suggesting that the NPs start to aggregate/agglomerate and the particle suspension becomes unstable over time

(A)



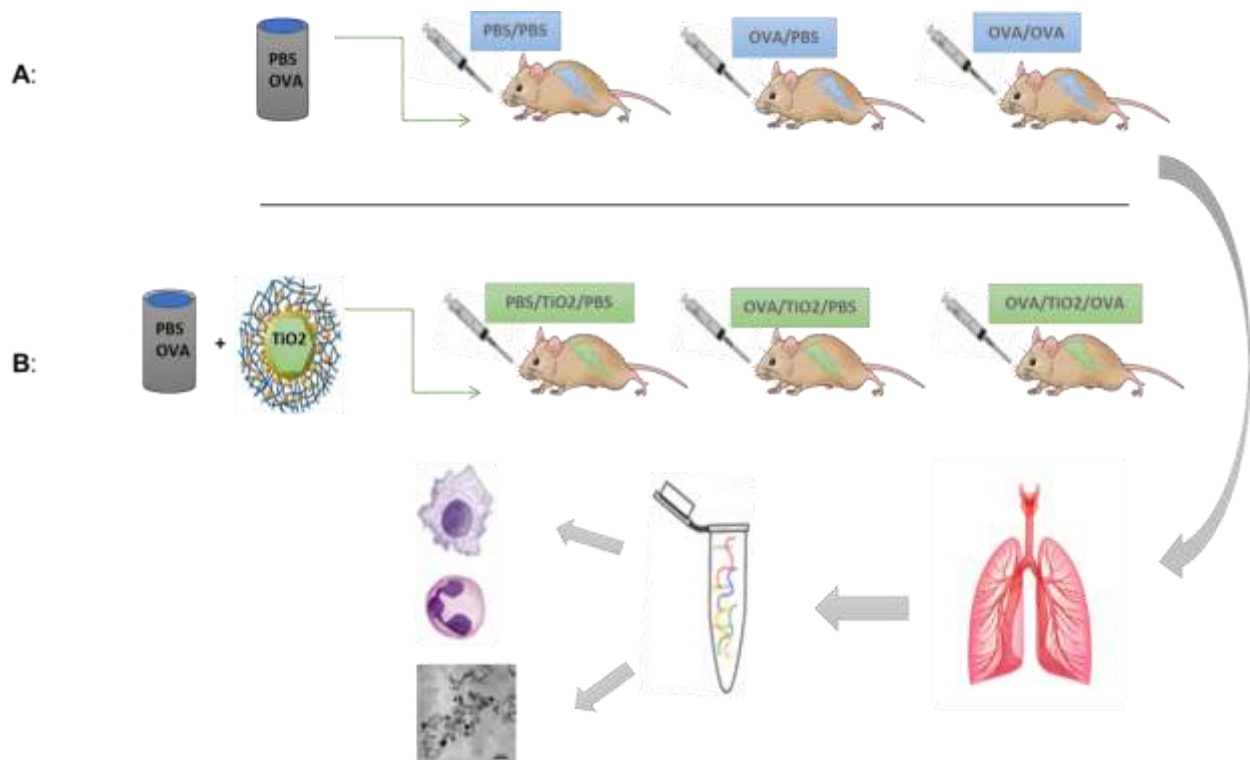
(B)



**Figure 7** Dynamic light (DLS) measurements of TiO<sub>2</sub> NPs suspensions with the maximum measurable concentration (0.001 mg/mL) using the intensity distribution. A comparison was performed between a freshly prepared suspension [A] and a suspension prepared 2 hours prior to the measurement [B]. Both samples [A & B] indicated a monomodal size distribution with a mean hydrodynamic diameter of around 185 nm and dispersity of 12% and 25%, respectively (Harfoush et al., 2020).

## **6.2 Inhaled exposure to titanium particles induces further airways inflammation in asthmatic mice**

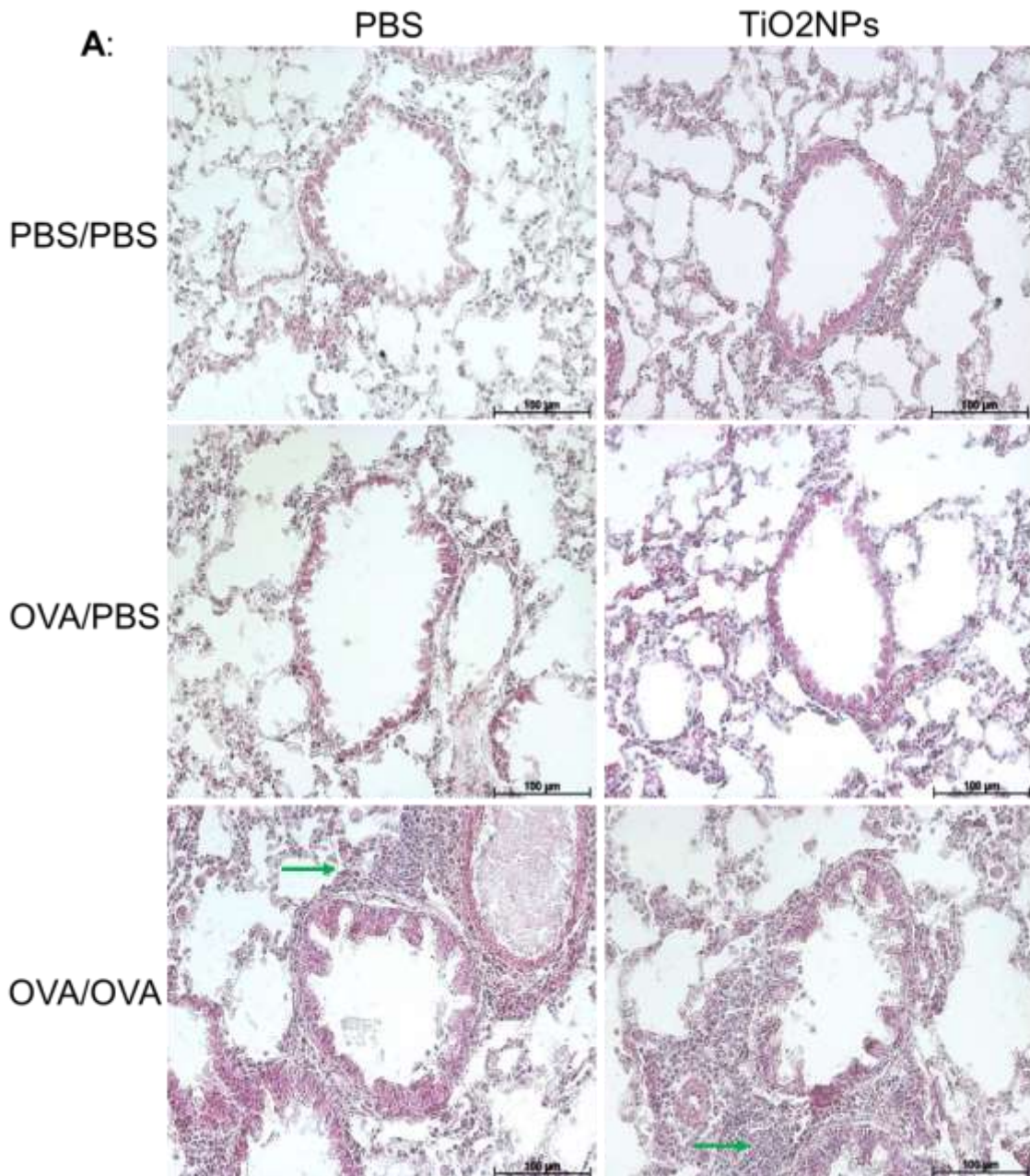
The effect of intranasal application of NPs was compared between the non-asthmatic and asthmatic experimental groups. The PBS/PBS and OVA/PBS groups with intraperitoneal OVA sensitization and only PBS challenge, serving as the control groups, showed no allergic airway reaction. On the other hand, the mice in the OVA/OVA groups receiving both intraperitoneal OVA sensitization and challenge, defining the asthma status, developed an asthmatic reaction (**Figure 8A**). In the second section (**Figure 8B**), the mice without or with induced airway inflammation reaction were intranasally administered with TiO<sub>2</sub> NPs and defined as PBS/TiO<sub>2</sub>/PBS, OVA/TiO<sub>2</sub>/PBS, and OVA/TiO<sub>2</sub>/OVA.

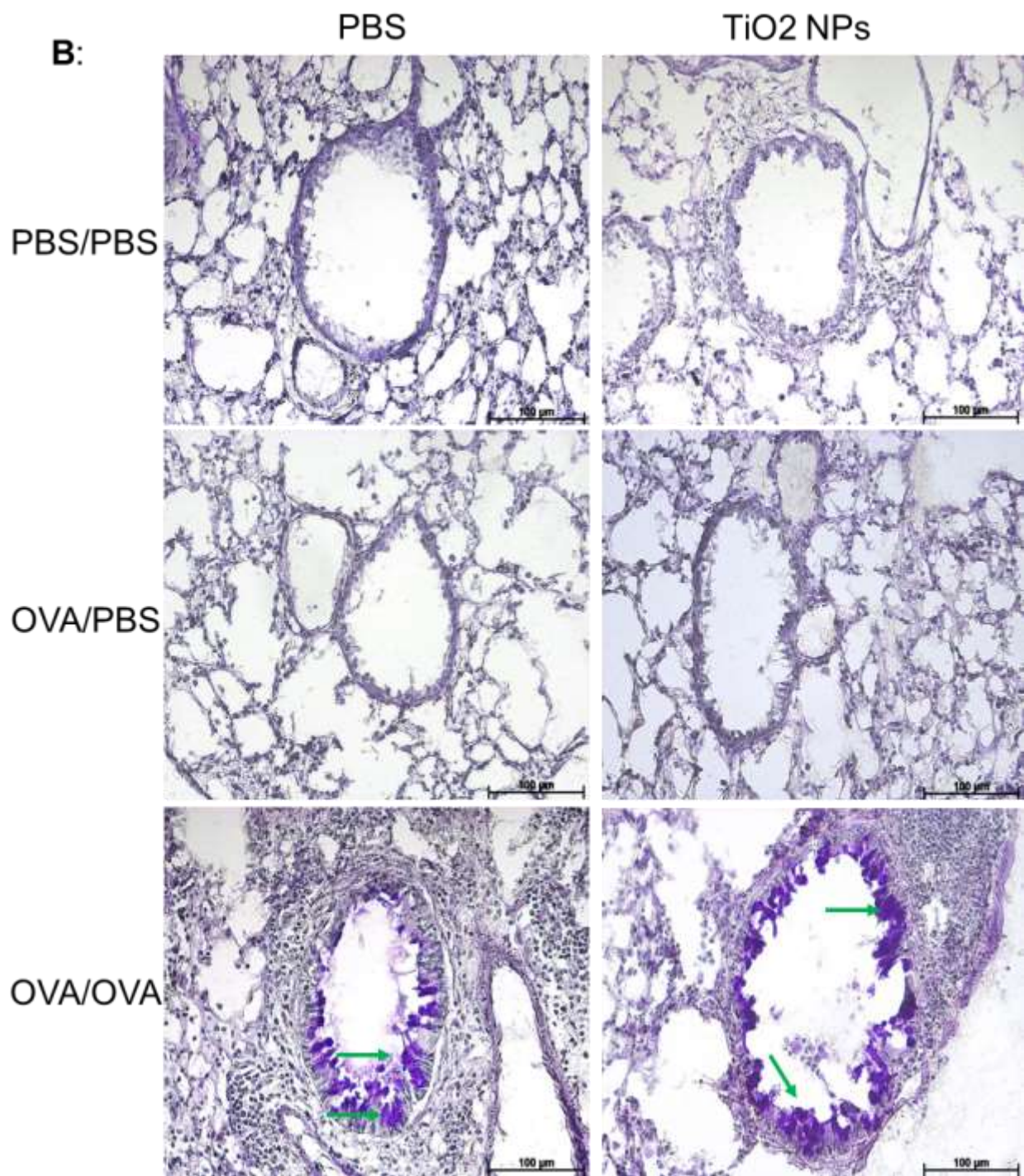


**Figure 8** Investigation of BALB/c female (9-week-old) mice in six test groups. Mice in the PBS/PBS group were neither sensitized nor challenged and therefore had no asthma [A]. However, those in the OVA/PBS group were sensitized to OVA but not challenged and therefore had no asthma [A]. The first two categories together define the non-asthmatic or control status. Mice in the third group with OVA/OVA were both sensitized and challenged with OVA and therefore had asthmatic reactions [A]. In [B], we applied TiO<sub>2</sub> NPs in combination with the previous treatment to the mice. Three new groups receiving NPs were defined as PBS/TiO<sub>2</sub>/PBS, OVA/TiO<sub>2</sub>/PBS, and OVA/TiO<sub>2</sub>/OVA [B]. Each of the first three groups consisted of 5 mice. Each of the second three groups was composed of 10 mice (Harfoush et al., 2020).

The H&E-stained lung sections obtained from the asthmatic mice (i.e., OVA/OVA) presented a large increase in the inflammatory cells and eosinophilic infiltration, compared to those in the control groups (**Figure 9A**). Moreover, these mice demonstrated a goblet cell hyperplasia and hypersecretion of mucus in the PAS-stained sections, compared to the controls (**Figure 9B, C**). In contrast, the non-asthmatic mice (i.e., PBS/PBS and OVA/PBS) had clear airways and less mucus in the respective lung sections (**Figure 9B, C**).

In half of the mice groups, TiO<sub>2</sub> NPs were administered in parallel with PBS or OVA. Administration of TiO<sub>2</sub> to the control groups (i.e., PBS/TiO<sub>2</sub>/PBS and OVA/TiO<sub>2</sub>/PBS) did not cause any remarkable inflammatory changes, compared to the non-treated groups. However, treatment with TiO<sub>2</sub> NPs in the OVA-challenged mice which had allergic airway inflammation (i.e. OVA/TiO<sub>2</sub>/OVA) further increased goblet cell counts, eosinophilic infiltration, and mucus production, compared to those in the untreated group asthma (i.e., OVA/OVA; **Figure 9A-C**).





**C: Number of goblet cells (PAS)**

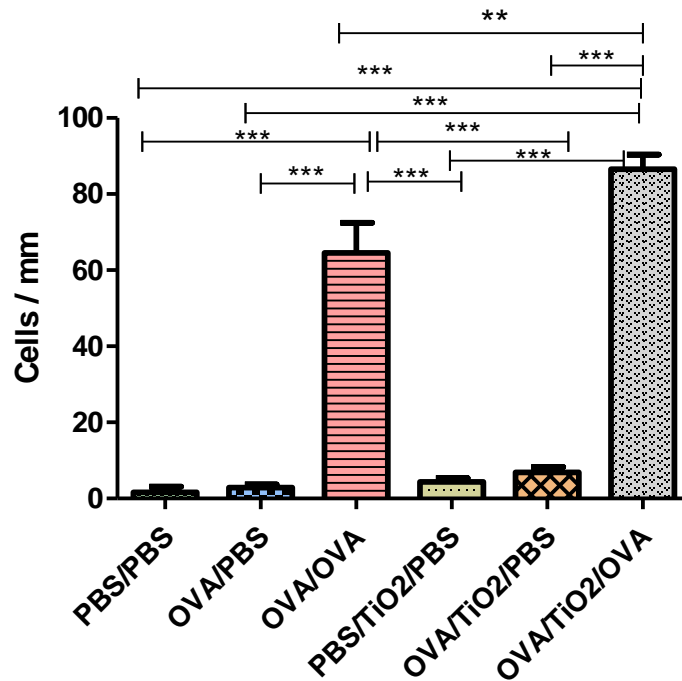


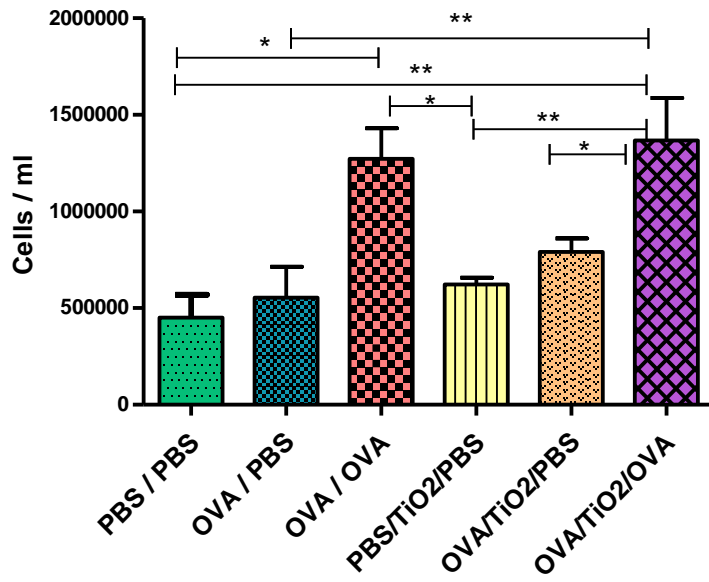
**Figure 9** Histological analysis of lung tissue; **A**) Representative photomicrographs of fixed lung sections stained with hematoxylin and eosin (H&E). Aggregations of inflammatory cells (arrow) were observed in the OVA-sensitized and -challenged mice (OVA/OVA) but not in the controls (PBS/PBS and OVA/PBS). However, the lungs of the OVA/OVA mice treated with TiO<sub>2</sub> NPs exhibited more inflammatory cells aggregates. **B**) Representative photomicrographs of fixed lung sections stained with periodic acid Schiff (PAS); Lung tissue sections showed goblet cell hyperplasia and increased mucus secretion (arrow) in the OVA/OVA and OVA/TiO<sub>2</sub>/OVA mice, compared to those in the controls, **C**) Quantification of goblet cell in PAS-stained lung sections showing a significant increase in goblet cell in the OVA/OVA group, compared to that in the PBS/PBS and OVA/PBS groups ( $P < 0.001$ ). TiO<sub>2</sub> NPs treatment in the asthmatic OVA/TiO<sub>2</sub>/OVA group increased significantly the number of goblet cells, compared to those in the asthmatic non-treated group (OVA/OVA;  $P < 0.01$ ). Results are expressed as mean  $\pm$  SEM for seven bronchial airways per mouse ( $n = 5$  mice per group), and the groups were compared using one-way ANOVA (Harfoush et al., 2020).

### **6.3 Titanium dioxide enhances eosinophil infiltration in the lungs of asthmatic mice**

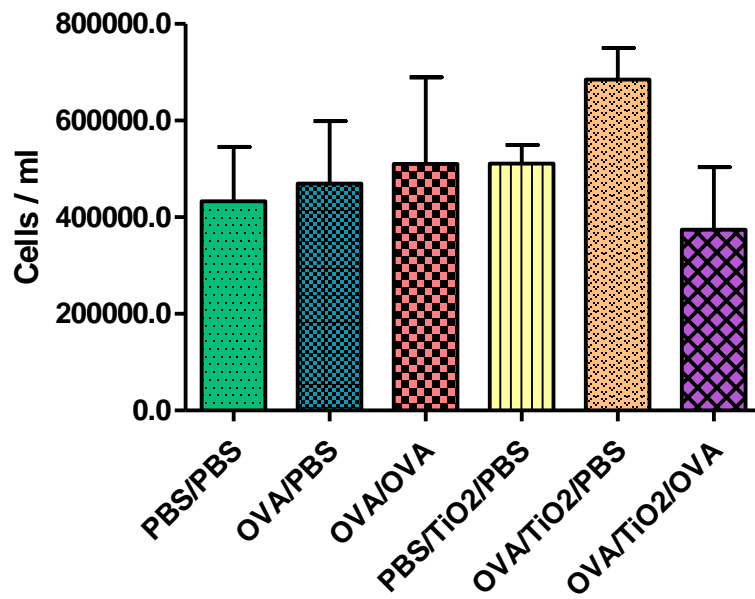
In the present research, the immune cell populations present in the BALF of the different experimental groups were also determined (**Figure 10A-E**). The OVA/OVA asthma mice showed a significant increase in total immune cells, compared with the PBS/PBS controls. Moreover, this increase was exacerbated after TiO<sub>2</sub> NP exposure (**Figure 10A**).

As the results revealed, in all experimental groups, the macrophages were present at almost the same levels, with an only slight increase in the OVA/OVA mice as compared to those in their non-asthmatic counterparts (**Figure 10B**). Moreover, eosinophils were significantly increased in the asthmatic mice; however, they were almost absent in the controls (**Figure 10C**). The TiO<sub>2</sub> NP treated mice showed a significant increase in eosinophil counts, compared to all other groups (**Figure 10C**). Regarding neutrophils, they were more numerous in the OVA/OVA asthmatic groups than in the controls. Besides, only PBS/TiO<sub>2</sub>/PBS mice showed a significant increase in the number of neutrophils as compared to the PBS group (**Figure 10D**). However, lymphocyte numbers were variably different among the groups. In this regard, the OVA/OVA group had a significantly larger number of lymphocytes than the respective non-asthmatic ones (**Figure 10E**). Accordingly, it can be concluded that the OVA model was functional and created an eosinophilic inflammatory environment enhanced in the presence of TiO<sub>2</sub> NPs.

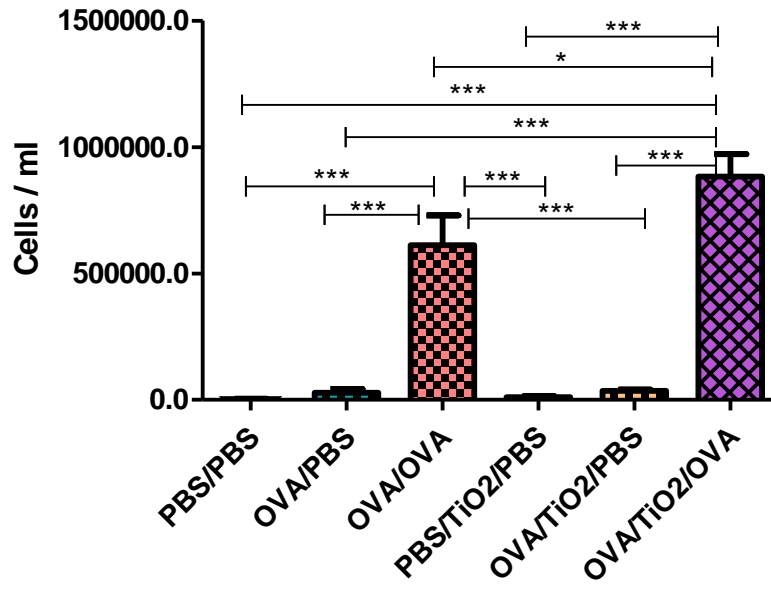
(A) Total cell count



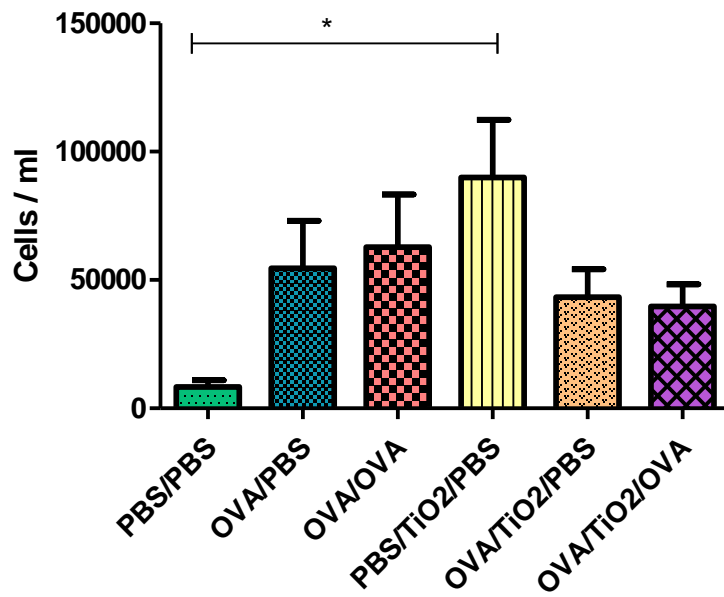
(B) Macrophages



(C) **Eosinophils**



(D) **Neutrophils**



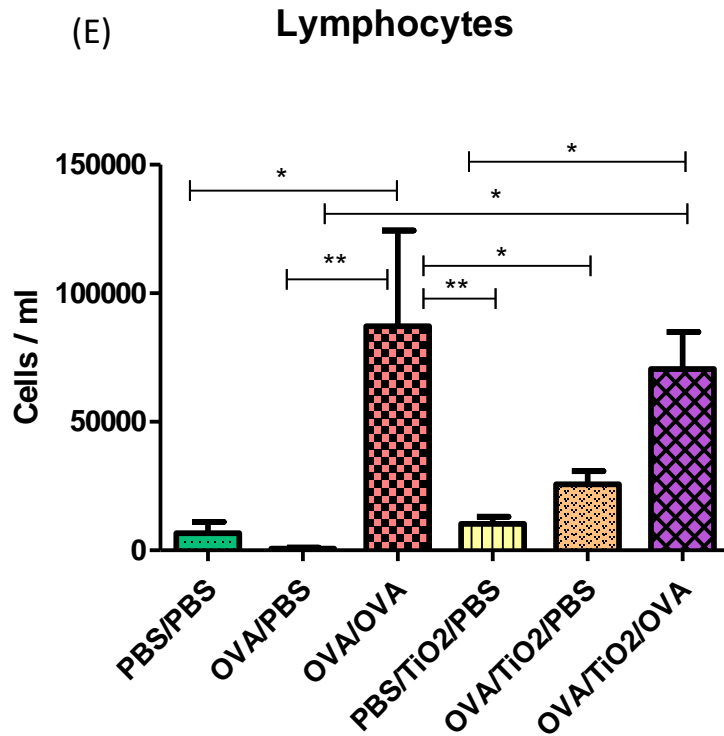


**Figure 10** Inflammatory cell count in BALF. Total cells [A], macrophages [B], eosinophils [C], neutrophils [D], and lymphocytes [E] counts in BALF obtained from different groups demonstrated an inflammatory response in the lungs after OVA exposure. Total cells, eosinophils, and lymphocytes counts were significantly increased in the OVA/OVA mice, compared to those in the PBS/PBS controls ( $P < 0.05$ ,  $P < 0.001$ , and  $P < 0.05$ , respectively). TiO<sub>2</sub> NPs treatment resulted in a significant increase in eosinophils count in the OVA/OVA mice ( $P < 0.05$ ), indicating a greater asthmatic response. Data are expressed as mean  $\pm$  SEM for 5 to 10 mice per group. Inter-group comparison was performed using one-way ANOVA (Harfoush et al., 2020).

To further characterize the inflammatory cell infiltrates in the lung tissues, double IF staining was performed by using different antibodies directed against macrophage marker F4/80 and neutrophil marker Ly6G (**Figure 11A**), as well as eosinophil marker Siglec-F and T lymphocytes marker CD3 $\epsilon$  (**Figure 11B**). All investigated cells were present in the different studied groups; however, eosinophils and T lymphocytes were more prominently found in the OVA/OVA and OVA/TiO<sub>2</sub>/OVA groups than in the controls.

Moreover, these results are in good agreement with those obtained from the BALF analysis.

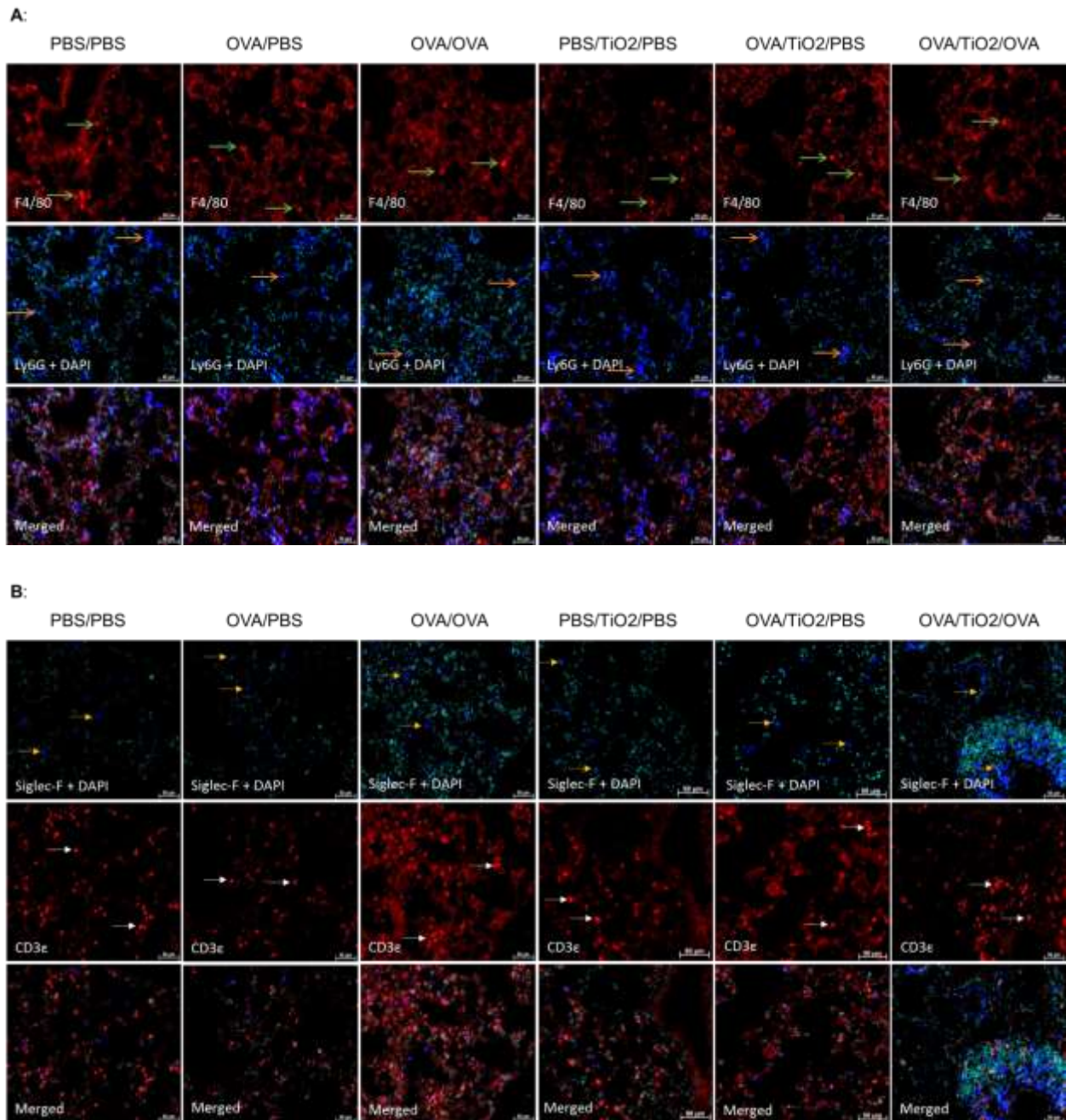


**Figure 11** Qualitative immunofluorescence staining of immune cells in the lung sections. **A)** Green arrows indicate alveolar macrophages [F4/80 positive, red] and orange arrows represent neutrophils [Ly6G positive, blue]. **B)** Eosinophils [siglec-F positive, blue] and T lymphocytes [CD3ε positive, red] as indicated by yellow and white arrows, respectively. Nucleus visualization in cyan using DAPI (Harfoush et al., 2020).

## **6.4 Intranasal administration of titanium dioxide nanoparticles during OVA-sensitization and challenge induces airway hyperresponsiveness**

The lung function analysis serves to evaluate the severity of airway hyperresponsiveness (AHR). The parameter which describes changes in the lung regarding hyperresponsiveness, is the sRaw. In order to confirm the influence of OVA-induced asthma on the airways, the changes in the airway resistance upon MCh stimulation were measured. The local effects of NPs in asthmatic groups were further evaluated by the measurement of airway resistance in response to the increased doses of inhaled MCh. In line with previous reports [23] our findings indicated that mice with severe asthma (i.e., OVA/OVA) showed increased airway resistance in response to MCh in a dose-dependent manner (**Figure 12**). In this respect, exposure to TiO<sub>2</sub> NPs tended to increase the airway resistance in the PBS/TiO<sub>2</sub>/PBS, OVA/TiO<sub>2</sub>/PBS, and OVA/TiO<sub>2</sub>/OVA groups, compared to that in the untreated ones (**Figure 12**).

## Airway Resistance

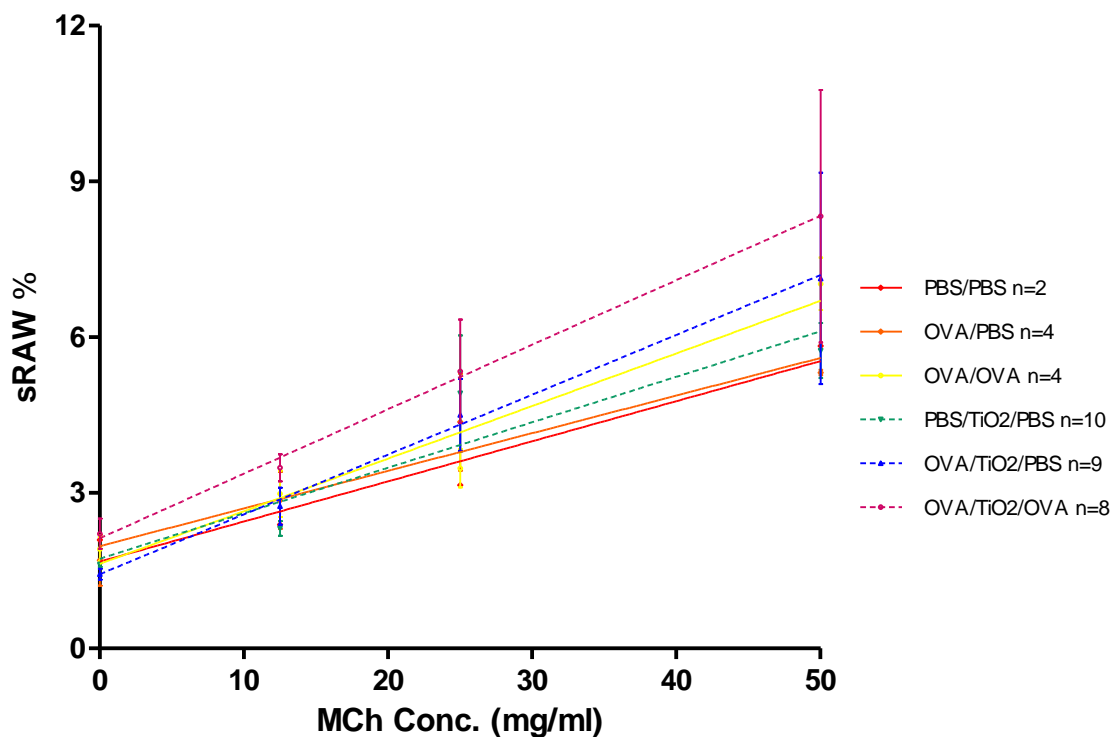


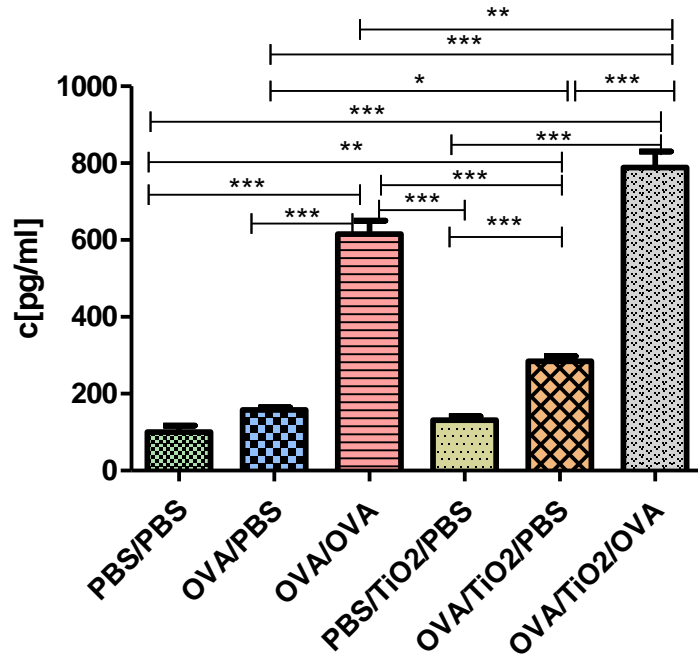
**Figure 12** Airway responsiveness to methacholine (Mch) and percentages of specific airway resistance (sRaw) in the controls, OVA-exposed group, TiO<sub>2</sub> NPs-exposed group, and OVA plus TiO<sub>2</sub> NP-exposed group, were measured upon Mch stimulation (0, 12.5, 25, and 50 mg/mL). Mice exposed to OVA showed an increase in sRaw, compared to the controls. Additional exposure to TiO<sub>2</sub> NPs, along with OVA, resulted in an increase in sRaw. Data are presented as mean±SEM, and n is presented in the graph for each condition (Harfoush et al., 2020).

## **6.5 Titanium dioxide treatment shifts the respiratory immune reaction towards a Th2-mediated response**

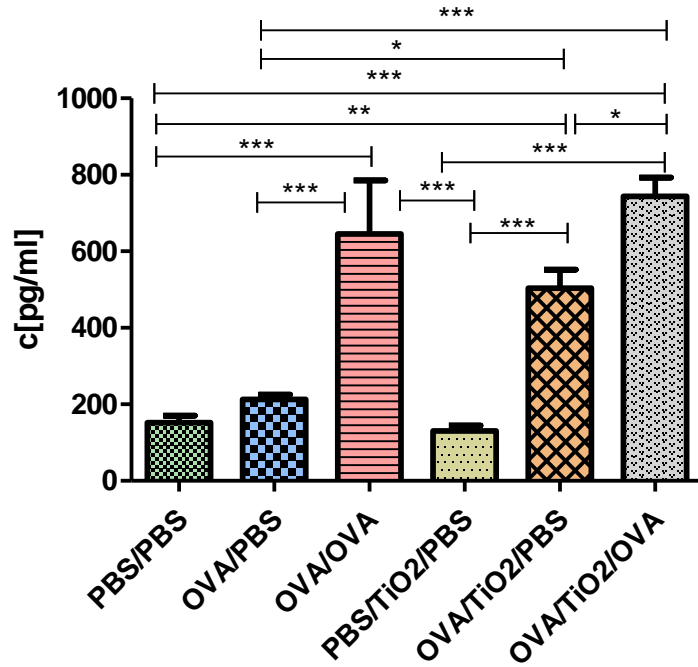
Th1/Th2 cytokines were assayed, the measurement revealed significant differences in cytokine levels among the groups (**Figure 13A-E**). In this regard, the OVA/OVA mice showed a significant increase in the IL-4, IL-5, and IL-13 levels as compared to the non-asthmatic groups (**Figure 13 A, B, C**). However, the PBS-challenged and OVA-sensitized group had no significant elevation in IL-4, IL-5, and IL-13 in comparison to the PBS controls. Furthermore, TiO<sub>2</sub> NPs in the presence of OVA (OVA/TiO<sub>2</sub>/PBS) were found to significantly increase the IL-4, IL-5 and IL-13 levels (**Figure 13A, B, C**). Interestingly, the results also revealed that OVA/OVA combined with TiO<sub>2</sub> NPs provoked the highest Th2-type cytokine production (IL-4 and IL-13). These results indicated that TiO<sub>2</sub> NPs exposure in the presence of OVA aggravated the asthmatic response; however, this was not observed for particles treatment alone. Although IFN- $\gamma$  levels remained higher after OVA sensitization and challenge, compared to the PBS controls, TiO<sub>2</sub> NP treatment exerted no apparent effect on the levels of IFN- $\gamma$  (**Figure 13D**).

Based on the evidence, elevated total serum IgE levels are associated with allergy. In line with this, circulating IgE levels were significantly increased in the OVA-treated group (OVA/OVA), compared to those in the non-sensitized group (PBS/PBS). Following TiO<sub>2</sub> NP treatment, the baseline levels of total IgE were not significantly increased in both OVA/TiO<sub>2</sub>/PBS and OVA/TiO<sub>2</sub>/OVA groups when compared to those in the OVA/PBS and OVA/OVA groups, respectively (**Figure 13E**).

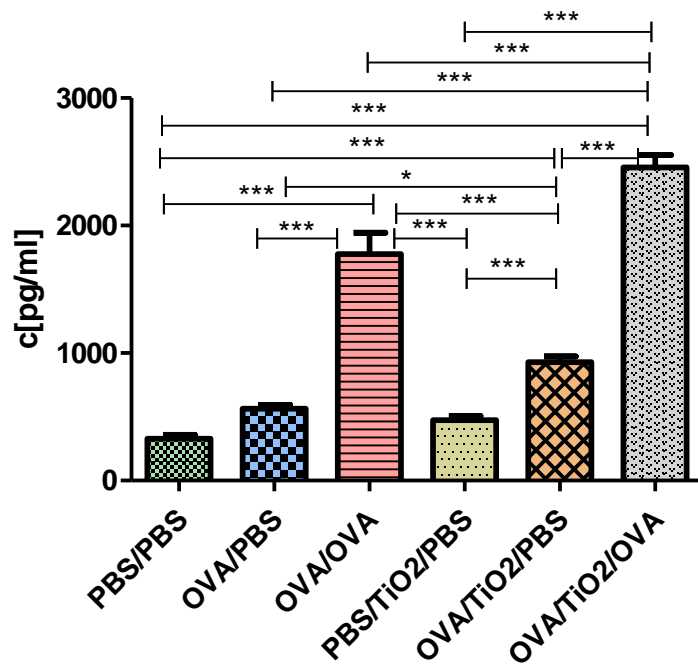
(A) IL-4



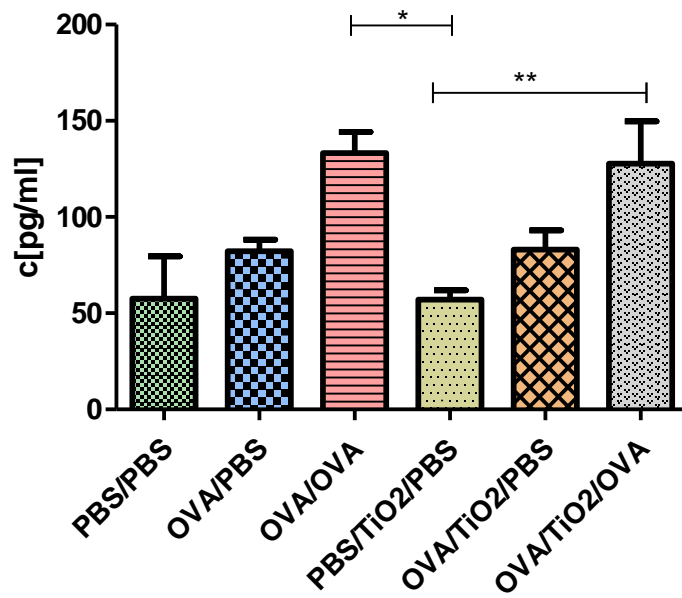
(B) IL-5



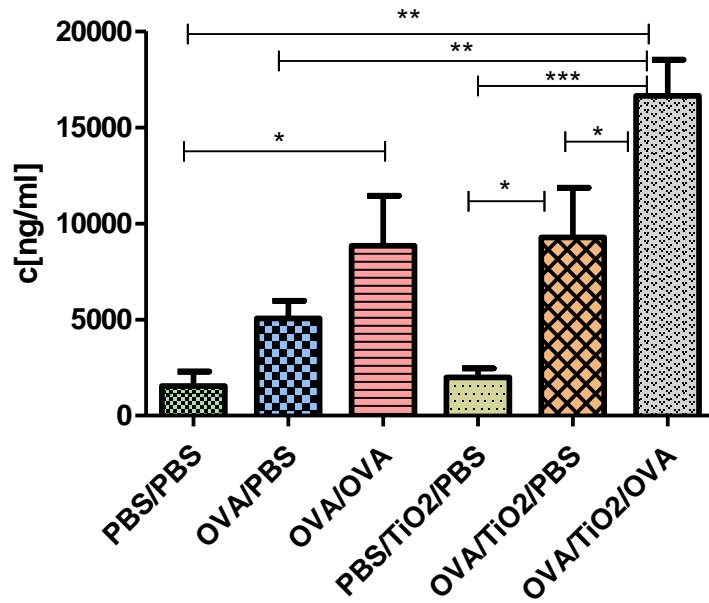
(C) IL-13



(D) INF- $\gamma$



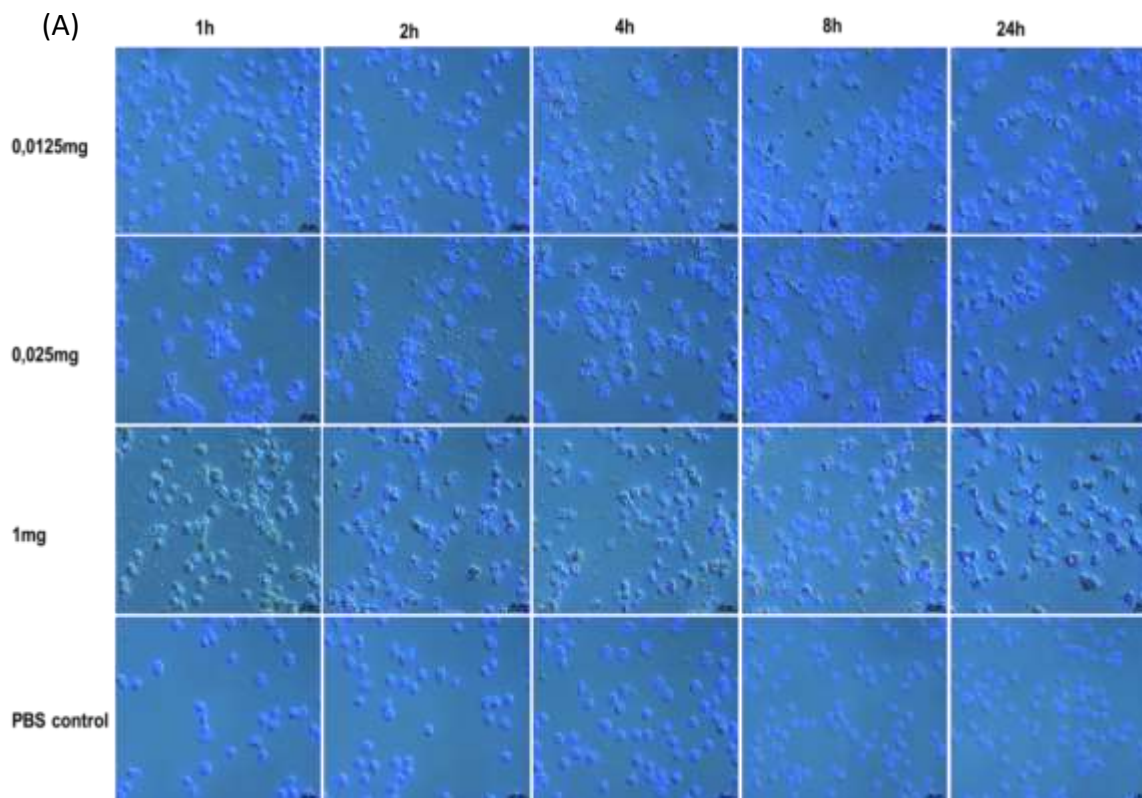
(E) Total IgE in serum

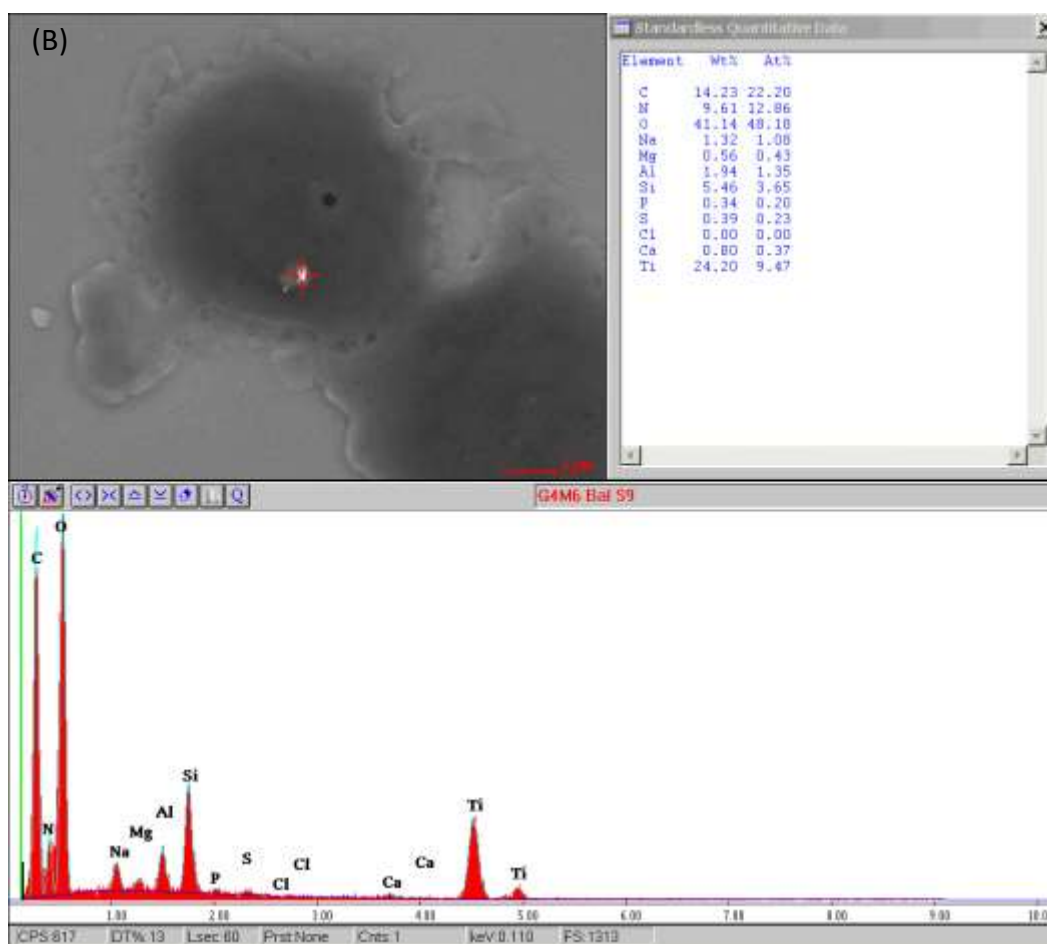


**Figure 13** Cytokine levels in lung homogenates and serum; **A, B, C**) Th2 cytokines (IL-4, IL-5, and IL-13), **D**) Th1 pro-inflammatory cytokine (IFN- $\gamma$  in lungs), and **E**) total IgE in serum. Asthmatic mice had an increase in Th2 cytokine levels, compared to those in healthy groups. Interleukin levels were higher following OVA-TiO<sub>2</sub> NPs treatment. Data are represented as mean $\pm$ SEM (n=5-10), and the groups were compared using one-way ANOVA (Harfoush et al., 2020).

## 6.6 Cellular uptake of titanium dioxide nanoparticles

As known before, the macrophages uptake NPs by phagocytosis [39]. To prove that, our BALF macrophages were isolated and incubated with different concentrations of TiO<sub>2</sub> NPs (**Figure 14A**). Agglomeration mostly occurs prior to phagocytosis, upon the contact of NPs with the cell culture medium. The TiO<sub>2</sub> NP aggregates were detected in almost all cells at different time points and concentrations. Moreover, there were agglomerates precipitated outside the macrophages. The morphological changes of the macrophages and halos seem to be the result of phagocytic activity (**Figure 14A**). In order to confirm our previous *in vitro* results, alveolar macrophages isolated from the BALF of TiO<sub>2</sub>-treated groups were first stained with Diff-Quick and then scanned with SEM, followed by EDX spectroscopy (**Figure 14B**). The TiO<sub>2</sub> NPs could be observed in the alveolar macrophages of the treated mice. This indicated the ability of macrophages to take up TiO<sub>2</sub> NPs *in vivo*.

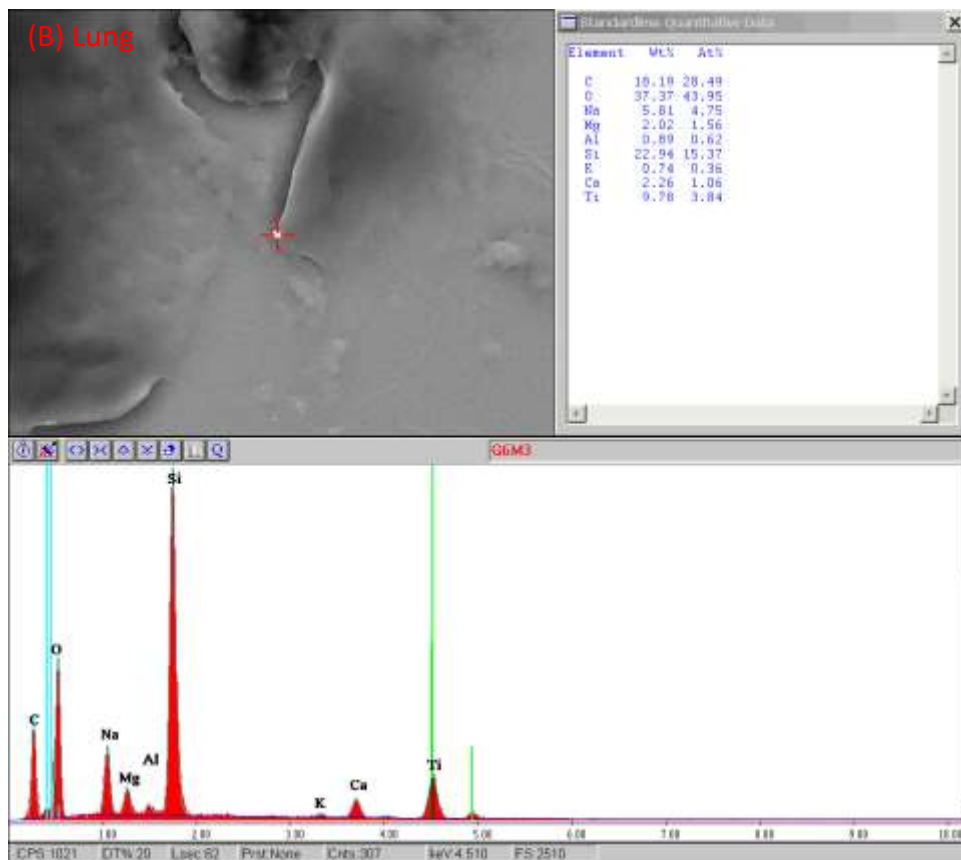
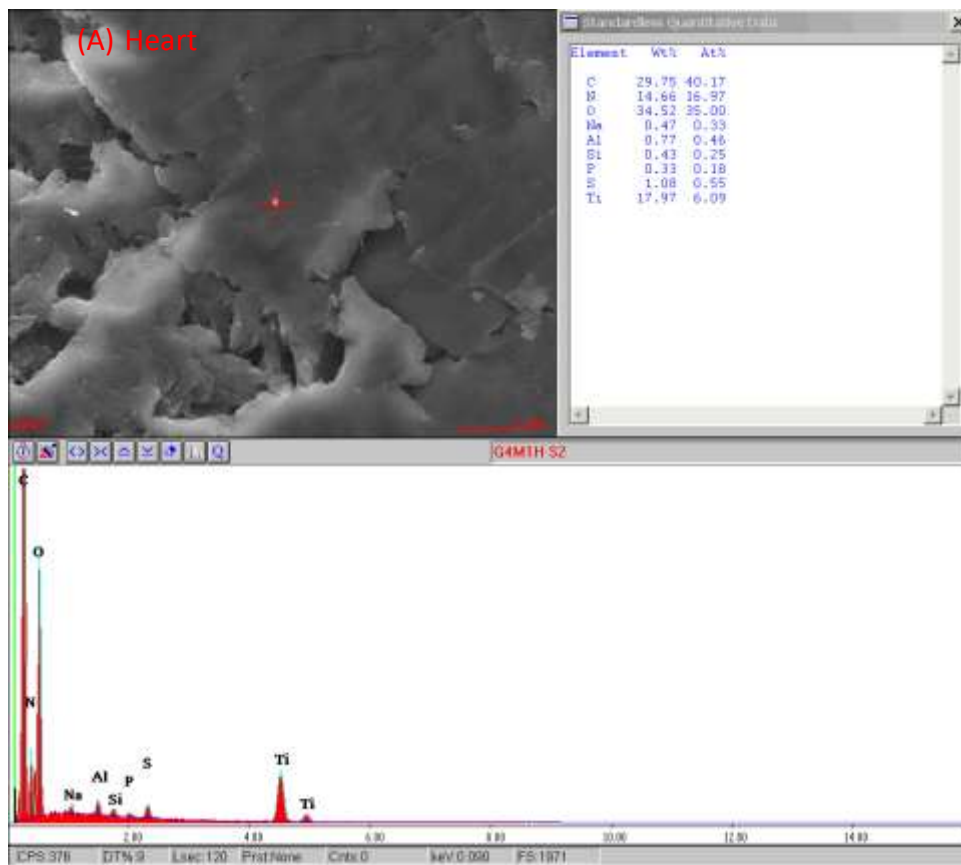


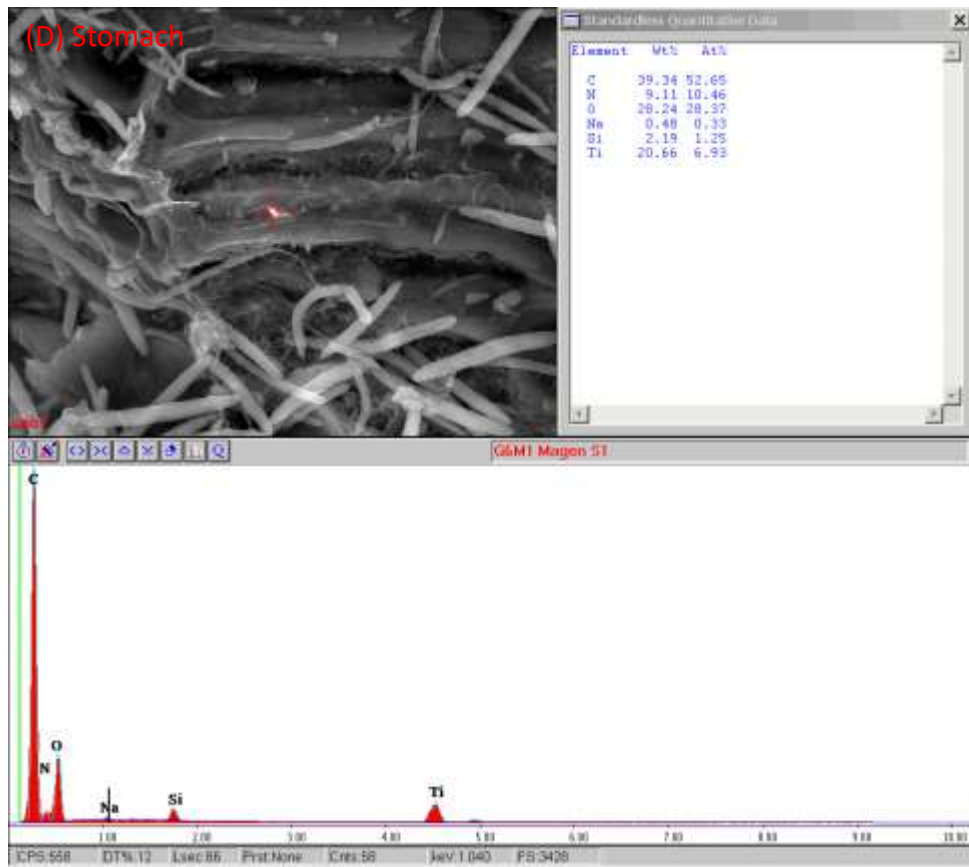
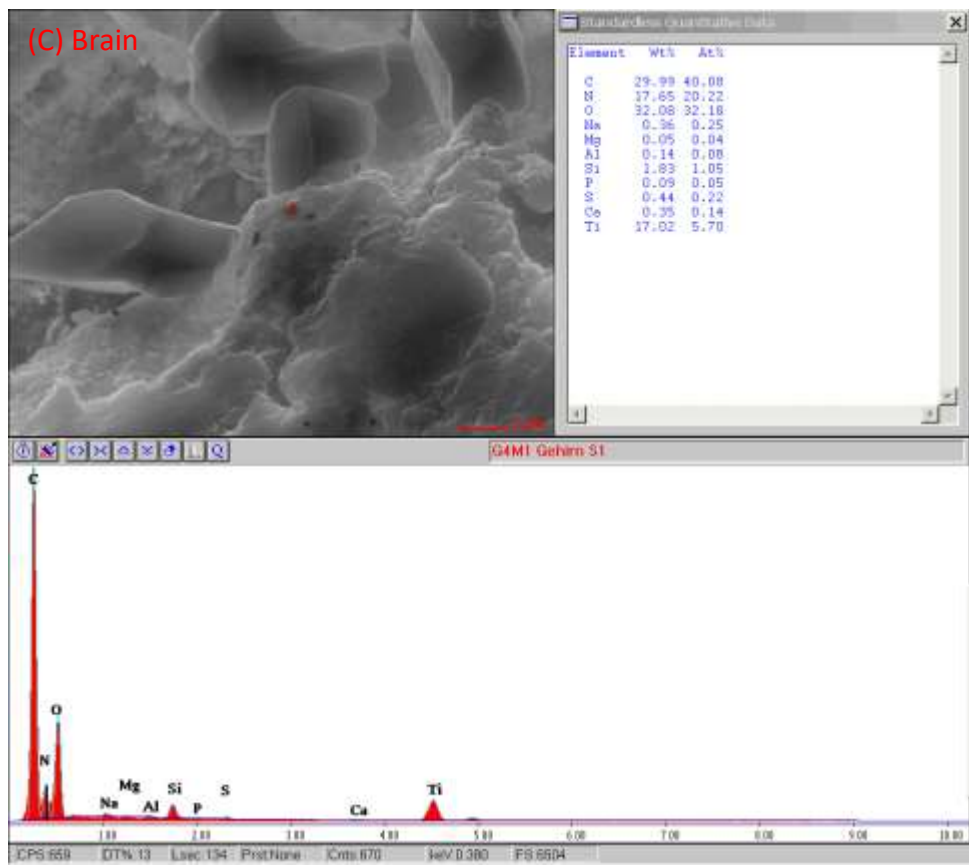


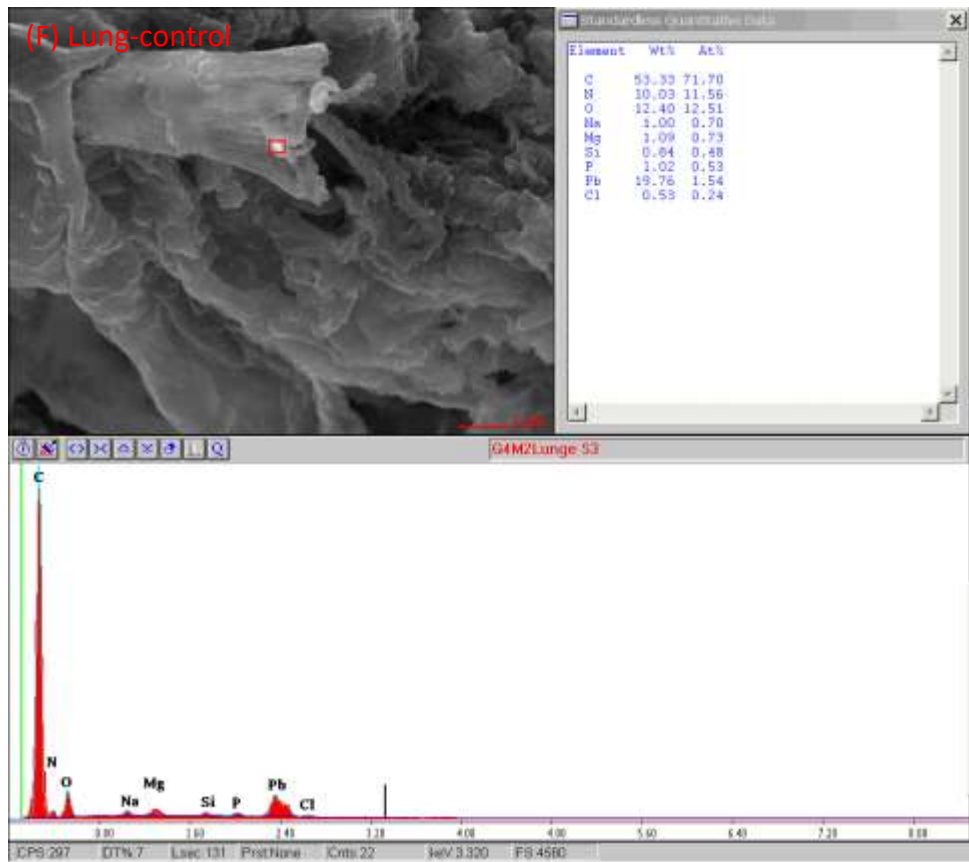
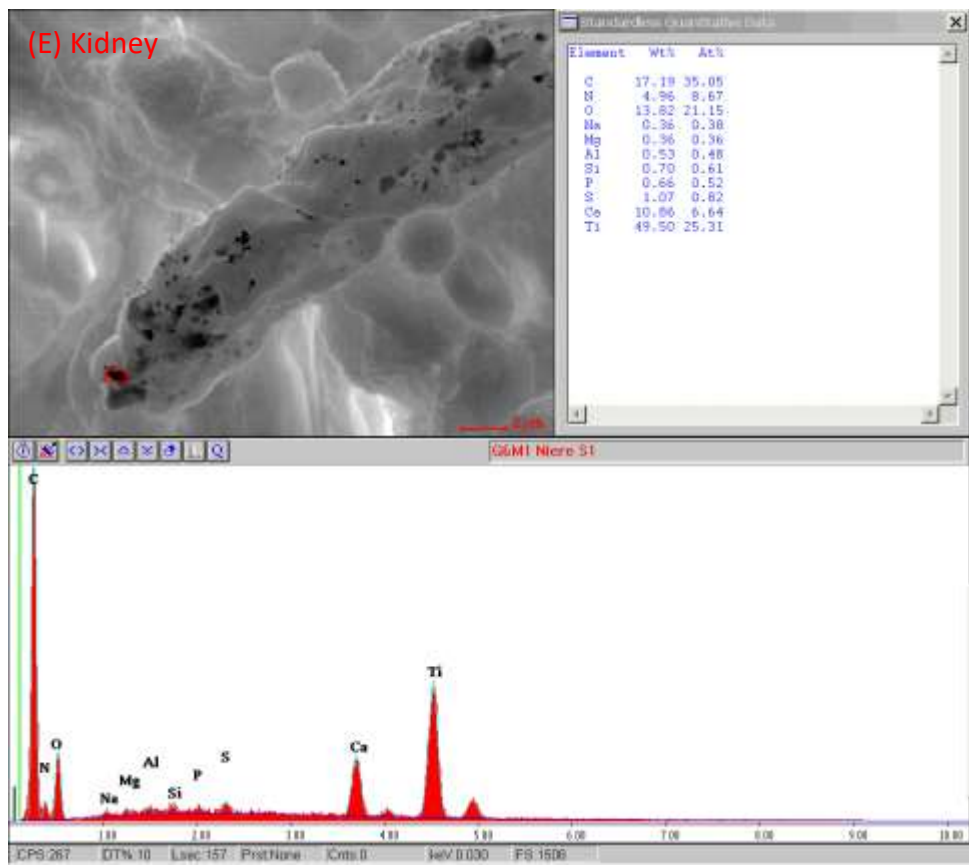
**Figure 14** Nanoparticle uptake in alveolar macrophages. Cultured alveolar macrophages [A] were exposed to TiO<sub>2</sub> NPs; (0.0125, 0.025, and 1 mg/ml) and PBS. Cellular uptake was analyzed after incubation for 1, 2, 4, 8, and 24 h. Adherent mouse alveolar macrophages were fixed and stained with DAPI before microscopic analysis. An example image of alveolar macrophage in BALF [B] was taken by SEM. The white spot inside the cell is a cluster of TiO<sub>2</sub> NPs. This was followed by EDX spectrum analysis showing a strong titanium signal, indicating the presence of TiO<sub>2</sub> NPs in alveolar macrophages. (The parameters are Wt%: weight percent, At%: atomic percent) (Harfoush et al., 2020).

## 6.7 Titanium dioxide nanoparticles distribution in extrapulmonary organs

To further evaluate the dynamics and distribution of intranasally administered TiO<sub>2</sub> NPs *in vivo*, SEM-EDX was performed (**Figure 15A**). As indicated in previous studies, NPs applied via the respiratory tract can cross the blood-air barrier for systemic dissemination [40][41]. In the present study, the SEM, followed by EDX scans, revealed the presence of TiO<sub>2</sub> NPs in the heart, lungs, brain, stomach, and kidney samples obtained from the TiO<sub>2</sub> NPs-treated mice (**Figure 15A-E**). Nonetheless, they were not observed in the untreated mice (**Figure 15F,G**, as examples).







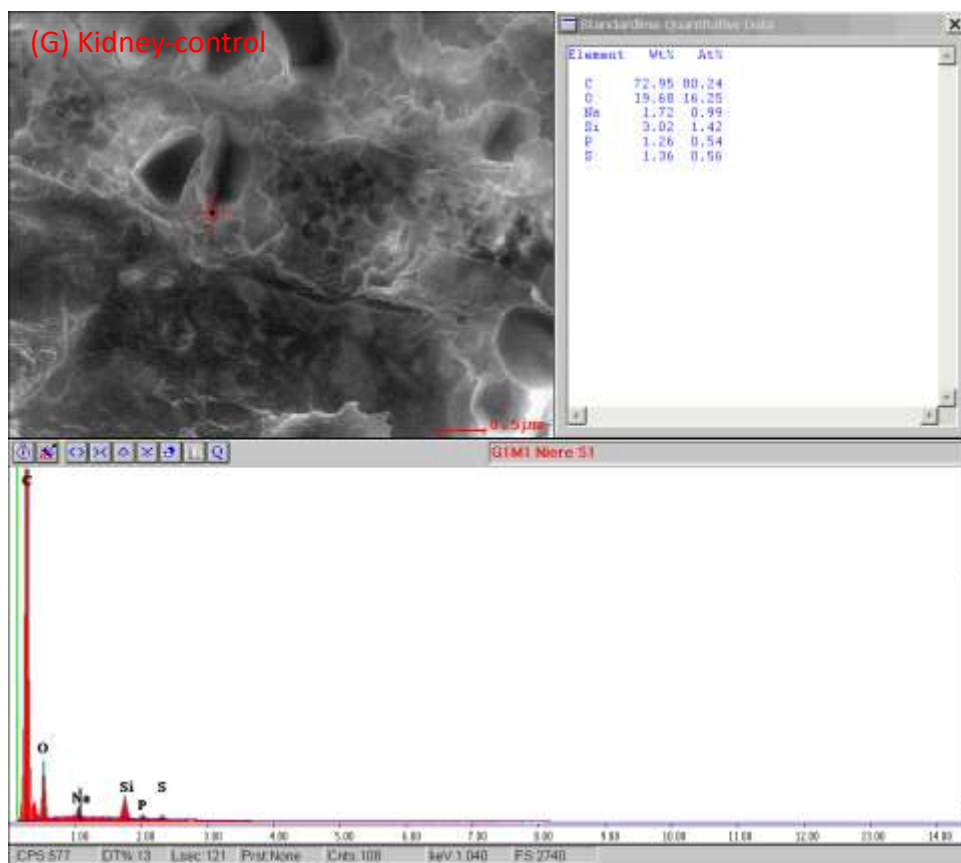


**Figure 15** Detection of TiO<sub>2</sub> NPs in different mice organs. Images of SEM, followed by EDX spectrum analysis, showing the presence of TiO<sub>2</sub> NPs in the organs of treated mice; **(A)** heart, **(B)** lung, **(C)** brain, **(D)** stomach, and **(E)** kidney, and the absence of TiO<sub>2</sub> NPs in the lung **(F)** and kidney **(G)** of untreated ones (Harfoush et al., 2020).

To thoroughly analyze the presence of TiO<sub>2</sub> NPs in more organs, ICP-MS was employed, revealing titanium traces in the heart, lungs, brain, stomach, kidneys, spleen, and liver (**Figure 16**).

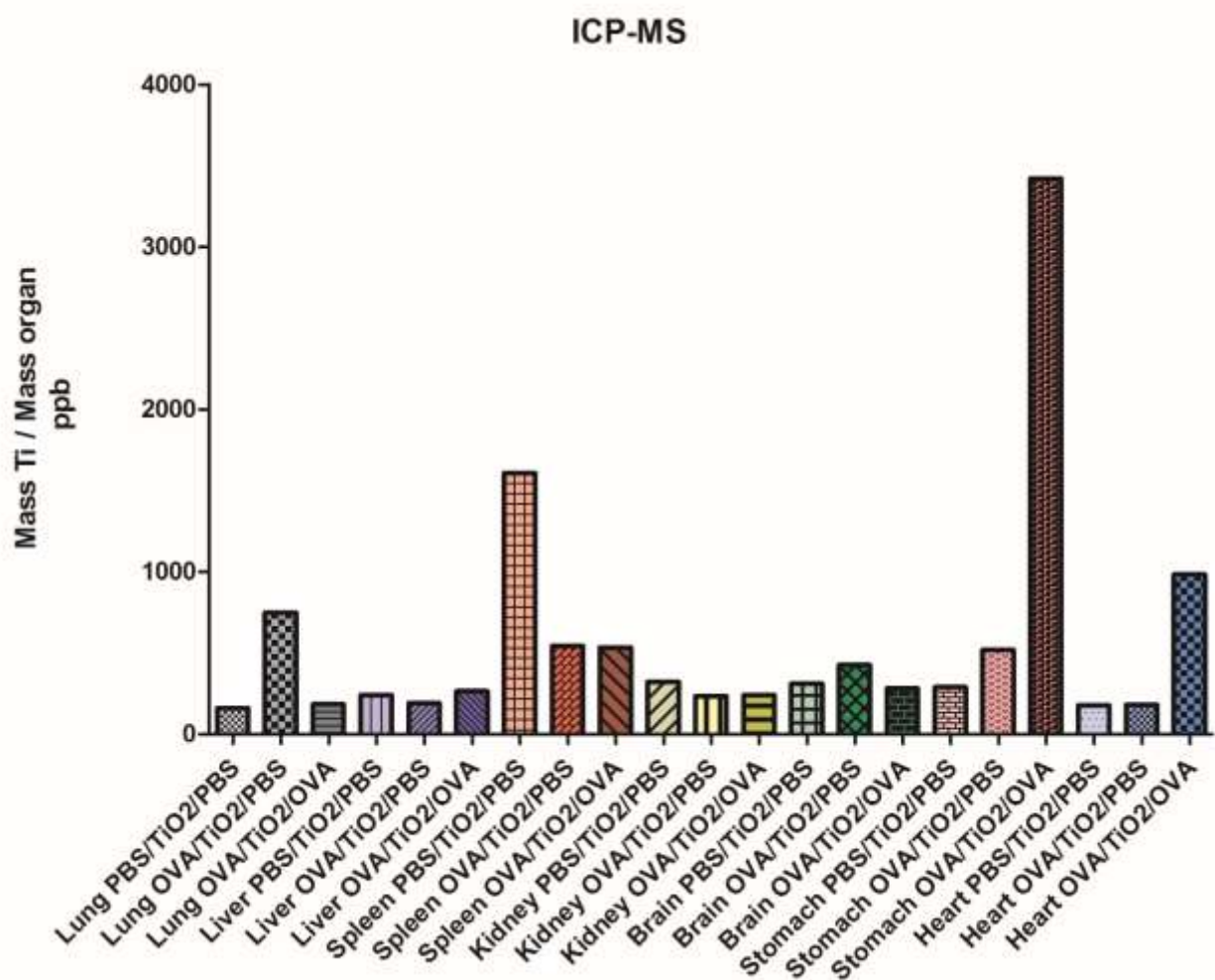
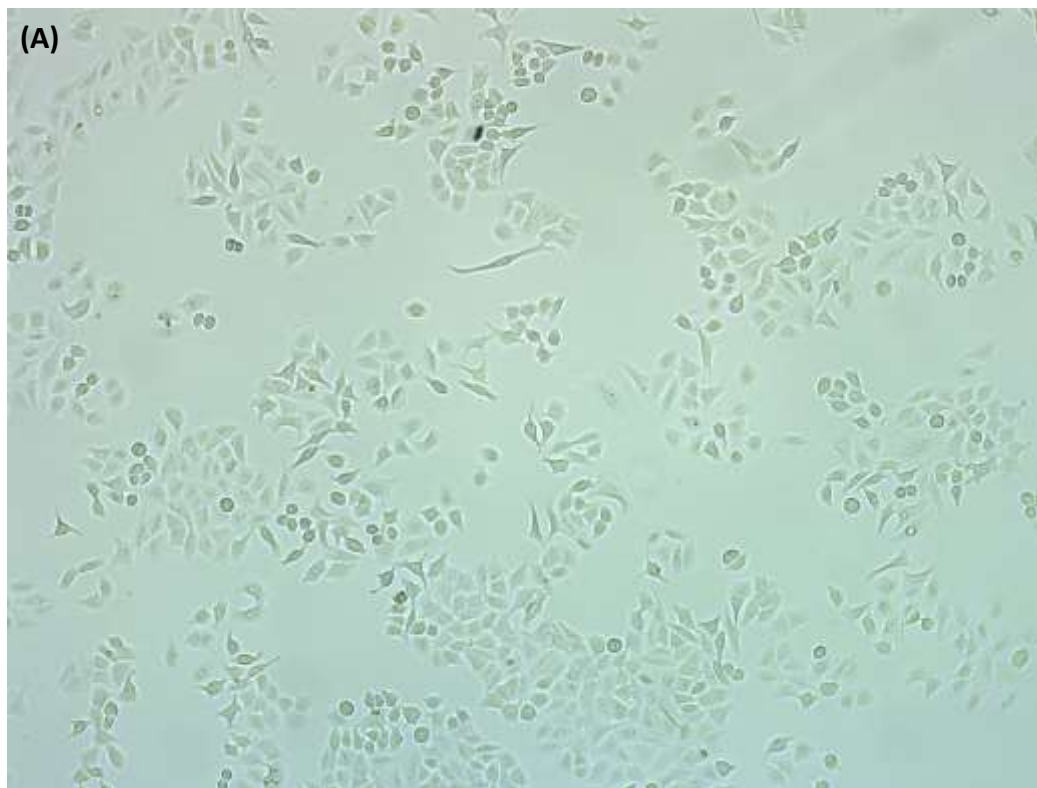


**Figure 16** ICP-MS of different organs showed traces of TiO<sub>2</sub> NP expressed as mass Ti / mass organ in ppb (Harfoush et al., 2020).

## 6.8 The isolation and identification of A549 cells under light microscope

A549 cells are adenocarcinomic human alveolar basal epithelial cells, and constitute a cell line that was used as models for the therapy development, drug metabolism, lung cancer studies, and as a transfection host. In **(Figure 17 A)** the untreated control cells are squamous, grow as a monolayer; attaching or adherent to the culture flask.

The cells were treated with 3 $\mu$ g/mL of SWCNTs **(Figure 17 B)**, DWCNTs **(Figure 17 C)**, and MWCNTs **(Figure 17 D)** for 6 hours. Black dispersions were observed in different sites of the cells, one can assume that the CNTs deposited and accumulated in the cells.



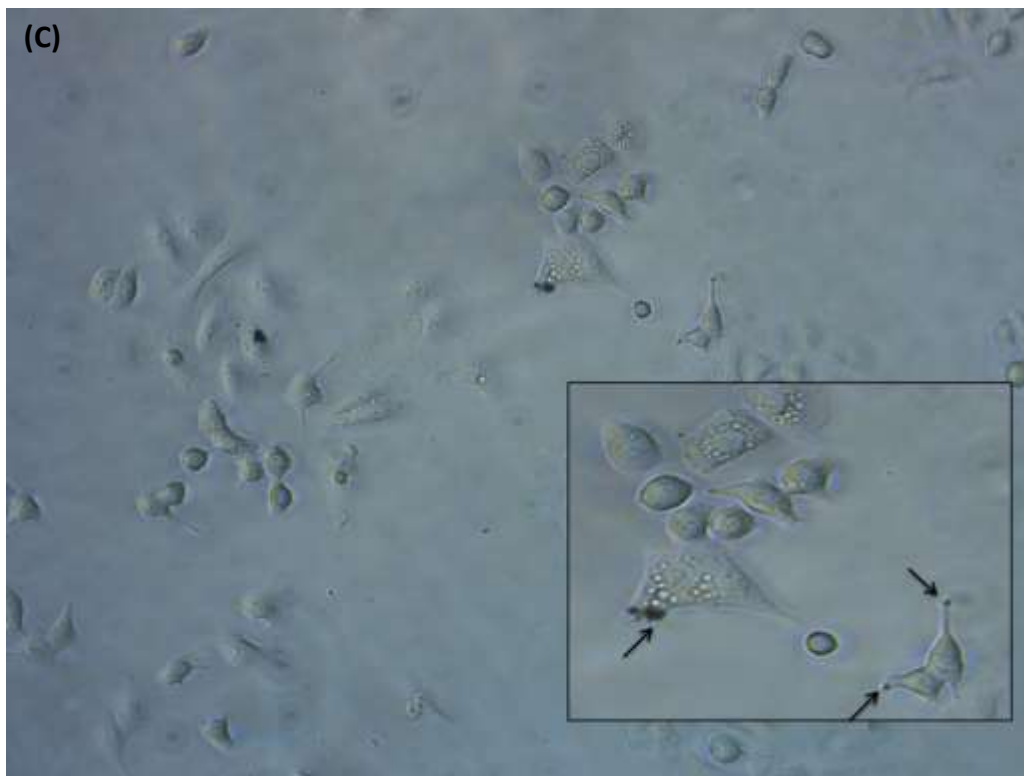
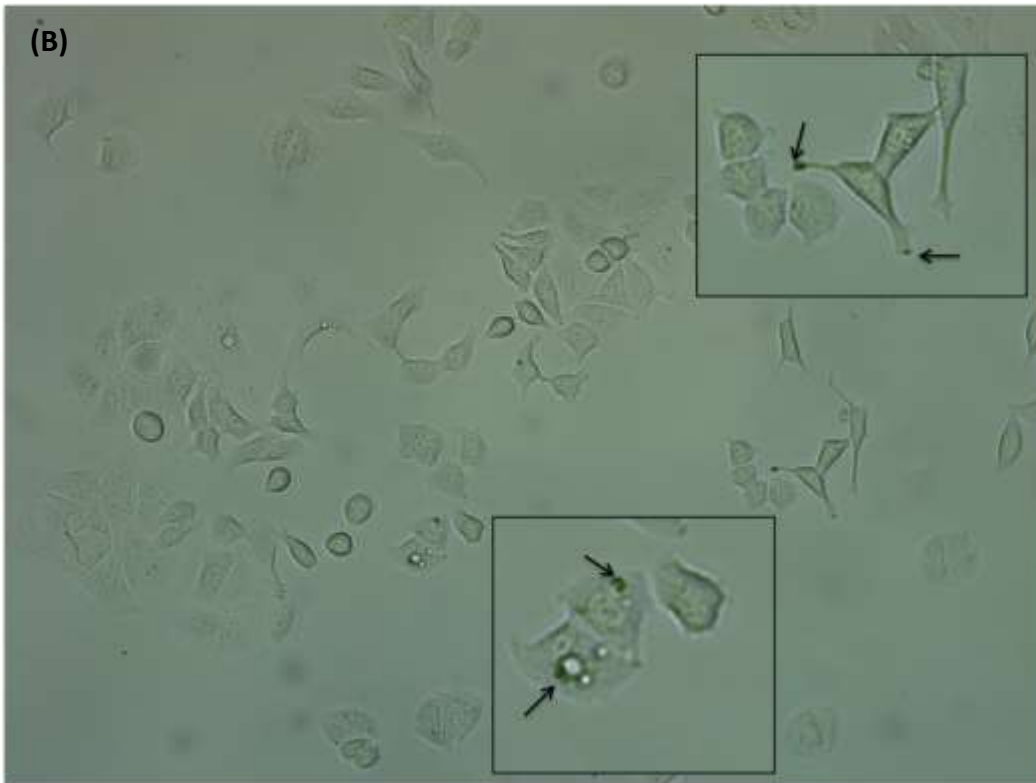
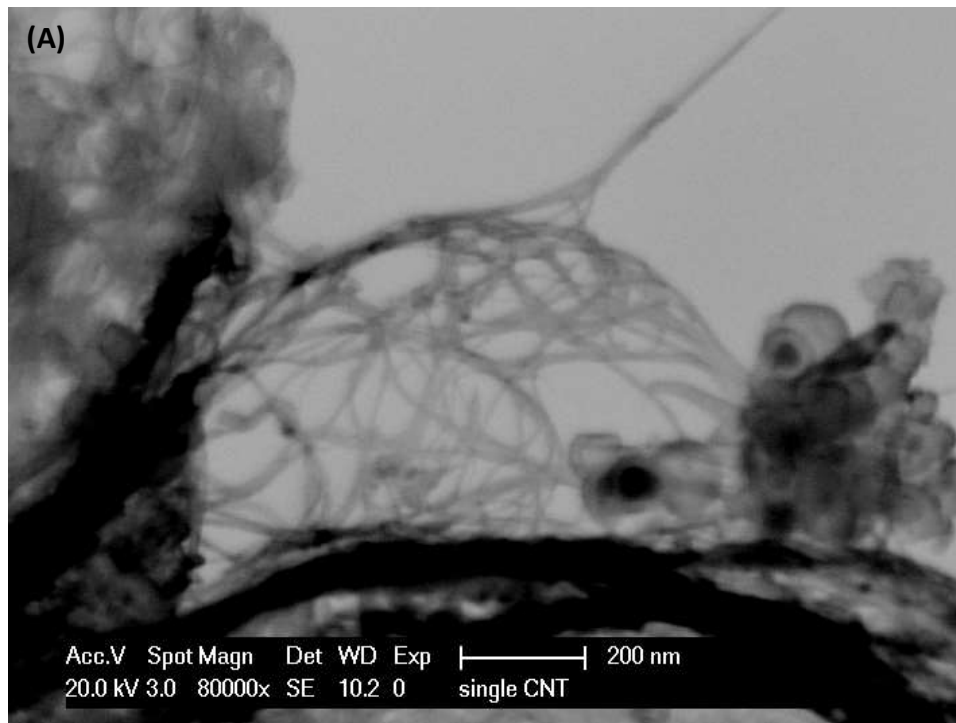




**Figure 17** Light microscope analysis of control A549 cells incubated with culture medium (**A**). Cells exposed to  $3\mu\text{g}/\text{mL}$  of SWCNTs (**B**), DWCNTs (**C**), and MWCNTs (**D**) for 6h. Black arrows represent the dispersed carbon nanotubes.

## 6.9 Characterization of single, double, and multi-walled carbon nanotubes

Characteristics of the three types of carbon nanotubes were provided by scanning electron microscopy (ThermoFisher XL 30 FEG ESEM; Eindhoven, NL). Figure 18 shows an area of high density tubes, aggregates/bundles of varying lengths and diameters of the three types of CNTs used in this study. Scanning electron microscopy (SEM) pictures of (SWCNTs, DWCNTs, and MWCNTs) are shown in (Figure 18 A, B, C) respectively.



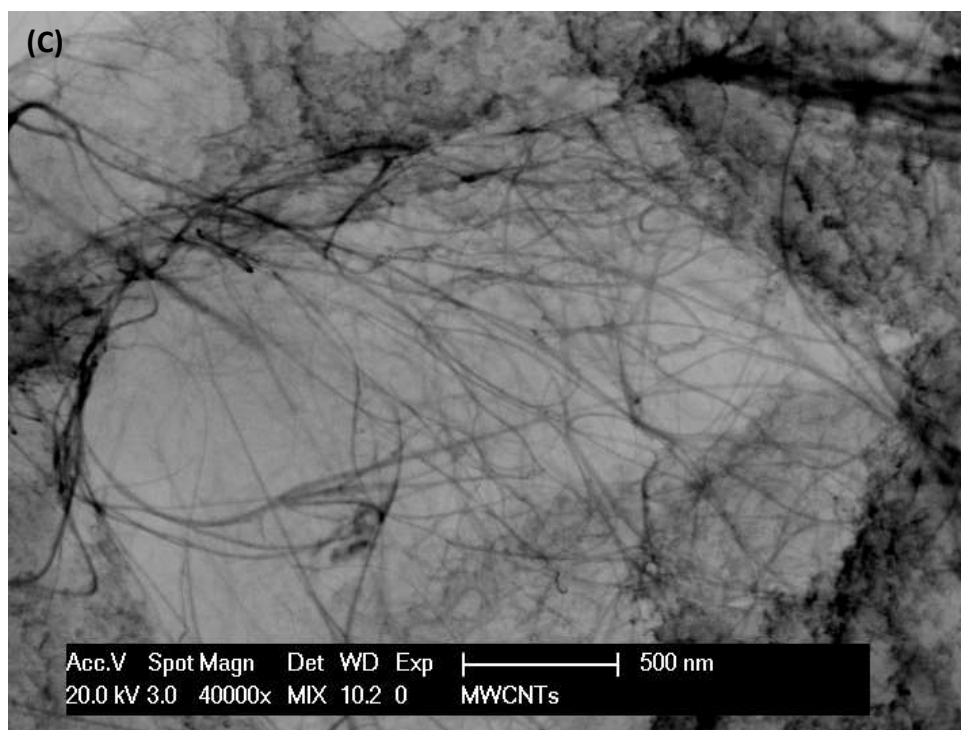
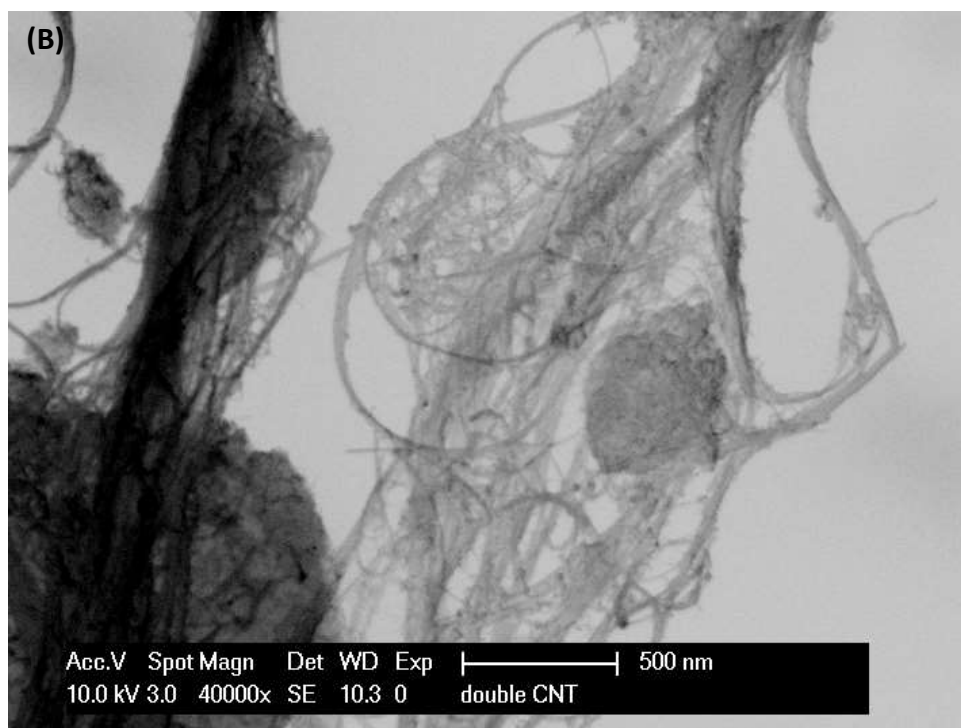
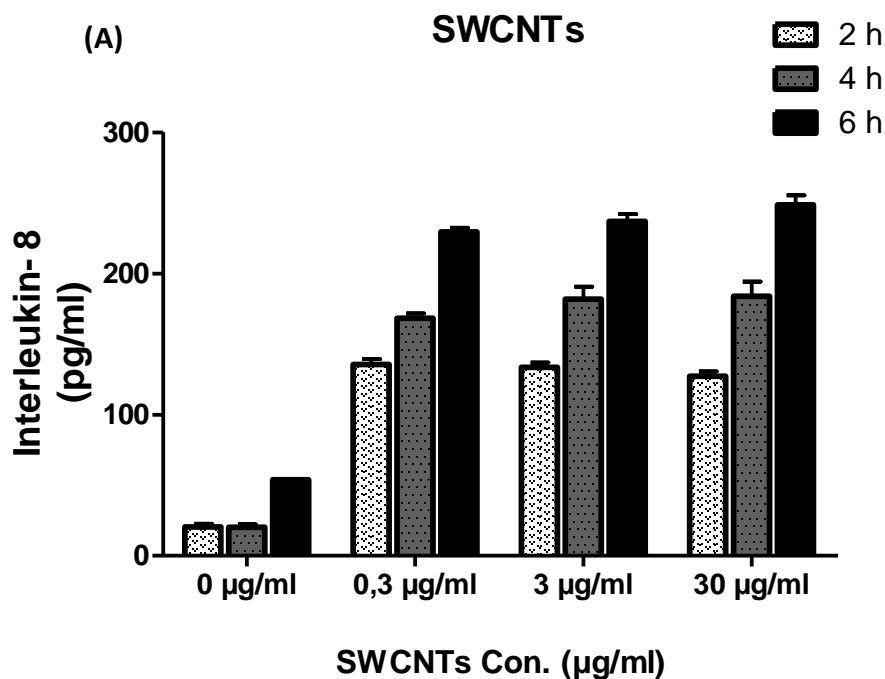


**Fig. 18** Scanning electron microscopic (SEM) images of dispersed SWCNTs, DWCNTs, and MWCNTs used in the experiments. Original magnification is 80000 $\times$  for (A), and 40000 $\times$  for (B, C), showing high density tubes and large aggregates of nanomaterials.

## 6.10 Carbon nanotubes treatment affects IL-8 levels

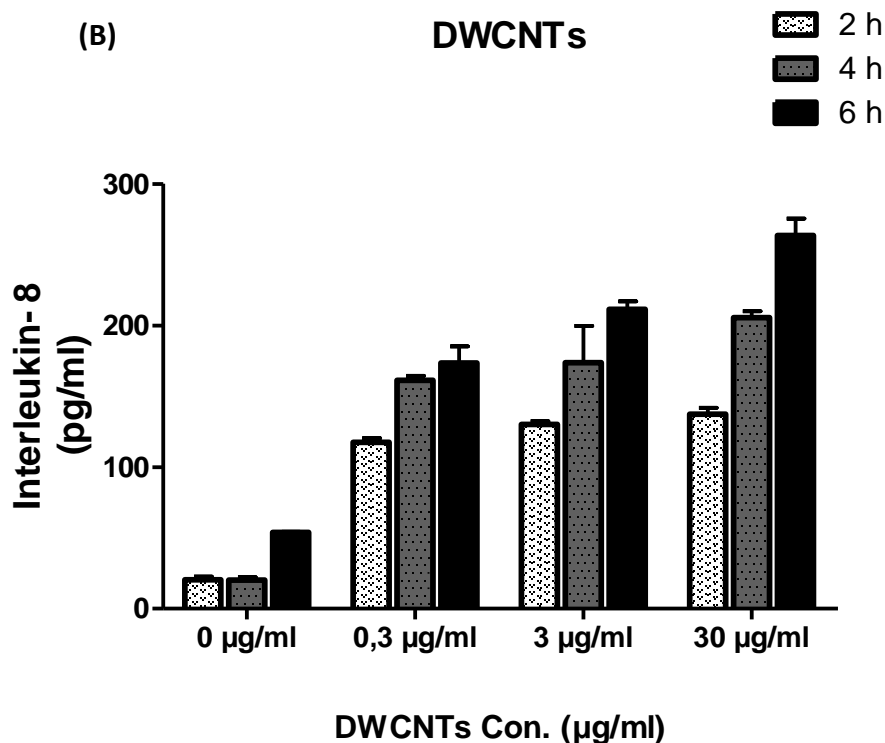
Interleukin-8 (IL-8) is a type of chemokine which belongs to the CXC family and has been found to be an activator and attractant for human neutrophils *in vitro*. It can be produced by a variety of cells, including epithelial cells, macrophages, neutrophils, and endothelial cells. Moreover, IL-8 and its related cytokines are produced by different tissues upon inflammation, infection, ischemia etc., and are thought to be a mediator for inflammatory response and a main cause of local neutrophil accumulation [44].

A549 cells were treated with different concentrations (0.3, 3 and 30  $\mu\text{g/ml}$ ) of SWCNTs, DWCNTs, and MWCNTs. In order to investigate the pro-inflammatory potential of CNTs, we analyzed the production of IL-8 at 2, 4, and 6 hours post-exposure to CNTs in the media supernatant of A549 cultures (**Figure 19**). In the supernatants of control untreated cells, IL-8 release was at very low value. When A549 cells were treated with the nanomaterials, IL-8 secretion was increased significantly in a time dependent manner for the three various types of CNTs. Notably, the dose 0.3 $\mu\text{g/ml}$  of SWCNTs (**Figure 19 A**) was sufficient to induce cellular inflammation. This inflammatory reaction was increased with increased incubation time. However, exposure to higher CNTs concentrations (3 and 30 $\mu\text{g/ml}$ ) did not induce higher level of IL-8 within the same time point. These results were seen for DWCNTs and MWCNTs respectively, (**Figure 19 B, C**).



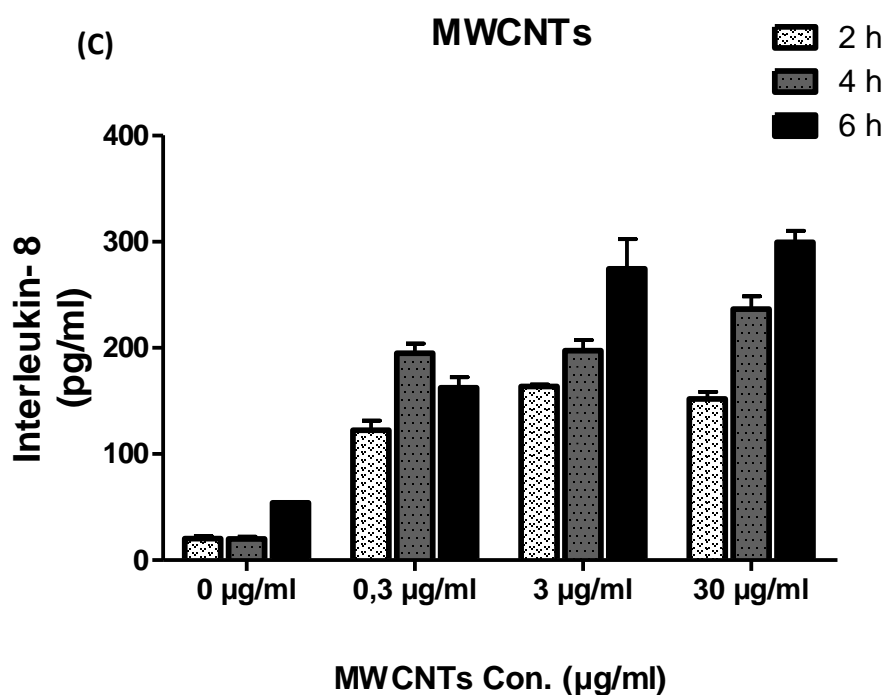
2h 0 µg/ml vs 4h 0 µg/ml	ns	4h 0 µg/ml vs 6h 0 µg/ml	***	6h 0 µg/ml vs 2h 0.3µg/ml	***
2h 0 µg/ml vs 6h 0 µg/ml	***	4h 0µg/ml vs 2h 0.3 µg/ml	***	6h 0 µg/ml vs 4h 0.3µg/ml	***
2h 0 µg/ml vs 2h 0.3µg/ml	***	4h 0 µg/ml vs 4h 0.3µg/ml	***	6h 0µg/ml vs 6h 0.3 µg/ml	***
2h 0 µg/ml vs 4h 0.3µg/ml	***	4h 0 µg/ml vs 6h 0.3 µg/ml	***	6h 0 µg/ml vs 2h 3 µg/ml	***
2h 0 µg/ml vs 6h 0.3µg/ml	***	4h 0 µg/ml vs 2h 3 µg/ml	***	6h 0 µg/ml vs 4h 3 µg/ml	***
2h 0 µg/ml vs 2h 3 µg/ml	***	4h 0 µg/ml vs 4h 3 µg/ml	***	6h 0 µg/ml vs 6h 3 µg/ml	***
2h 0 µg/ml vs 4h 3 µg/ml	***	4h 0µ g/ml vs 6h 3 µg/ml	***	6h 0 µg/ml vs 2h 30 µg/ml	***
2h 0 µg/ml vs 6h 3µg/ml	***	4h 0 µg/ml vs 2h 30 µg/ml	***	6h 0 µg/ml vs 4h 30 µg/ml	***
2h 0 µg/ml vs 2h 30µg/ml	***	4h 0 µg/ml vs 4h 30 µg/ml	***	6h 0 µg/ml vs 6h 30 µg/ml	***
2h 0 µg/ml vs 4h 30 µg/ml	***	4h 0 µg/ml vs 6h 30 µg/ml	***	6h 0.3 µg/ml vs 2h 3µg/ml	***
2h 0 µg/ml vs 6h 30 µg/ml	***	4h 0.3µg/ml vs 6h 0.3µg/ml	***	6h 0.3 µg/ml vs 4h 3µg/ml	***
2h 0.3µ g/ml vs 4h 0.3µg/ml	***	4h 0.3 µg/ml vs 2h 3 µg/ml	***	6h 0.3 µg/ml vs 6h 3µg/ml	ns
2h 0.3 µg/ml vs 6h 0.3µg/ml	***	4h 0.3 µg/ml vs 4h 3 µg/ml	ns	6h 0.3 µg/ml vs 2h 30 µg/ml	***
2h 0.3 µg/ml vs 2h 3 µg/ml	ns	4h 0.3 µg/ml vs 6h 3 µg/ml	***	6h 0.3 µg/ml vs 4h 30 µg/ml	***
2h 0.3 µg/ml vs 4h 3 µg/ml	***	4h 0.3 µg/ml vs 2h 30 µg/ml	***	6h 0.3 µg/ml vs 6h 30 µg/ml	**
2h 0.3 µg/ml vs 6h 3 µg/ml	***	4h 0.3 g/ml vs 4h 30 g/ml	ns	6h 3 µg/ml vs 2h 30 µg/ml	***
2h 0.3 µg/ml vs 2h 30 µg/ml	ns	4h 0.3µg/ml vs 6h 30 µg/ml	***	6h 3 µg/ml vs 4h 30 µg/ml	***
2h 0.3 µg/ml vs 4h 30 µg/ml	***	4h 3 µg/ml vs 6h 3 µg/ml	***	6h 3 µg/ml vs 6h 30 µg/ml	ns
2h 0.3 µg/ml vs 6h 30 µg/ml	***	4h 3 µg/ml vs 2h 30 µg/ml	***		
2h 3 µg/ml vs 4h 3 µg/ml	***	4h 3 µg/ml vs 4h 30 µg/ml	ns		
2h 3 µg/ml vs 6h 3 µg/ml	***	4h 3 µg/ml vs 6h 30 µg/ml	***		
2h 3 µg/ml vs 2h 30 µg/ml	ns	4h 30 µg/ml vs 6h 30 µg/ml	***		
2h 3 µg/ml vs 4h 30 µg/ml	***				
2h 3 µg/ml vs 6h 30 µg/ml	***				

2h 30 µg/ml vs 4h 30 µg/ml	***			
2h 30 µg/ml vs 6h 30 µg/ml	***			



2h 0 µg/ml vs 4h 0 g/ml	ns	4h 0 µg/ml vs 6h 0 µg/ml	ns	6h 0 µg/ml vs 2h 0.3µg/ml	***
2h 0 µg/ml vs 6h 0 g/ml	ns	4h 0 µg/ml vs 2h 0.3µg/ml	***	6h 0 µg/ml vs 4h 0.3µg/ml	***
2h 0 µg/ml vs 2h 0.3 g/ml	***	4h 0 µg/ml vs 4h 0.3µg/ml	***	6h 0 µg/ml vs 6h 0.3µg/ml	***
2h 0 µg/ml vs 4h 0.3 g/ml	***	4h 0 µg/ml vs 6h 0.3µg/ml	***	6h 0 µg/ml vs 2h 3 µg/ml	***
2h 0 µg/ml vs 6h 0.3 g/ml	***	4h 0 µg/ml vs 2h 3 µg/ml	***	6h 0 µg/ml vs 4h 3 g/ml	***
2h 0 µg/ml vs 2h 3 µg/ml	***	4h 0 µg/ml vs 4h 3 µg/ml	***	6h 0 µg/ml vs 6h 3 µg/ml	***
2h 0 µg/ml vs 4h 3 µg/ml	***	4h 0 µg/ml vs 6h 3 µg/ml	***	6h 0 µg/ml vs 2h 30 µg/ml	***
2h 0 µg/ml vs 6h 3 µg/ml	***	4h 0 µg/ml vs 2h 30 µg/ml	***	6h 0 µg/ml vs 4h 30 µg/ml	***
2h 0 µg/ml vs 2h 30 µg/ml	***	4h 0 µg/ml vs 4h 30 µg/ml	***	6h 0 µg/ml vs 6h 30 µg/ml	***
2h 0 µg/ml vs 4h 30 µg/ml	***	4h 0 µg/ml vs 6h 30 µg/ml	***	6h 0.3 g/ml vs 2h 3 µg/ml	**
2h 0 µg/ml vs 6h 30 µg/ml	***	4h 0.3 µg/ml vs 6h 0.3µg/ml	ns	6h 0.3 µg/ml vs 4h 3µg/ml	ns
2h 0.3 µg/ml vs 4h 0.3µg/ml	**	4h 0.3 µg/ml vs 2h 3µg/ml	ns	6h 0.3 µg/ml vs 6h 3µg/ml	*
2h 0.3 µg/ml vs 6h 0.3µg/ml	***	4h 0.3 µg/ml vs 4h 3µg/ml	ns	6h 0.3 µg/ml vs 2h 30µg/ml	*
2h 0.3 µg/ml vs 2h 3 µg/ml	ns	4h 0.3 µg/ml vs 6h 3µg/ml	***	6h 0.3 µg/ml vs 4h 30µg/ml	ns
2h 0.3 µg/ml vs 4h 3 µg/ml	***	4h 0.3µg/ml vs 2h 30 µg/ml	ns	6h 0.3 µg/ml vs 6h 30µg/ml	***

2h 0.3 µg/ml vs 6h 3 µg/ml	***	4h 0.3 µg/ml vs 4h 30µg/ml	**	6h 3 µg/ml vs 2h 30 µg/ml	***
2h 0.3 µg/ml vs 2h 30 g/ml	ns	4h 0.3 µg/ml vs 6h 30 µg/ml	***	6h 3 µg/ml vs 4h 30 µg/ml	ns
2h 0.3 µg/ml vs 4h 30 µg/ml	***	4h 3 µg/ml vs 6h 3 µg/ml	**	6h 3 µg/ml vs 6h 30 µg/ml	***
2h 0.3 µg/ml vs 6h 30 µg/ml	***	4h 3 µg/ml vs 2h 30 µg/ml	*		
2h 3 µg/ml vs 4h 3 µg/ml	**	4h 3 µg/ml vs 4h 30 µg/ml	*		
2h 3 µg/ml vs 6h 3 µg/ml	***	4h 3 µg/ml vs 6h 30 µg/ml	***		
2h 3 µg/ml vs 2h 30 µg/ml	ns	4h 30 µg/ml vs 6h 30 µg/ml	***		
2h 3 µg/ml vs 4h 30 µg/ml	***				
2h 3 µg/ml vs 6h 30 µg/ml	***				
2h 30 µg/ml vs 4h 30 µg/ml	***				
2h 30 µg/ml vs 6h 30 µg/ml	***				



2h 0 µg/ml vs 4h 0 µg/ml	ns	4h 0 µg/ml vs 6h 0 µg/ml	ns	6h 0 µg/ml vs 2h 0.3µg/ml	***
2h 0 µg/ml vs 6h 0 µg/ml	ns	4h 0 µg/ml vs 2h 0.3 µg/ml	***	6h 0 µg/ml vs 4h 0.3 vg/ml	***
2h 0 µg/ml vs 2h 0.3 g/ml	***	4h 0 µg/ml vs 4h 0.3 µg/ml	***	6h 0 µg/ml vs 6h 0.3 µg/ml	***
2h 0 µg/ml vs 4h 0.3 µg/ml	***	4h 0µg/ml vs 6h 0.3 µg/ml	***	6h 0 µg/ml vs 2h 3 µg/ml	***
2h 0 µg/ml vs 6h 0.3 µg/ml	***	4h 0 µg/ml vs 2h 3 µg/ml	***	6h 0 µg/ml vs 4h 3 µg/ml	***
2h 0 µg/ml vs 2h 3 µg/ml	***	4h 0 µg/ml vs 4h 3 µg/ml	***	6h 0 µg/ml vs 6h 3 µg/ml	***
2h 0 µg/ml vs 4h 3 µg/ml	***	4h 0 µg/ml vs 6h 3 µg/ml	***	6h 0 µg/ml vs 2h 30 µg/ml	***
2h 0 µg/ml vs 6h 3 µg/ml	***	4h 0 µg/ml vs 2h 30 µg/ml	***	6h 0 µg/ml vs 4h 30 µg/ml	***
2h 0 µg/ml vs 2h 30 g/ml	***	4h 0 µg/ml vs 4h 30 µg/ml	***	6h 0 µg/ml vs 6h 30 µg/ml	***
2h 0 µg/ml vs 4h 30 µg/ml	***	4h 0 µg/ml vs 6h 30 µg/ml	***	6h 0.3 µg/ml vs 2h 3µg/ml	ns

2h 0 µg/ml vs 6h 30 µg/ml	***	4h 0.3 µg/ml vs 6h 0.3µg/ml	ns	6h 0.3 µg/ml vs 4h 3 µg/ml	ns
2h 0.3 g/ml vs 4h 0.3 µg/ml	***	4h 0.3 µg/ml vs 2h 3 µg/ml	ns	6h 0.3 µg/ml vs 6h 3 µg/ml	***
2h 0.3 µg/ml vs 6h 0.3µg/ml	*	4h 0.3 µg/ml vs 4h 3 µg/ml	ns	6h 0.3 µg/ml vs 2h 30 µg/ml	ns
2h 0.3 µg/ml vs 2h 3µg/ml	*	4h 0.3 µg/ml vs 6h 3 µg/ml	***	6h 0.3 µg/ml vs 4h 30µg/ml	***
2h 0.3 µg/ml vs 4h 3 µg/ml	***	4h 0.3 µg/ml vs 2h 30 µg/ml	*	6h 0.3 µg/ml vs 6h 30µg/ml	***
2h 0.3 µg/ml vs 6h 3µg/ml	***	4h 0.3 µg/ml vs 4h 30 µg/ml	*	6h 3 µg/ml vs 2h 30 µg/ml	***
2h 0.3 µg/ml vs 2h 30µg/ml	ns	4h 0.3 µg/ml vs 6h 30 µg/ml	***	6h 3 µg/ml vs 4h 30 µg/ml	*
2h 0.3 µg/ml vs 4h 30µg/ml	***	4h 3 µg/ml vs 6h 3 µg/ml	***	6h 3 µg/ml vs 6h 30 µg/ml	ns
2h 0.3 µg/ml vs 6h 30µg/ml	***	4h 3 µg/ml vs 2h 30 µg/ml	**		
2h 3 µg/ml vs 4h 3 µg/ml	ns	4h 3 µg/ml vs 4h 30 µg/ml	*		
2h 3 µg/ml vs 6h 3 µg/ml	***	4h 3 µg/ml vs 6h 30 µg/ml	***		
2h 3 µg/ml vs 2h 30 µg/ml	ns	4h 30 µg/ml vs 6h 30 µg/ml	***		
2h 3 µg/ml vs 4h 30 µg/ml	***				
2h 3 µg/ml vs 6h 30 µg/ml	***				
2h 30 µg/ml vs 4h 30µg/ml	***				
2h 30 µg/ml vs 6h 30µg/ml	***				

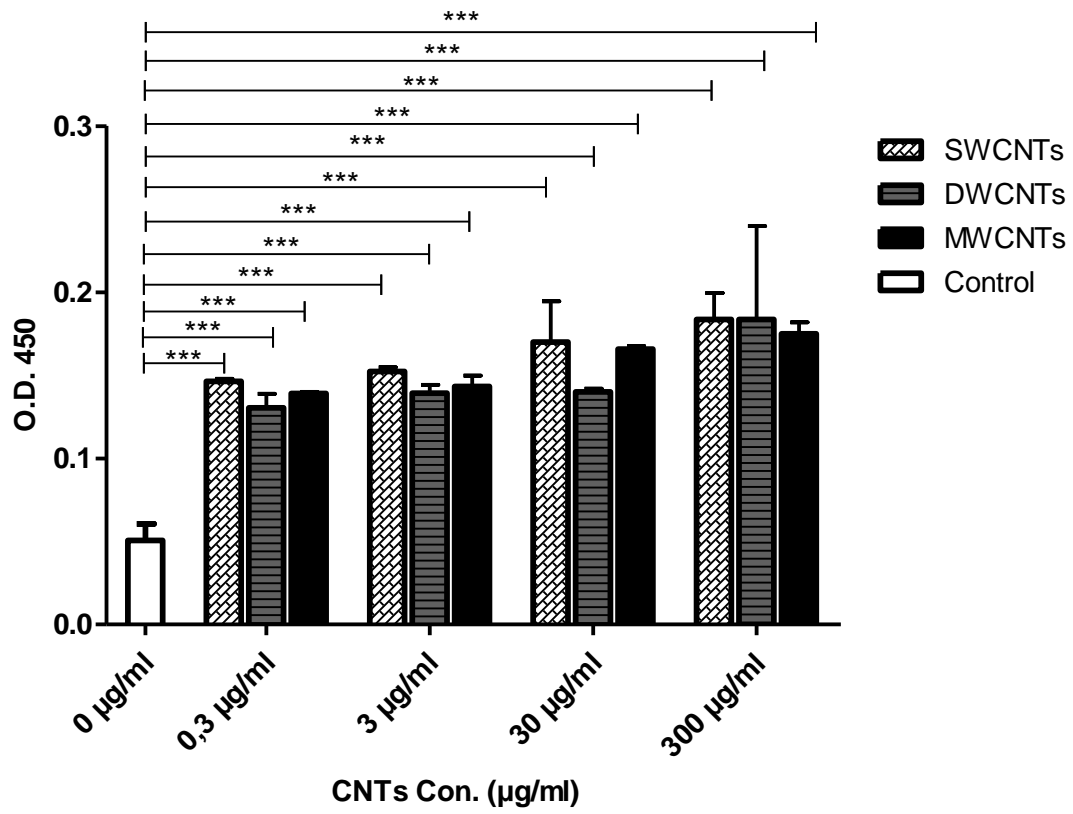
**Figure 19** Effects of different CNTs exposure on the cellular inflammation in A549 cells. Following treatment with CNTs at 0.3, 3, and 30µg/mL, IL-8 levels were measured in the supernatant of A549 cell culture at 2 (**A**), 4 (**B**), and 6 h (**C**). Results are expressed as mean ± SEM, and groups were compared using one way ANOVA followed by post-hoc Tukey test.

## 6.11 Cytotoxicity induced by carbon nanotubes

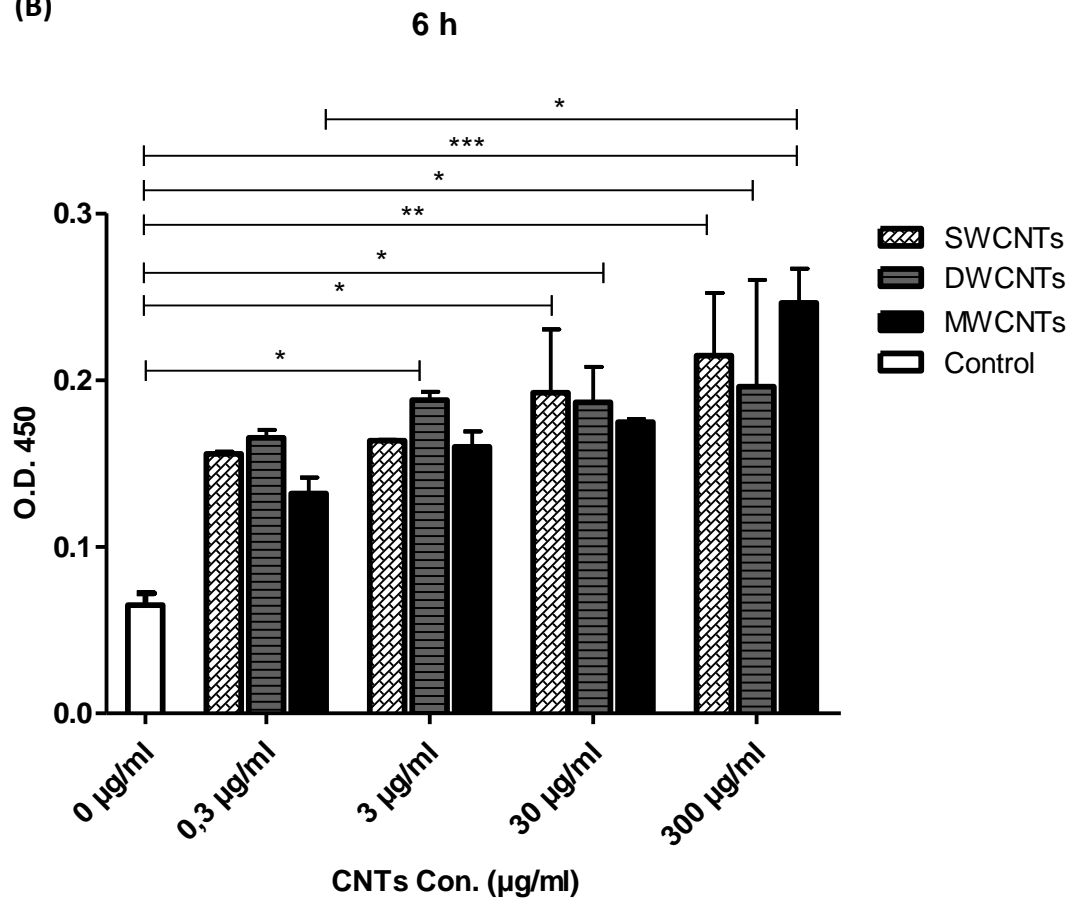
This method is based on determining the LDH enzyme which is released into the cytoplasm and then into cultural medium after the cell damage. The LDH content of supernatants from CNTs treated A549 cells is shown in (**Figure 20**). As indicated by LDH release, over the range of used doses, no evidence of increased toxicity was detected after 2 hours of incubation with CNTs at different doses (data not shown). However, after 4 h the levels of LDH were slightly increased with the increasing concentration, which coincides with a noted decrease of cell viability in response to different CNTs treatment (**Figure 20 A**). A significant increase in the cytotoxicity was found also after 6 h of treatment incubation compared to controls, and the highest increase was seen after exposure to 300 $\mu$ g/ml of MWCNTs (**Figure 20 B**). Moreover, there had been a significant reduction in cell viability compared to control culture observed after 24 h of cell incubation with CNTs, this was accompanied by the dose-time dependent increase in LDH levels (**Figure 20 C**).

(A)

4 h



(B)



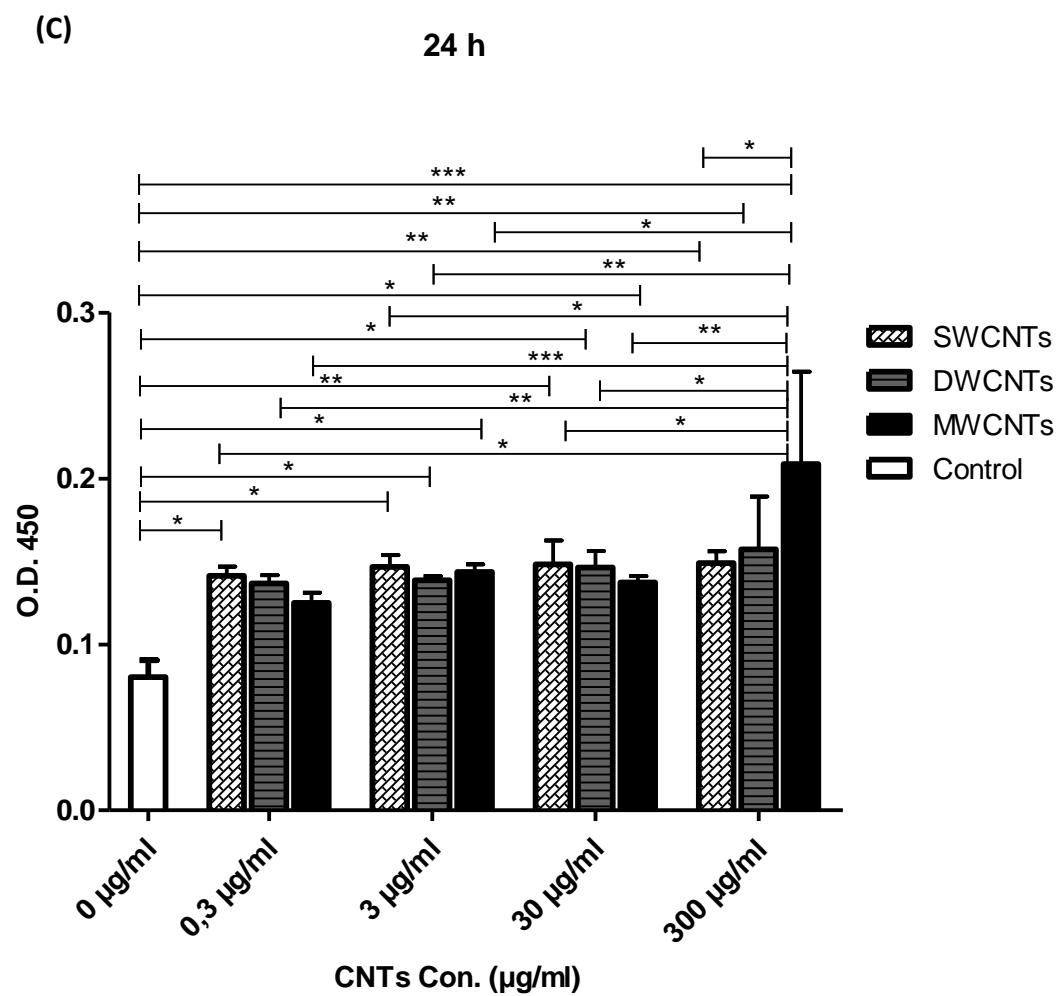
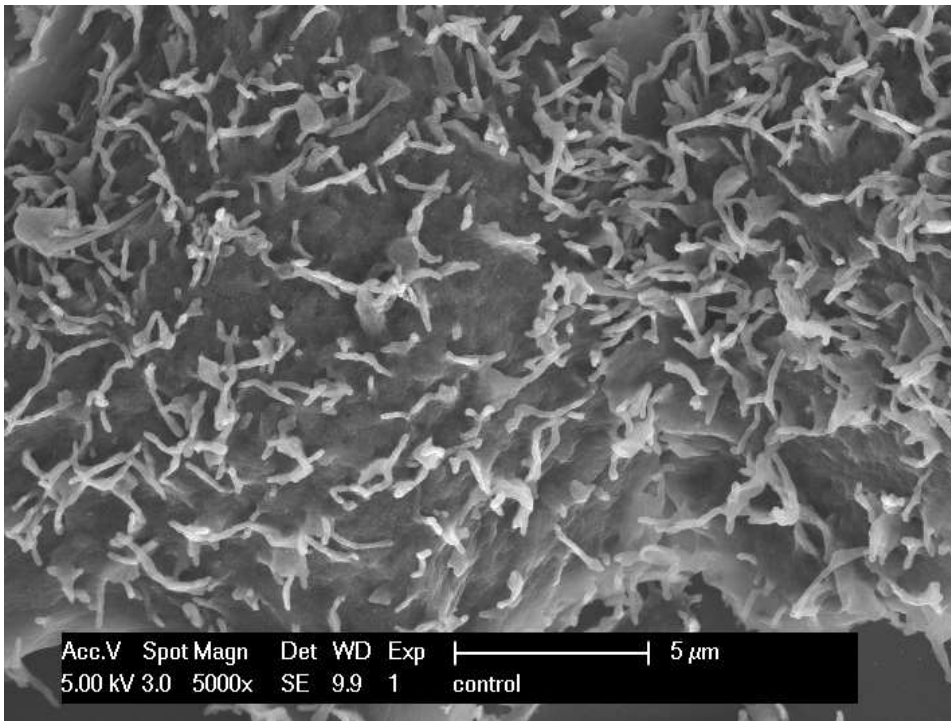
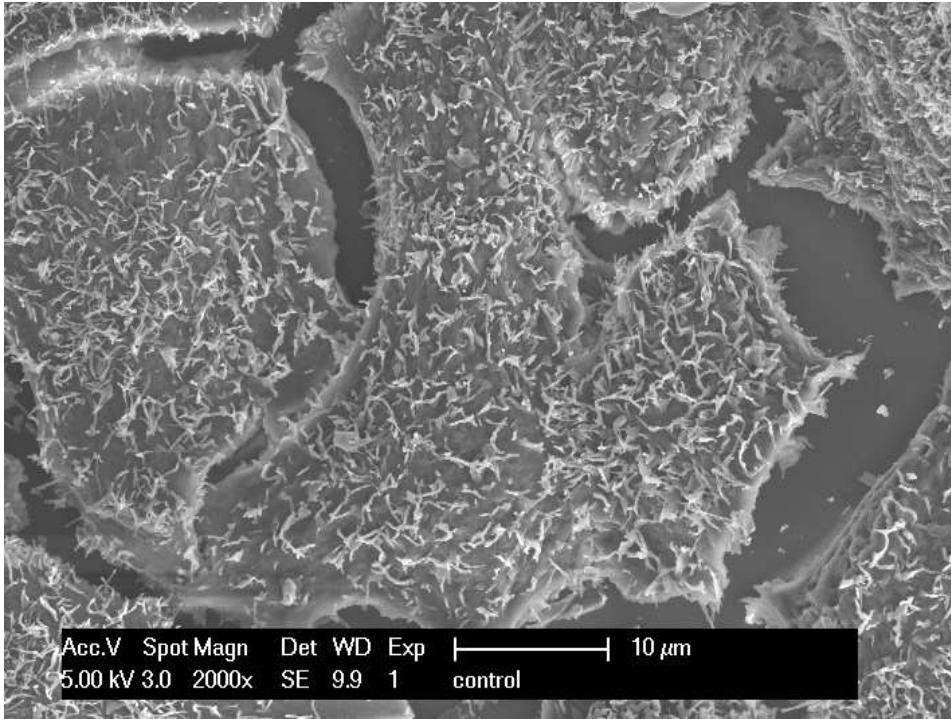


**Figure 20** LDH release (shown as O.D. 450) in the culture of A549 cells incubated with CNTs. Control cells were incubated in RPMI 1640 culture media containing 10% fetal calf serum and 1% penicillin/streptomycin. Treated cells were incubated with SWCNTs, DWCNTs and MWCNTs at (0.3, 3, 30, and 300µg/mL) for 4 (A), 6 (B), and 24 (C) h. Data are expressed as mean ± SEM. Significance between the groups was tested using one way ANOVA. Statistical significance was calculated by one-way analysis of variance (ANOVA) followed by Tukey’s test ( $p < 0.05$ ).

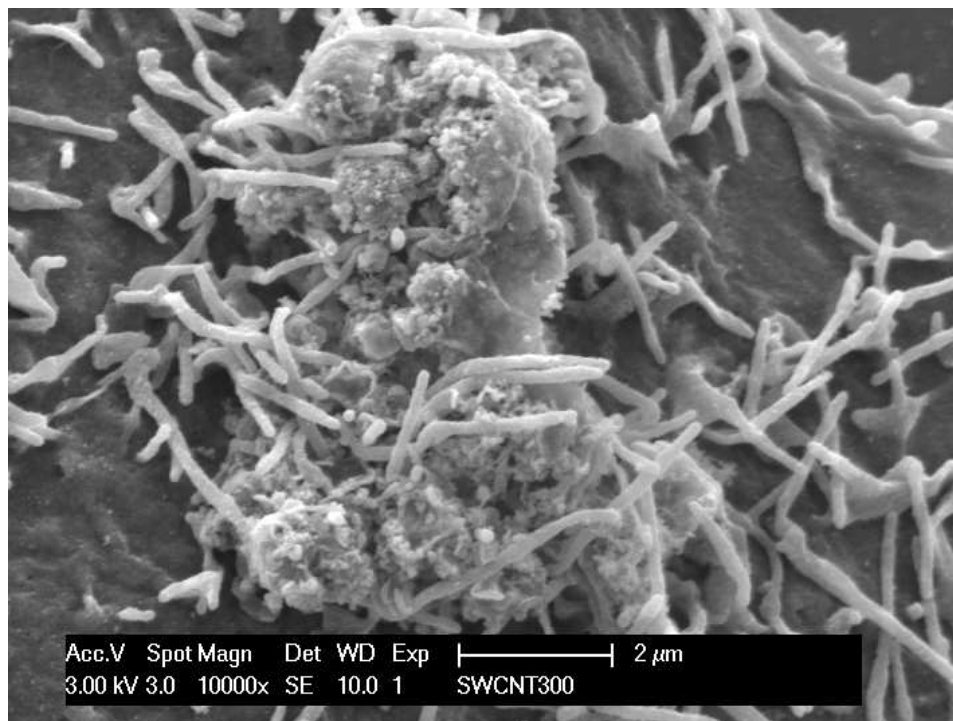
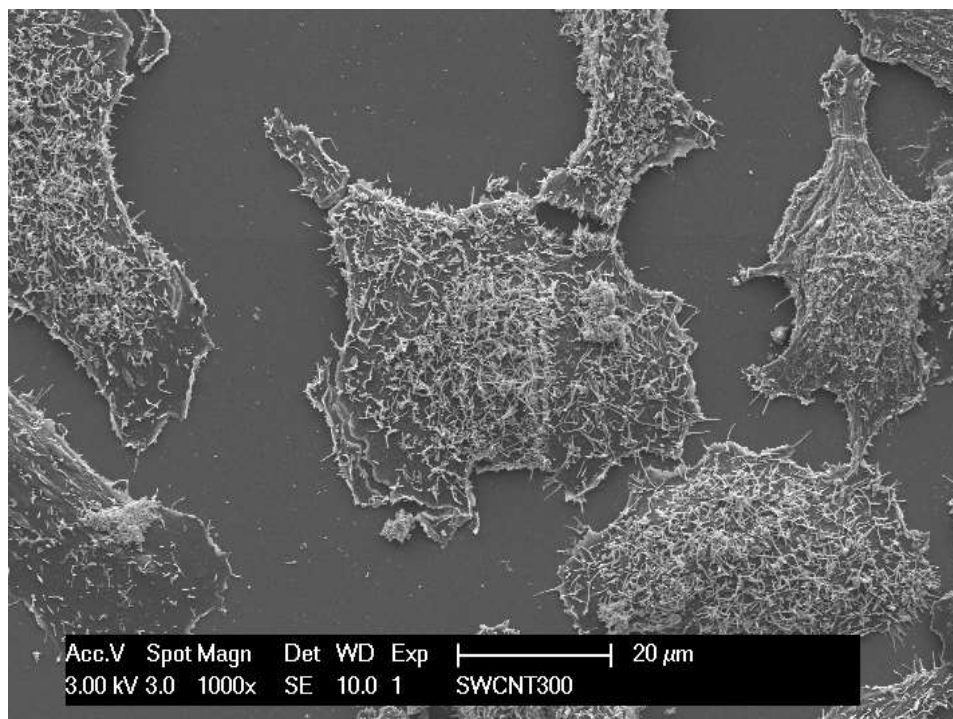
## 6.12 Carbon nanotubes challenge and-cell interaction

Scanning electron microscopy (SEM) analysis was conducted to show the cellular alterations induced after 4 hours of incubation with 3  $\mu\text{g/ml}$  CNTs. A549 control cell surface appeared covered by regular microvilli (**Figure 21 A**). Microvilli structure and blebs were also observed on the cell surface after incubation with 3  $\mu\text{g/ml}$  of SWCNTs, DWCNTs, and MWCNTs (**Figure 21 B, C, D**) respectively. More than one carbon nanotube agglomerate was seen entering into the cell, although this entry was more evident in cells exposed to DWCNTs (**Figure 21 C**). Moreover, SEM micrographs showed CNTs aggregates directly in contact with microvilli and located across the cell membrane, confirming their existence inside the cells. Similar results have been observed by the three carbon nanotubes configurations.

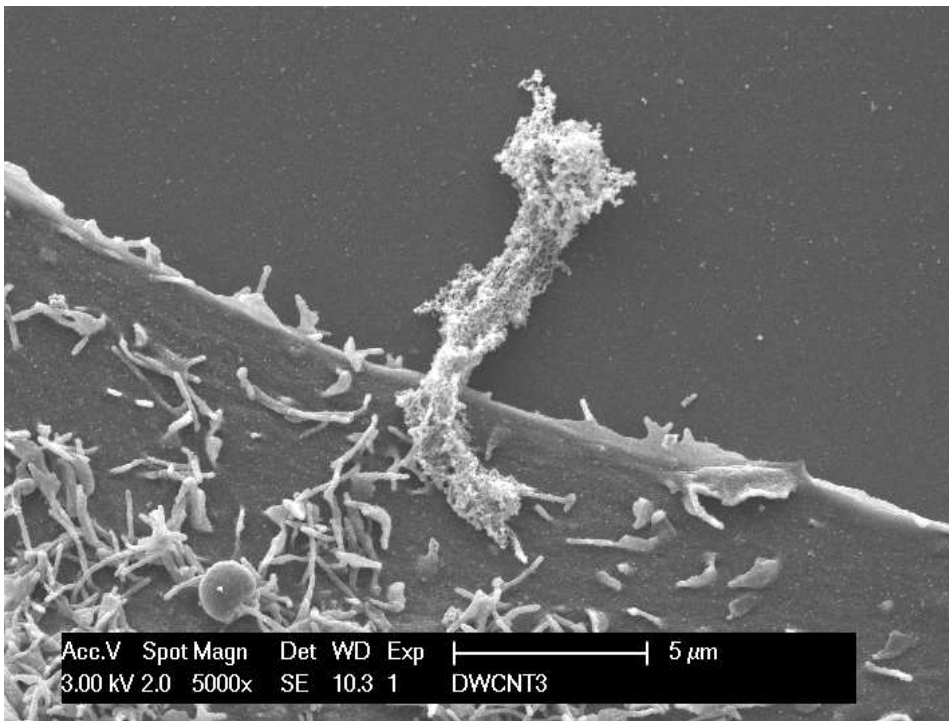
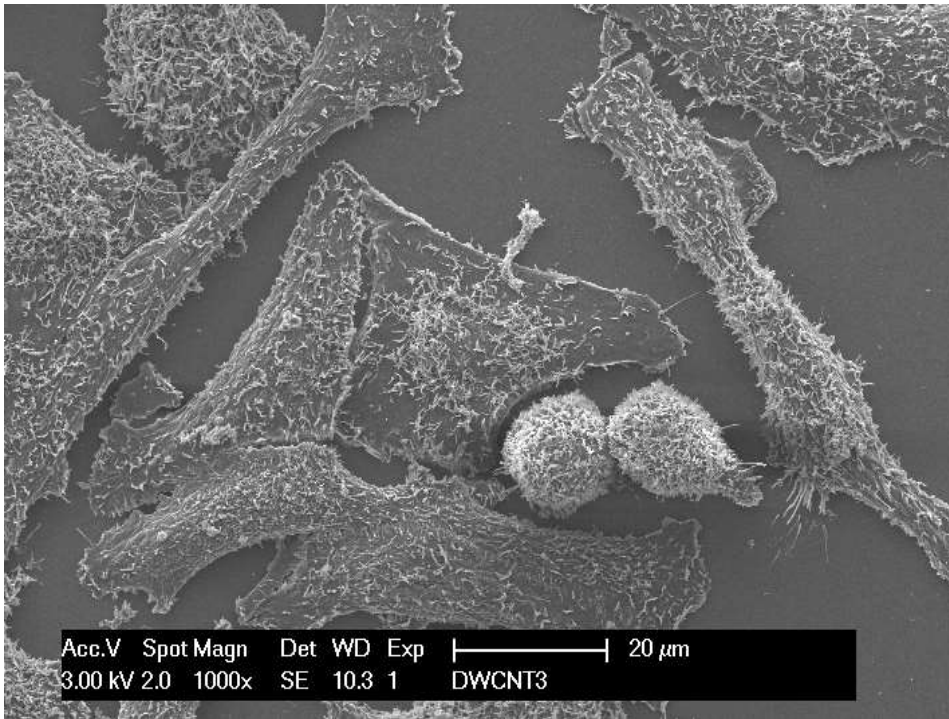
(A)



(B)



(c)



(D)

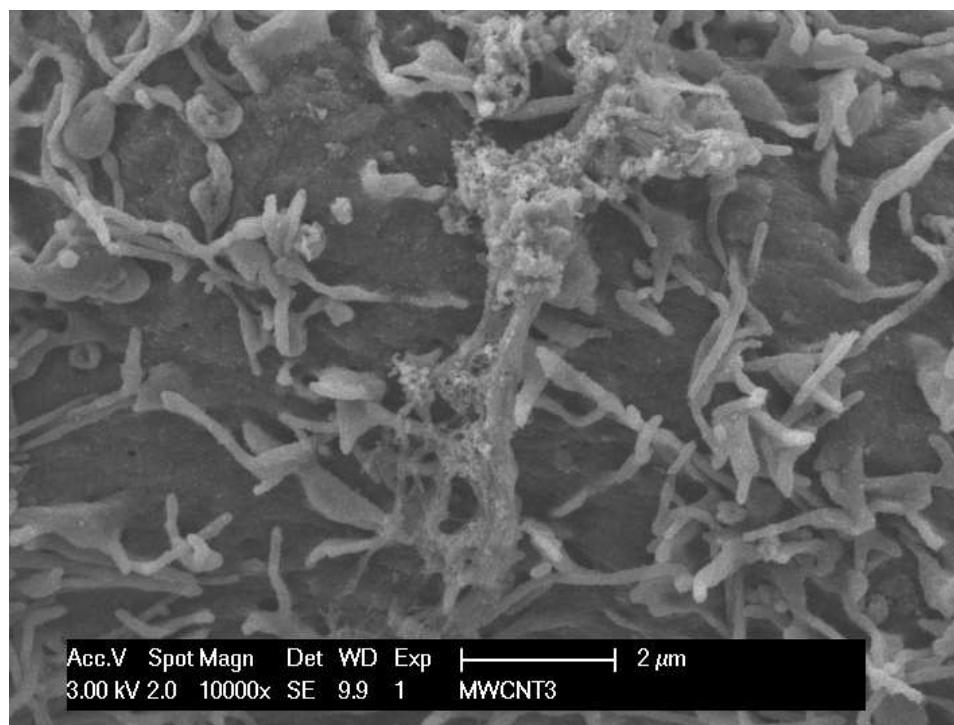
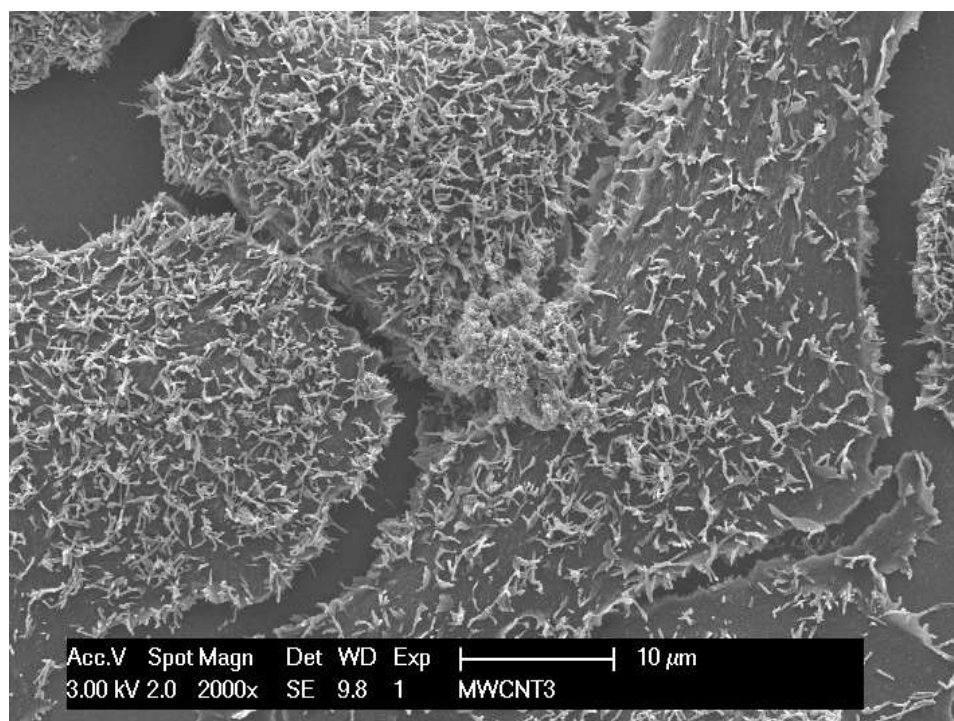


**Figure 21** SEM photographs of A549 cell line before and after incubation with CNTs. (A) control cells were incubated with medium alone. Treated cells were exposed to 3 μg/ml of SWCNTs (B), DWCNTs (C) and MWCNTs (D) for 4 hours. Arrows indicate the carbon nanotubes.

## 7. Discussion

Nanosize particles show greater deposition in the alveoli of individuals with chronic obstructive pulmonary disease (COPD) and asthma, where they might induce response or exacerbate disease [45]. The  $\text{TiO}_2$  has recently become part of our everyday life style [46]; accordingly, this compound and its derivative NPs are widely used in the fields of technology and medicine as well [46]. Additionally,  $\text{TiO}_2$  NPs might be found in cosmetics, sunscreens, toothpaste, paints, and food supplements. When inhaled, these particles have been classified as Group 2B carcinogen by the International Agency for Research on Cancer (IARC).

Mishra et al. [23] reported that  $\text{TiO}_2$  NPs increased allergic airway inflammation and Socs3 expression via the NF- $\kappa$ B pathway in a mouse model of asthma. Moreover, Kim et al. [47] demonstrated inflammasome activation in asthmatic lungs after  $\text{TiO}_2$  NP exposure, suggesting the probable contributive influence of targeting the inflammasome on controlling the airway inflammation induced by NPs. In a human study performed by Heller et al. (2018), the pigment-grade  $\text{TiO}_2$  NPs, when inhaled and ingested, were reported to be associated with chronic inflammatory degenerative diseases. The authors also demonstrated that pancreatic  $\text{TiO}_2$  pigment nanocrystals could enter the bloodstream and were associated with type II diabetes mellitus [48].

In line with previous reports in the OVA mouse model, our findings indicated that intranasal exposure to  $\text{TiO}_2$  NPs increased the AHR measured during MCh administration. Moreover,  $\text{TiO}_2$  NPs were able to enhance eosinophil infiltration in the lungs of asthmatic mice, in comparison to those in the controls. Eosinophil is well recognized as a major effector cell in the asthmatic airways. Interestingly, their significant elevation is reported to be associated with extreme allergic reactions [49]. Our results also revealed a significant neutrophil influx in the non-allergic mice in comparison to that in the PBS controls.

Neutrophils and their products are the key mediators of the inflammatory alterations observed in the airways [50]. This neutrophilic influx is the essential feature of TiO<sub>2</sub> NPs-induced inflammation in the PBS control mice, therefore, high-dose TiO<sub>2</sub> NP inhalation may also have occupational consequences for non-asthmatics.

In addition, TiO<sub>2</sub> NPs significantly increased the number of goblet cells and consequently mucus secretion in the OVA/TiO<sub>2</sub>/OVA mice, compared to that in the OVA/OVA ones. The significant increase in the serum levels of IL-4 and IL-13 in the OVA/TiO<sub>2</sub>/OVA group was indicative of a strong Th2 response to TiO<sub>2</sub> NPs exposure. Nonetheless, no alterations in IFN- $\gamma$  levels were observed; therefore, Th1 was not involved. The OVA-treated mice showed higher total IgE levels following TiO<sub>2</sub> NPs exposure; however, this increase was not significant.

Our results are consistent with the previous published reports which show the local effects of TiO<sub>2</sub> NPs on airway inflammation [23,51-54].

However, to date, the research that has addressed the biodistribution of TiO<sub>2</sub> NPs into mice organs after intranasal administration are limited. Therefore, the current work was conducted to describe the systemic uptake of TiO<sub>2</sub> NPs and their translocation into extrapulmonary organs. Our findings indicated that intranasally administered TiO<sub>2</sub> NPs translocated through the lungs and accumulated in the organs (i.e., liver, spleen, kidney, brain, stomach, and heart) as examined by SEM-EDX followed by ICP-MS. These particles are small enough to pass through the respiratory tissues into the bloodstream to disseminate into distant organs [55][56]. In addition, the detection of TiO<sub>2</sub> NPs in the brain tissue was indicative of the ability of these particles to pass across the blood-brain barrier into the central nervous system following intranasal application, probably via the olfactory bulb by neuronal transport [57] [58].

Furthermore, the present study was the first describing the combination of *in vitro* and *in vivo* uptake of TiO<sub>2</sub> NPs by alveolar macrophages. Based on the evidence, the NPs have the ability to

activate phagocytic cells, like macrophages, to take them up. The halos around the macrophages with less NPs precipitation, as well as the macrophage morphological changes, seem to be the result of phagocytic activity [59]. This was confirmed by *in vivo* studies (using SEM) showing TiO<sub>2</sub> NPs inside the BALF-macrophages of NPs-exposed mice.

Our data also revealed the presence of TiO<sub>2</sub> NPs aggregates both inside and outside the cells at different time points. This supports the results of our DLS measurements indicating the instability of TiO<sub>2</sub> NPs and their aggregation/agglomeration over time.

Together, the inhalation of nanosized TiO<sub>2</sub>, in combination with OVA, aggravates asthmatic features. The asthmatic exacerbation induced by TiO<sub>2</sub> NPs is mainly eosinophilic-mediated and enhanced by goblet cell hyperplasia, mucus hypersecretion, increased cytokine levels, and AHR. In view of the findings presented in this study, TiO<sub>2</sub> NPs alone did not induce strong inflammatory response and asthmatic features in the healthy mice (i.e., non-asthmatics). However, the ability of these particles to translocate from the lungs into different organs underscores the need for assessing the risk and harmful toxicological potential of these particles in human health. Our data could provide implications for human health, particularly for asthmatic individuals. Based on our findings, it is recommended that the individuals suffering from asthma or other respiratory diseases (e.g., COPD) limit their exposure to products contain TiO<sub>2</sub> NPs. These results carry important implications for occupational and environmental health policy, especially for pre-existing asthmatic populations and workers in industries exposed to TiO<sub>2</sub> NPs products by various routes. In the second part of our study, other type of interesting nanomaterials was studied; carbon nanotubes (CNTs) are a group of carbon allotropes with interesting characteristics that make them productive materials in many disciplines of nanotechnology including optics and therapeutics, healthcare domains and electronics equipment [60].

CNTs are classified as single-walled carbon nanotubes (SWCNTs), double-walled carbon nanotubes (DWCNTs) and multi-walled carbon nanotubes (MWCNTs) depending on the number of carbon sidewalls present and the way they are arranged.

*In vitro* comparative studies of the SWCNTs, DWCNTs and MWCNT toxicity are few. The purpose of this study is to investigate the biological effects of a range of nanomaterials in order to gain an understanding of the mechanisms by which carbon nanotubes of varying dimensions interact with A549 cells.

To characterize the level of CNTs-induced inflammation, IL-8 levels were measured at 2, 4, and 6 hours from the media supernatant of A549 cultures using ELISA. The dose 0.3 $\mu$ g/ml of all CNTs was sufficient to induce cellular inflammation as compared to controls. IL-8 levels remained almost the same as SWCNTs concentrations increased from 0.3 to 3 and 30  $\mu$ g/ml during the same time point. Which indicates that the increase was time dependent and dose independent.

Interestingly, our findings were found to be similar to the results seen with DWCNTs and MWCNTs, except those after 4 and 6 hours; where IL-8 levels were increased in a dose-and-time dependent manner. For the longer exposure (6 h) at the higher concentration (30  $\mu$ g/ml) of all CNTs, the maximum IL-8 level and inflammatory response was found. Our results are in line with previous reports, which indicated that MWCNTs are able to induce expression of IL-8 in A549 cells, mediated by NF- $\kappa$ B and oxidative activation [61], furthermore, our studies compare IL-8 secretion for all the three various types of carbon nanomaterials in different time points and different doses.

In addition, our existing data suggest that the studied industrial CNTs have a toxic effect, causing the cell damage and apoptosis, as revealed by LDH level as a marker of cell death. Adding CNTs to the A549 culture caused a small statistically significant decrease in cell viability after 4, 6 hours as marked increase in LDH levels. However, this increase was significantly higher after 24 hours

in a dose- and time dependent manner. This was in agreement with Cavallo et al. and Kim et al. [62][63] who concentrated only on MWCNTs in their studies and demonstrated their ability to induce cell growth inhibition and genotoxicity.

In a similar context, Murr et al. and Palomaki et al. reported decreased cell viability when exposed to CNTs, without any quantitative differences between single- double- and multiwalled nanotubes [64][65].

Moreover, our SEM images showed CNTs aggregates located across the plasma membrane and in association with the microvilli, confirming their presence inside the cell and suggesting a rapid cellular uptake within 4 hours cell. This was consistent with the data published by Fraczek-Szczypta et al. showing a possible agglomeration of MWCNTs surrounded by different cells releasing toxics [66].

The particle entering may occur directly through membrane halos as reported previously [62] [67]. Other researches have reported the endocytosis as the cellular uptake mechanism of CNTs [68]. They penetrate through the cellular lipid bilayer membrane of cellular walls that may lead to the inflammation and also cytotoxicity.

Similar results have been observed by a study on A549 cells exposed to MWCNTs [69], reporting that negatively charged MWCNTs may facilitate their transport through the cell membrane. These findings are consistent with the published reports revealing several mechanisms to show MWCNTs enter into cells by uptake mechanisms [62,66,70,71], which have been suggested that together the size and shape of nanomaterials could affect the cellular uptake pathways [72][73].

Finally, we presented for the first time, interesting comparative experiments between single, double and multi-walled carbon nanotubes in cell culture environment.

According to our obtained results, all types of carbon nanotubes have toxic side effects on A549 cell line, but the manifestations and mechanisms remain poorly understood, which must be considered in the future in comparative toxicological studies.

## 8. Conclusion

Our data revealed the presence of TiO<sub>2</sub> NPs aggregates both inside and outside the cells at different time points. This supports the results of our DLS measurements indicating the instability of TiO<sub>2</sub> NPs and their aggregation/agglomeration over time.

Together, the inhalation of nanosized TiO<sub>2</sub>, in combination with OVA, aggravates asthmatic features. The asthmatic exacerbation induced by TiO<sub>2</sub> NPs is mainly eosinophilic-mediated and enhanced by goblet cell hyperplasia, mucus hypersecretion, increased cytokine levels, and AHR. In view of the findings presented in this study, TiO<sub>2</sub> NPs alone did not induce strong inflammatory response and asthmatic features in the healthy mice (i.e., non-asthmatics). However, the ability of these particles to translocate from the lungs into different organs underscores the need for assessing the risk and harmful toxicological potential of these particles in human health. Our data could provide implications for human health, particularly for asthmatic individuals. Based on our findings, it is recommended that the individuals suffering from asthma or other respiratory diseases (e.g., COPD) limit their exposure to products contain TiO<sub>2</sub> NPs. These results carry important implications for occupational and environmental health policy, especially for pre-existing asthmatic populations and workers in industries exposed to TiO<sub>2</sub> NPs products by various routes. In the second part of our study, another type of interesting nanomaterials was studied; carbon nanotubes (CNTs) are a group of carbon allotropes with interesting characteristics that make them productive materials in many disciplines of nanotechnology including optics and therapeutics, healthcare domains and electronics equipment [60].

## 9. References

1. Sahin-Yilmaz A, Naclerio RM: Anatomy and physiology of the upper airway. *Proc Am Thorac Soc* 2011, 8: 31-39.
2. van CP, Sys L, De BT, Watelet JB: Anatomy and physiology of the nose and the paranasal sinuses. *Immunol Allergy Clin North Am* 2004, 24: 1-17.
3. Widdicombe J: Physiologic control. Anatomy and physiology of the airway circulation. *Am Rev Respir Dis* 1992, 146: S3-S7.
4. Mei D, Tan WSD, Wong WSF: Pharmacological strategies to regain steroid sensitivity in severe asthma and COPD. *Curr Opin Pharmacol* 2019, 46: 73-81.
5. Fanta CH: Asthma. *N Engl J Med* 2009, 360: 1002-1014.
6. Duerr CU, McCarthy CD, Mindt BC, Rubio M, Meli AP, Pothlichet J *et al.*: Type I interferon restricts type 2 immunopathology through the regulation of group 2 innate lymphoid cells. *Nat Immunol* 2016, 17: 65-75.
7. Holgate ST, Arshad HS, Roberts GC, Howarth PH, Thurner P, Davies DE: A new look at the pathogenesis of asthma. *Clin Sci (Lond)* 2009, 118: 439-450.
8. Lambrecht BN, Hammad H: The airway epithelium in asthma. *Nat Med* 2012, 18: 684-692.
9. Heck S, Nguyen J, Le DD, Bals R, Dinh QT: Pharmacological Therapy of Bronchial Asthma: The Role of Biologicals. *Int Arch Allergy Immunol* 2015, 168: 241-252.
10. Omlor AJ, Le DD, Schlicker J, Hannig M, Ewen R, Heck S *et al.*: Local Effects on Airway Inflammation and Systemic Uptake of 5 nm PEGylated and Citrated Gold Nanoparticles in Asthmatic Mice. *Small* 2017, 13.
11. Beck-Broichsitter M, Thieme M, Nguyen J, Schmehl T, Gessler T, Seeger W *et al.*: Novel 'nano in nano' composites for sustained drug delivery: biodegradable nanoparticles encapsulated into nanofiber non-wovens. *Macromol Biosci* 2010, 10: 1527-1535.
12. Nguyen J, Reul R, Betz T, Dayyoub E, Schmehl T, Gessler T *et al.*: Nanocomposites of lung surfactant and biodegradable cationic nanoparticles improve transfection efficiency to lung cells. *J Control Release* 2009, 140: 47-54.
13. Puglia C, Santonocito D: Cosmeceuticals: Nanotechnology-Based Strategies for the Delivery of Phytocompounds. *Curr Pharm Des* 2019, 25: 2314-2322.
14. Deci MB, Liu M, Dinh QT, Nguyen J: Precision engineering of targeted nanocarriers. *Wiley Interdiscip Rev Nanomed Nanobiotechnol* 2018.

15. Omlor AJ, Nguyen J, Bals R, Dinh QT: Nanotechnology in respiratory medicine. *Respir Res* 2015, 16: 64.
16. Nguyen J, Walsh CL, Motion JP, Perttu EK, Szoka F: Controlled nucleation of lipid nanoparticles. *Pharm Res* 2012, 29: 2236-2248.
17. Gatti AM, Kirkpatrick J, Gambarelli A, Capitani F, Hansen T, Eloy R *et al.*: ESEM evaluations of muscle/nanoparticles interface in a rat model. *J Mater Sci Mater Med* 2008, 19: 1515-1522.
18. Kim BG, Lee PH, Lee SH, Park MK, Jang AS: Effect of TiO<sub>2</sub> Nanoparticles on Inflammasome-Mediated Airway Inflammation and Responsiveness. *Allergy Asthma Immunol Res* 2017, 9: 257-264.
19. Su M, Zhang Y, Liu G, Xu L, Zhang L, Yang Z: Urban ecosystem health assessment: perspectives and Chinese practice. *Int J Environ Res Public Health* 2013, 10: 5874-5885.
20. Ko JW, Shin NR, Je-Oh L, Jung TY, Moon C, Kim TW *et al.*: Silica dioxide nanoparticles aggravate airway inflammation in an asthmatic mouse model via NLRP3 inflammasome activation. *Regul Toxicol Pharmacol* 2020, 112: 104618.
21. Donaldson K, Tran L, Jimenez LA, Duffin R, Newby DE, Mills N *et al.*: Combustion-derived nanoparticles: a review of their toxicology following inhalation exposure. *Part Fibre Toxicol* 2005, 2: 10.
22. Nel A: Atmosphere. Air pollution-related illness: effects of particles. *Science* 2005, 308: 804-806.
23. Mishra V, Baranwal V, Mishra RK, Sharma S, Paul B, Pandey AC: Titanium dioxide nanoparticles augment allergic airway inflammation and Socs3 expression via NF-kappaB pathway in murine model of asthma. *Biomaterials* 2016, 92: 90-102.
24. Mizutani N, Nabe T, Yoshino S: Exposure to multiwalled carbon nanotubes and allergen promotes early- and late-phase increases in airway resistance in mice. *Biol Pharm Bull* 2012, 35: 2133-2140.
25. Mitchell LA, Gao J, Wal RV, Gigliotti A, Burchiel SW, McDonald JD: Pulmonary and systemic immune response to inhaled multiwalled carbon nanotubes. *Toxicol Sci* 2007, 100: 203-214.
26. Kinaret P, Ilves M, Fortino V, Rydman E, Karisola P, Lahde A *et al.*: Inhalation and Oropharyngeal Aspiration Exposure to Rod-Like Carbon Nanotubes Induce Similar Airway Inflammation and Biological Responses in Mouse Lungs. *ACS Nano* 2017, 11: 291-303.
27. Cavallo D, Fanizza C, Ursini CL, Casciardi S, Paba E, Ciervo A *et al.*: Multi-walled carbon nanotubes induce cytotoxicity and genotoxicity in human lung epithelial cells. *J Appl Toxicol* 2012, 32: 454-464.

28. El-Gazzar AM, Abdelgied M, Alexander DB, Alexander WT, Numano T, Iigo M *et al.*: Comparative pulmonary toxicity of a DWCNT and MWCNT-7 in rats. *Arch Toxicol* 2019, 93: 49-59.
29. Murr LE, Garza KM, Soto KF, Carrasco A, Powell TG, Ramirez DA *et al.*: Cytotoxicity assessment of some carbon nanotubes and related carbon nanoparticle aggregates and the implications for anthropogenic carbon nanotube aggregates in the environment. *Int J Environ Res Public Health* 2005, 2: 31-42.
30. Magrez A, Kasas S, Salicio V, Pasquier N, Seo JW, Celio M *et al.*: Cellular toxicity of carbon-based nanomaterials. *Nano Lett* 2006, 6: 1121-1125.
31. Manna SK, Sarkar S, Barr J, Wise K, Barrera EV, Jejelowo O *et al.*: Single-walled carbon nanotube induces oxidative stress and activates nuclear transcription factor-kappaB in human keratinocytes. *Nano Lett* 2005, 5: 1676-1684.
32. Maynard AD, Baron PA, Foley M, Shvedova AA, Kisin ER, Castranova V: Exposure to carbon nanotube material: aerosol release during the handling of unrefined single-walled carbon nanotube material. *J Toxicol Environ Health A* 2004, 67: 87-107.
33. Cousins DJ, Lee TH, Staynov DZ: Cytokine coexpression during human Th1/Th2 cell differentiation: direct evidence for coordinated expression of Th2 cytokines. *J Immunol* 2002, 169: 2498-2506.
34. Georas SN, Guo J, De FU, Casolaro V: T-helper cell type-2 regulation in allergic disease. *Eur Respir J* 2005, 26: 1119-1137.
35. Gandhi VD, Vliagoftis H: Airway epithelium interactions with aeroallergens: role of secreted cytokines and chemokines in innate immunity. *Front Immunol* 2015, 6: 147.
36. Herz U, Braun A, Ruckert R, Renz H: Various immunological phenotypes are associated with increased airway responsiveness. *Clin Exp Allergy* 1998, 28: 625-634.
37. Joachim RA, Sagach V, Quarcoo D, Dinh T, Arck PC, Klapp BF: Upregulation of tumor necrosis factor-alpha by stress and substance p in a murine model of allergic airway inflammation. *Neuroimmunomodulation* 2006, 13: 43-50.
38. Hirayama D, Iida T, Nakase H: The Phagocytic Function of Macrophage-Enforcing Innate Immunity and Tissue Homeostasis. *Int J Mol Sci* 2017, 19.
39. Krpetic Z, Porta F, Caneva E, Dal S, V, Scari G: Phagocytosis of biocompatible gold nanoparticles. *Langmuir* 2010, 26: 14799-14805.
40. Geiser M, Kreyling WG: Deposition and biokinetics of inhaled nanoparticles. *Part Fibre Toxicol* 2010, 7: 2.
41. Nemmar A, Hoet PH, Vanquickenborne B, Dinsdale D, Thomeer M, Hoylaerts MF *et al.*: Passage of inhaled particles into the blood circulation in humans. *Circulation* 2002, 105: 411-414.

42. Xin W, Severino J, Venkert A, Yu H, Knorr D, Yang JM *et al.*: Fabrication and Characterization of Solid Composite Yarns from Carbon Nanotubes and Poly(dicyclopentadiene). *Nanomaterials (Basel)* 2020, 10.
43. Fujita K, Obara S, Maru J, Endoh S: Cytotoxicity profiles of multi-walled carbon nanotubes with different physico-chemical properties. *Toxicol Mech Methods* 2020, 1-36.
44. Baggiolini M, Clark-Lewis I: Interleukin-8, a chemotactic and inflammatory cytokine. *FEBS Lett* 1992, 307: 97-101.
45. Byrne JD, Baugh JA: The significance of nanoparticles in particle-induced pulmonary fibrosis. *Mcgill J Med* 2008, 11: 43-50.
46. Skocaj M, Filipic M, Petkovic J, Novak S: Titanium dioxide in our everyday life; is it safe? *Radiol Oncol* 2011, 45: 227-247.
47. Kim BG, Lee PH, Lee SH, Park MK, Jang AS: Effect of TiO<sub>2</sub> Nanoparticles on Inflammasome-Mediated Airway Inflammation and Responsiveness. *Allergy Asthma Immunol Res* 2017, 9: 257-264.
48. Heller A, Jarvis K, Coffman SS: Association of Type 2 Diabetes with Submicron Titanium Dioxide Crystals in the Pancreas. *Chem Res Toxicol* 2018, 31: 506-509.
49. Sampson AP: The role of eosinophils and neutrophils in inflammation. *Clin Exp Allergy* 2000, 30 Suppl 1: 22-27.
50. Jasper AE, McIver WJ, Sapey E, Walton GM: Understanding the role of neutrophils in chronic inflammatory airway disease. *F1000Res* 2019, 8.
51. de HC, Hassing I, Bol M, Bleumink R, Pieters R: Ultrafine but not fine particulate matter causes airway inflammation and allergic airway sensitization to co-administered antigen in mice. *Clin Exp Allergy* 2006, 36: 1469-1479.
52. Larsen ST, Roursgaard M, Jensen KA, Nielsen GD: Nano titanium dioxide particles promote allergic sensitization and lung inflammation in mice. *Basic Clin Pharmacol Toxicol* 2010, 106: 114-117.
53. Rossi EM, Pylkkanen L, Koivisto AJ, Nykasenoja H, Wolff H, Savolainen K *et al.*: Inhalation exposure to nanosized and fine TiO<sub>2</sub> particles inhibits features of allergic asthma in a murine model. *Part Fibre Toxicol* 2010, 7: 35.
54. Vandebriel RJ, Vermeulen JP, van Engelen LB, de JB, Verhagen LM, de la Fonteyne-Blankestijn LJ *et al.*: The crystal structure of titanium dioxide nanoparticles influences immune activity in vitro and in vivo. *Part Fibre Toxicol* 2018, 15: 9.
55. van RB, Landsiedel R, Fabian E, Burkhardt S, Strauss V, Ma-Hock L: Comparing fate and effects of three particles of different surface properties: nano-TiO<sub>2</sub>, pigmentary TiO<sub>2</sub> and quartz. *Toxicol Lett* 2009, 186: 152-159.

56. Nurkiewicz TR, Porter DW, Hubbs AF, Cumpston JL, Chen BT, Frazer DG *et al.*: Nanoparticle inhalation augments particle-dependent systemic microvascular dysfunction. *Part Fibre Toxicol* 2008, 5: 1.
57. Nel A, Xia T, Madler L, Li N: Toxic potential of materials at the nanolevel. *Science* 2006, 311: 622-627.
58. Wang J, Liu Y, Jiao F, Lao F, Li W, Gu Y *et al.*: Time-dependent translocation and potential impairment on central nervous system by intranasally instilled TiO<sub>2</sub> nanoparticles. *Toxicology* 2008, 254: 82-90.
59. Omlor AJ, Le DD, Schlicker J, Hannig M, Ewen R, Heck S *et al.*: Local Effects on Airway Inflammation and Systemic Uptake of 5 nm PEGylated and Citrated Gold Nanoparticles in Asthmatic Mice. *Small* 2017, 13.
60. Mohanta D, Patnaik S, Sood S, Das N: Carbon nanotubes: Evaluation of toxicity at biointerfaces. *J Pharm Anal* 2019, 9: 293-300.
61. Ye SF, Wu YH, Hou ZQ, Zhang QQ: ROS and NF-kappaB are involved in upregulation of IL-8 in A549 cells exposed to multi-walled carbon nanotubes. *Biochem Biophys Res Commun* 2009, 379: 643-648.
62. Cavallo D, Fanizza C, Ursini CL, Casciardi S, Paba E, Ciervo A *et al.*: Multi-walled carbon nanotubes induce cytotoxicity and genotoxicity in human lung epithelial cells. *J Appl Toxicol* 2012, 32: 454-464.
63. Kim JS, Song KS, Joo HJ, Lee JH, Yu IJ: Determination of cytotoxicity attributed to multiwall carbon nanotubes (MWCNT) in normal human embryonic lung cell (WI-38) line. *J Toxicol Environ Health A* 2010, 73: 1521-1529.
64. Murr LE, Garza KM, Soto KF, Carrasco A, Powell TG, Ramirez DA *et al.*: Cytotoxicity assessment of some carbon nanotubes and related carbon nanoparticle aggregates and the implications for anthropogenic carbon nanotube aggregates in the environment. *Int J Environ Res Public Health* 2005, 2: 31-42.
65. Palomaki J, Karisola P, Pylkkanen L, Savolainen K, Alenius H: Engineered nanomaterials cause cytotoxicity and activation on mouse antigen presenting cells. *Toxicology* 2010, 267: 125-131.
66. Fraczek-Szczypta A, Menaszek E, Syeda TB, Misra A, Alavijeh M, Adu J *et al.*: Effect of MWCNT surface and chemical modification on in vitro cellular response. *J Nanopart Res* 2012, 14: 1181.
67. Ramasamy M, Das M, An SS, Yi DK: Role of surface modification in zinc oxide nanoparticles and its toxicity assessment toward human dermal fibroblast cells. *Int J Nanomedicine* 2014, 9: 3707-3718.
68. Witzmann FA, Monteiro-Riviere NA: Multi-walled carbon nanotube exposure alters protein expression in human keratinocytes. *Nanomedicine* 2006, 2: 158-168.

69. Fanizza C, Casciardi S, Incoronato F, Cavallo D, Ursini CL, Ciervo A *et al.*: Human epithelial cells exposed to functionalized multiwalled carbon nanotubes: interactions and cell surface modifications. *J Microsc* 2015, 259: 173-184.
70. Kostarelos K, Lacerda L, Pastorin G, Wu W, Wieckowski S, Luangsivilay J *et al.*: Cellular uptake of functionalized carbon nanotubes is independent of functional group and cell type. *Nat Nanotechnol* 2007, 2: 108-113.
71. Cheng C, Muller KH, Koziol KK, Skepper JN, Midgley PA, Welland ME *et al.*: Toxicity and imaging of multi-walled carbon nanotubes in human macrophage cells. *Biomaterials* 2009, 30: 4152-4160.
72. Magrez A, Horvath L, Smajda R, Salicio V, Pasquier N, Forro L *et al.*: Cellular toxicity of TiO<sub>2</sub>-based nanofilaments. *ACS Nano* 2009, 3: 2274-2280.
73. Antonelli A, Serafini S, Menotta M, Sfara C, Pierige F, Giorgi L *et al.*: Improved cellular uptake of functionalized single-walled carbon nanotubes. *Nanotechnology* 2010, 21: 425101.
74. Harfoush SA, Nguyen J, Heck S, Mahdy A, Bals R, Dinh QT: Nanoparticles and air pollutants as potential stimulators of asthmatic reaction. *Frontiers in Nanoscience and Nanotechnology* 2019, 6: 1-6.
75. Harfoush SA, Hannig M, Le DD, Heck S, Leitner M, Omlor AJ *et al.*: High-dose intranasal application of titanium dioxide nanoparticles induces the systemic uptakes and allergic airway inflammation in asthmatic mice. *Respiratory Research* 2020, 21: 168.
76. Buhl R, Hamelmann E: Future perspectives of anticholinergics for the treatment of asthma in adults and children. *Therapeutics and Clinical Risk Management* 2019, 15: 473-485.

## 10. Abbreviation

**TiO<sub>2</sub>:** titanium dioxide

**OVA:** ovalbumin

**SEM:** scanning electron microscopy

**ICP-MS:** inductively coupled plasma mass spectrometry

**Th:** T helper

**IL:** interleukin

**WHO:** World Health Organization

**NPs:** nanoparticles

**ECHA:** the European Chemicals Agency

**RAC:** Committee for Risk Assessment

**TEM:** transmission electron microscopy

**PBS:** phosphate-buffered saline

**BALF:** bronchoalveolar lavage fluid

**H&E:** hematoxylin and eosin

**PAS:** periodic acid Schiff

**IF:** immunofluorescence

**ELISA:** enzyme-linked immunosorbent assay

**Ig:** immunoglobulin

**IFN- $\gamma$ :** interferon-gamma

**EDX:** energy-dispersive X-ray spectroscopy

**AHR:** airway hyperresponsiveness

**sRaw:** specific airway resistance

**MCh:** methacholine

**COPD:** chronic obstructive pulmonary disease

**CNTs:** carbon nanotubes

**SWCNTs:** single walled carbon nanotubes

**DWCNTs:** double walled carbon nanotubes

**MWCNTs:** multi walled carbon nanotubes

**ml:** millilitre

**L:** litre

**µl:** microliter

**FDA:** Food and Drug Administration

## 11. Publications

List of papers and manuscripts that are published during the PhD study:

**1. Shaza Abdunnasser Harfoush**, Juliane Nguyen, Sebastian Heck, Ahmed Mahdy, Robert Bals and Quoc Thai Dinh. **Nanoparticles and air pollutants as potential stimulators of asthmatic reaction.** *Frontiers in Nanoscience and Nanotechnology*. 2019 Oct 11.

**2. Shaza Abdunnasser Harfoush**, Robert Bals and Quoc Thai Dinh. **Nanoparticles could be a promising candidate for asthma therapy.** *Nanotechnology and Advanced Material Science*. 2019 Oct 06.

**3. Shaza Abdunnasser Harfoush**, Matthias Hannig, Duc Dung Le, Sebastian Heck, Maximilian Leitner, Albert J. Omlor, Isabella Tavernaro, Annette Kraegeloh, Ralf Kautenburger, Guido Kickelbick, Andreas Beilhack, Markus Bischoff, Juliane Nguyen, Martina Sester, Robert Bals and Quoc Thai Dinh. **High-dose intranasal application of titanium dioxide nanoparticles induces the systemic uptakes and allergic airway inflammation in asthmatic mice.** *Respiratory Research*. 2020 July 02.

**4. Maximilian Leitner**, Sebastian Heck, Kenny Nguyen, Phu Quyen Nguyen, **Shaza Abdunnasser Harfoush**, Eva Rosenkranz, Robert Bals and Quoc Thai Dinh. **Allergic airway inflammation induces upregulation of the expression of IL-23R by macrophages and not in CD3<sup>+</sup>T cells and CD11c<sup>+</sup> F4/80<sup>-</sup> dendritic cells of the lung.** *Cell and Tissue Research*. 2022 April 27.

Posters:

**1. Shaza Abdunasser Harfoush**, Albert Joachim Omlor, Raphael Ewen, Duc Dung Le, Janine Schlicker, Sebastian Heck, Robert Bals, Juliane Nguyen, and Quoc Thai Dinh. The effects and uptake of gold nanoparticles in asthmatic mice.

**European Academy of Allergy and Clinical Immunology (EAACI) 2018 in München**

**2. Shaza Abdunasser Harfoush**, Sebastian Heck, Francois Daubeuf, Duc Dung Le, Martina Sester, Dominique Bonnet, Robert Bals, Nelly Frossard, and Quoc Thai Dinh. CXCL12 neutraligand chalcone 4 inhibits migration of intraganglionic DC in an OVA-sensitized mouse model for allergic airway inflammation.

**European Academy of Allergy and Clinical Immunology (EAACI) 2018 in München**

**3. Shaza Abdunasser Harfoush**, Matthias Hannig, Duc Dung Le, Sebastian Heck, Maximilian Leitner, Albert J. Omlor, Isabella Tavernaro, Annette Kraegeloh, Ralf Kautenburger, Guido Kickelbick, Andreas Beilhack, Markus Bischoff, Juliane Nguyen, Martina Sester, Robert Bals and Quoc Thai Dinh. Effects of titanium dioxide nanoparticles on airway inflammation in experimental asthma model.

**Kongress der Deutschen Gesellschaft für Pneumologie und Beatmungsmedizin (DGP) 2019**  
in München

## **12. Acknowledgments / Danksagung**

An dieser Stelle möchte ich allen Coautoren danken, die zum Gelingen dieser Arbeit beigetragen haben.

Ich bedanke mich herzlich bei Herrn Prof. Dr. Quoc Thai Dinh für das Übergebendes Themas und für die ausgezeichnete Supervision und Hilfestellung bei dieser interessanten Forschungsarbeit.

Frau Prof. Dr. Martina Sester danke ich für die ihre gute Betreuung vonseiten der Abteilung für Transplantations- und Infektionsimmunologie.

Des Weiteren danke ich Herrn Prof. Dr. Dr. Robert Bals, Herrn Prof. Dr. Matthias Hannig und Herrn Nobert Putz, für die fachliche Unterstützung des Promotionsverfahrens.

*Aus datenschutzrechtlichen Gründen wird der Lebenslauf in der elektronischen Fassung der Dissertation nicht veröffentlicht.*

**Tag der mündlichen Prüfung: 18. April 2023**

**Dekan: Prof. Dr. Michael D. Menger**

**Berichterstatter: Prof. Dr. Martina Sester**

**Prof. Dr. Robert Bals**



